Preparation of Thiol Conjugates of the Mycotoxin Deoxynivalenol and their Occurrence in Nature

Ana Stanić

Dissertation for the Degree of Ph.D.

Department of Chemistry

Faculty of Mathematics and Natural Sciences

University of Oslo

2016

"An expert is a man who has made all the mistakes which can be made, in a narrow field."

- Niels Bohr

"The first principle is that you must not fool yourself and you are the easiest person to fool."

- Richard Feynman

Dedicated to my Mom and Dad

ACKNOWLEDGMENTS

The work presented in this thesis has been carried mainly at the Chemistry and Toxicology Department of Norwegian Veterinary Institute and partially at the Department of Chemistry, University of Oslo, during the period August 2013–July 2016.

An acknowledgment to Hans-Ulrich Humpf from the Institute of Food Chemistry, University of Münster, Germany, for kindly providing us with standards for breakdown products of DON (norDONs).

I would like to start with the fact that I lost 4 teeth during my PhD. There were moments where stress just piled up, nothing was working as it should, and I was often at the edge of a mini-nervous breakdown, and all I wanted to do was to break the instruments I was working on, spill my reactions down the sink, or set the lab on fire like a pyromaniac. I cried myself to sleep like a little girl, with worry over whether I will manage to finish it in time, and if I do actually finish it, then what?

All of these thoughts were running through my head on a daily basis, and yet, as crazy as it sounds, if I had the chance I would absolutely do it all over again. The reason for that are in the first place my three worlds-best supervisors. If I got the chance to pick them myself, I would not make a better choice. It was a supervisor lottery and they deserve much more from just a written gratitude in this thesis, but for now this is the best I can give. If I ever become rich and famous (or at least manage to marry rich) I promise more support.

To my main supervisor, **Dr. Silvio Uhlig** - thank you for always being calm and patient and for always listening to my monologues. For guiding me in the best possible way and giving me an opportunity to get this degree and the honor to work with the best group of people I could imagine. **Dr. Christopher Owen Miles** – thank you for numerous hours that you spent in my office explaining and discussing the scientific and non-scientific things and advising me. Thank you for all the pineapple lumps, baked muffins and cakes sneaked out from the meetings on the 5th floor that ended up on my office desk. **Prof. Frode Rise** – thank you for teaching me so much about NMR and for always making me laugh throughout this PhD with your witty and honest comments. To all three of you, **thank you**, not only for unselfishly transferring all of your knowledge to me, but to teaching me how to be a good scientist and to be critical. The three of you are the most knowledgeable people I have met, yet the most modest ones. Above everything you are great human beings and if I ever become half a person or a scientist as you are, I will consider it my personal success. Thank you for being not only scientific supervisors, but also unpaid psychologists. For holding mini-motivational speeches each time you noticed I had a bad

Thank you all for being patient with me!

Ana Stanic

Oslo, December 2016

SUMMARY

Cereal crops (such as oats, wheat, barley, rye, corn etc.) are often contaminated with toxigenic fungi during field or storage conditions, which can consequently lead to food and feed contamination with mycotoxins and to crop losses. One of the most common and worldwide occurring genera of fungi infecting crops is *Fusarium*, including species that may produce mycotoxins like trichothecenes, fumonisins and zearalenone. Trichothecenes inhibit protein synthesis by binding to the ribosomes. Based on their chemical structure, they are further divided into Type A, B, C and D. The Type B trichothecenes, characterized by the presence of a carbonyl group at the C-8 position, is not the most acutely toxic subgroup, but it is the most prevalent in North America and Europe. The economically most relevant mycotoxin, belonging to the Type B group of trichothecenes, is 4-deoxynivalenol (DON). It contains several structural features that enable plants or animals to biotransform the molecule, thereby decreasing or eliminating its toxicity. These features are an epoxy ring, hydroxyl groups and an *α,β*-unsaturated carbonyl group. Some of the plant biotransformation products of DON (e.g. deoxynivalenol 3-β-D-glucoside) are well known and characterized. More recent studies used carbon isotope labelled DON in metabolomic studies in wheat and tentatively identified new conjugates such as DON–glutathione (DON–GSH), DON–cysteinylglycine (DON–CysGly) and DON–cysteine (DON–Cys). As the thiol addition may either occur irreversibly on the 12,13-epoxide group of DON or reversibly at the 9,10-conjugated double bond, it was necessary to synthesize these conjugates in order to identify the biotransformation products in real samples.

The main focus of this work was to get insight into the reaction between DON and different thiols, including biologically significant compounds as L-cysteine and L-glutathione.

The reaction between the model thiol 2-mercaptoethanol and DON was initially used to optimize the reaction conditions and to develop a liquid chromatography–mass spectrometry (LC–MS) method to follow the reaction and to analyze the products. The reactions were tested in a pH range of 7.3–10.7, and with several thiols (2-aminoethane thiol, sodium methanethiolate, sodium 2-mercaptoethanesulfonate, L–cysteine and L–glutathione). The pattern in the LC–MS chromatograms of the reaction between DON and tested thiols was similar – what was shown to be the C-13 (epoxide) conjugate was always the earliest eluting peak, while there were several C-10 (Michael) adducts that were isomerizing and their ratios changing with time. The reactions occurred fastest under the basic conditions, but also occurred at physiological pH. The reaction was also carried out between 2-mercaptoethanol and trichothecenes that differentiate from DON in a way that is significant to prove the binding position of a thiol, such as T-2 tetraol that has hydroxyl group at C-8 and therefore lacking a conjugated double bond, and deepoxy-DON that contains reduced 12,13-epoxy ring.

A DON-13-mercaptoethanol and 10,13-double adduct was purified and characterized using nuclear magnetic resonance (NMR). Once major reaction products were characterized, optimized conditions (basic pH and thiol excess) were applied and used to synthesize and purify epoxide

and thermodynamically favored Michael adducts of DON–GSH and DON–Cys conjugates. In order to prepare analytical standards, conjugates were quantified using qNMR (ERETIC2).

The effect of the synthesized conjugates (DON-13-mercaptoethanol, DON-10,13-dimercaptoethanol, DON-10-Cys and DON-13-Cys) on cell proliferation and metabolic activity, as well as the expression of proinflammatory cytokines was tested. All of the tested compounds displayed significantly lower toxicity *in vitro* compared to DON.

The reaction mixtures containing DON and two dipeptides, CysGly and γ-GluCys, and *N*-acetylcysteine (NAC) were also prepared and followed over time for the comparative analysis of real samples and together with the obtained standards were used in the analysis of oats and spring wheat samples from Norway that were naturally contaminated with DON and in an extract of wheat spikelets that were artificially treated with DON. The LC–HRMS analysis showed that the main products of the artificially contaminated wheat were C-10 conjugates of DON and GSH, Cys and CysGly, while the naturally contaminated wheat and oat samples contained predominantly C-13-linked conjugates with GSH, Cys, CysGly and NAC.

ABBREVIATIONS

1D	one-dimensional
2D	two-dimensional
3ADON	3-acetyldeoxynivalenol
15ADON	15-acetyldeoxynivalenol
ABC	ATP-binding cassette
AFB_1	aflatoxin B_1
AFG_1	aflatoxin G_1
AFM_1	aflatoxin M_1
ATA	alimentary toxic aleukia
ATP	adenosine triphosphate
CoA	coenzyme A
COSY	correlation spectroscopy
CYP P450	cytochrome pigment 450
Cys	cysteine
Cys-Gly	cysteinylglycine
Deepoxy-DON	deepoxy deoxynivalenol
DEPT	distortionless enhancement by polarization transfer
DHAR	dehydroascorbate reductase
DMATS	dimethylallyl tryptophan synthase
DMEs	drug metabolizing enzymes
DON	deoxynivalenol
DON-15-GlcA	DON-15-*O*-β-D-glucuronide

DON-3-Glc	deoxynivalenol 3-β-D-glucoside
DON-3-GlcA	DON-3-*O*-β-D-glucuronide
ELISA	enzyme-linked immunosorbent assay
ERETIC	electronic reference to access in-vivo concentration
FHB	*Fusarium* head blight
FID	free induction decay
FX	fusarenon X
GC	gas chromatography
GSH	glutathione
GSSG	glutathione disulfide
GST	glutathione *S*-transferase
HMBC	hetero-nuclear multiple-bond correlation spectroscopy
HSQC	hetero-nuclear single-quantum correlation spectroscopy
IL-1β	interleukin-1 beta
ILSI	International Life Science Institute
LC	liquid chromatography
LIT	linear ion trap
LPS	lipopolysaccharide
LSD	D-lysergic acid diethylamide
mCPBA	*meta*-chloroperoxybenzoic acid
MRP1	multidrug resistance-associated protein 1
MS	mass spectrometry
NAC	*N*-acetylcysteine
NEO	neosolaniol
NIV	nivalenol

NMR	nuclear magnetic resonance
NOE	nuclear Overhauser effect
NOESY	nuclear Overhauser effect correlation spectroscopy
NPC	normal phase chromatography
NRPS	non-ribosomal peptide synthetase
OTA	ochratoxin
Pgp	P-glycoprotein
PKS	polyketide synthases
PULCON	pulse length based concentration determination
Q	quadrupole
QIT	quadrupole ion trap
qNMR	quantitative nuclear magnetic resonance
RF	radio frequency
ROESY	rotating-frame Overhauser spectroscopy
ROS	reactive oxygen species
RPC	reversed phase chromatography
SULTs	sulfotransferases
TLC	thin-layer chromatography
TNFα	tumor necrosis factor α
TOCSY	total correlation spectroscopy
TOF	time-of-flight
UDP	uridine diphosphate
ZEA	zearalenone
γGT	γ-glutamyl transpeptidase

Contents

APPENDIX

Paper I

Stanic, A.; Uhlig, S.; Solhaug, A.; Rise, F.; Wilkins, A. L.; Miles, C. O., Nucleophilic Addition of Thiols to Deoxynivalenol. *J. Agric. Food. Chem.* **2015**, *63*, 7556–7566.

Paper II

Stanic, A.; Uhlig, S.; Solhaug, A.; Rise, F.; Wilkins, A. L.; Miles, C. O., Preparation and Characterization of Cysteine Adducts of Deoxynivalenol. *J. Agric. Food. Chem.* **2016**, *64*, 4777–4785.

Paper III

Stanic, A.; Uhlig, S.; Sandvik, M.; Rise, F.; Wilkins, A. L.; Miles, C. O., Characterization of Deoxynivalenol–Glutathione Conjugates Using Nuclear Magnetic Resonance Spectroscopy and Liquid Chromatography–High-Resolution Mass Spectrometry. *J. Agric. Food. Chem.* **2016**, *64*, 6903–6910.

Paper IV

Uhlig, S.; **Stanic, A**.; Hofgaard, I.; Kluger, B.; Schuhmacher, R.; Miles, C., Glutathione-Conjugates of Deoxynivalenol in Naturally Contaminated Grain Are Primarily Linked via the Epoxide Group. *Toxins* **2016**, *8*, 1–12.

1. INTRODUCTION

1.1. Fungi – taxonomy and general features

The traditional division of the living organisms into two domains, Prokaryota and Eukaryota, and five kingdoms, Animalia, Plantae, Protista, Monera and Fungi, was first proposed by Robert Whittaker in 1959.[1] (Figure 1)
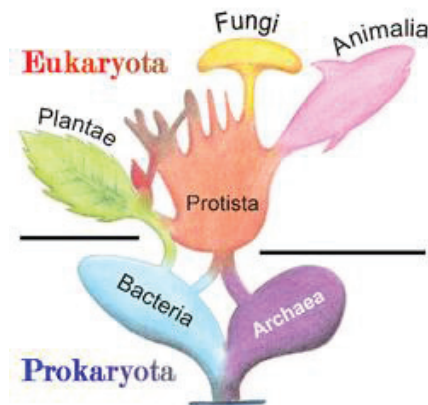
Figure 1. Five-kingdom taxonomic classification, proposed by Robert Whittaker (1959). Figure taken from Wikipedia.[2]

However, with the latest developments in molecular methods and improvements in understanding evolutionary relationships, there are new attempts to develop a classification based on mutually related monophyletic units, meaning that all organisms included in a kingdom are offspring of a common ancestor. In 2005, the International Society of Protistologists published a revision of the classification, dividing Eukaryotes into six clusters that may represent the basic groupings similar to traditional ''kingdoms''[3] (Figure 2). Based on that division, fungi, as well as animals, belong to the super-group Opisthokonta. In that same classification, the further division of Fungi is to Ascomycota, Basidiomycota, Chytridiomycetes, Microsporidia, Urediniomycetes, Ustilaginomycetes, Zygomycota and Glomeromycota—the latter being a group of fungi once placed in Zygomycota. Some more recent classifications do not accept Zygomycota as a phylum, as it has been recognized as polyphyletic and distributed among the phylum Glomeromycota and four subphyla Mucoromycotina, Kickxellomycotina, Zoopagomycotina and

Entomophthoromycotina.[4] As the methods for studying the evolution of fungi develop and improve further, the classification system will continue to undergo changes.

A simplified definition for the Fungi would describe them as a group of eukaryotic organisms that include unicellular microorganisms such as yeasts, as well as multicellular fungus like molds or fungi known as mushrooms.
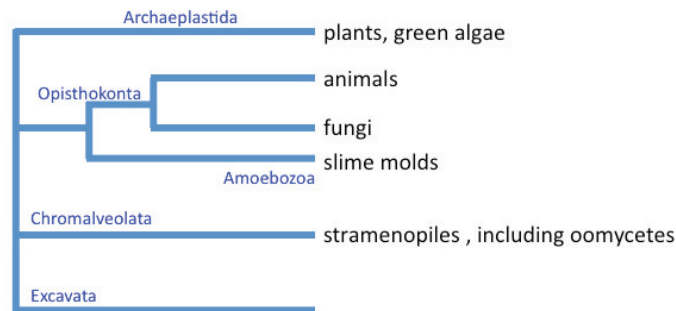
Figure 2. Relationships between plants and animals and the organisms previously considered as the kingdom of Fungi. Adapted from the Tree of Life Web Project.[5] Names in blue refer to the super-groups in the classification published by Adl et al.[3]

The fungi diverged from plants and animals around one billion years ago,[6] explaining why some of the morphological, biochemical and genetic features are shared, while others are unique, distinguishing them from the other kingdoms. Fungi, like animals, are lacking chloroplasts and are heterotrophic organisms. Thus, they make use of three different trophic strategies to obtain carbon and may occur as saprotrophs, necrotrophs, and biotrophs.[7] They also have vacuoles[8] and cell walls like plants, but unlike plants the cell wall is built from glucans and chitin,[9] which is an *N*-acetylglucosamine polymer and a characteristic component of the exoskeletons of arthropods and insects. Fungi produce spores, and have both sexual and asexual reproduction (Figure 3).

The environment is what triggers developmental states that lead to the creation of specialized structures for sexual or asexual reproduction—if the environmental conditions are favorable, asexual reproduction is advantageous, since the environment would be ideal for the clones of that individual. If the environmental conditions are poor, the goal would be to make genetically different offspring that will be better adapted to a new environment.[10] Asexual reproduction is by fragmentation, budding or the production of asexual spores: sporangiospores and conidia. Fungus sexual reproductive stage is called teleomorph, and asexual reproductive stage is called anamorph.[11] Since fungi used to be classified based on the structures associated with sexual reproduction, fungi that are lacking a sexual stage do not fit into those classifications and were named "Fungi imperfecti" or Deuteromycota.[12]
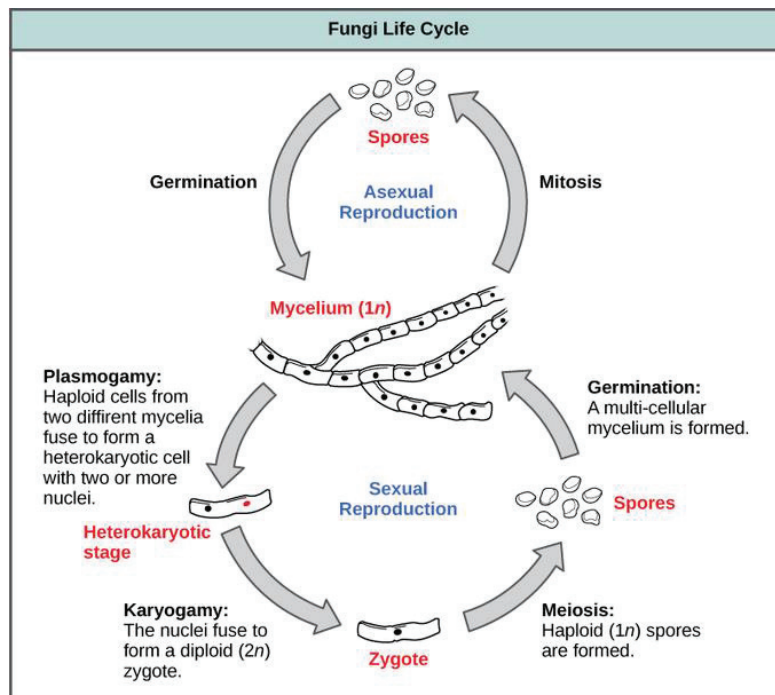
Figure 3. Types of fungal reproduction.[13]

Fungi are abundant worldwide and are involved in a wide range of processes—they can be decomposers, symbionts on algae and cyanobacteria,[14] plants, animals or fungi, but also parasites and pathogens of other organisms. Parasitic fungi infecting animals or humans elicit diseases collectively called mycoses (e.g., aspergillosis, candidiasis) while dietary, respiratory, dermal, and other exposures to the toxins produced by some types of fungi (molds) produce diseases collectively called mycotoxicoses.[15] Mycotoxins are toxic secondary metabolites produced by a type of fungus, commonly known as molds. Mycotoxicoses are examples of "poisoning by natural means", and in such a way analogous to the conditions caused by exposure to pesticides or heavy metal residues.[15] There are many historical instances of the occurrence of mycotoxicoses. One example is "Saint Anthony's fire", the Middle Age name for ergotism, a poisoning caused by the consumption of foods prepared from grain that was contaminated with ergot bodies (sclerotia of parasitic *Claviceps* spp.). The symptoms were convulsive and gangrenous and sometimes explained as "bewitchment"—a possession with evil spirits.[16] Another example of a mycotoxicosis is alimentary toxic aleukia (ATA), caused by the ingestion of grain contaminated with mycotoxins from *Fusarium* and *Stachybotris* species, and held responsible for the death of at least 100,000 Russian people between 1942 and 1948.[17] The investigation of the cause of the hepatotoxic disease in ruminants (cattle, sheep, deer, goats), facial eczema, started about 100 years ago in New Zealand.[18] It was only in 1959 that the toxin sporidesmin, produced by saprophytic fungus *Pithomyces chartarum*, was isolated and its exact structure was determined in 1962.[19]. However, what is considered as the beginning of modern

mycotoxicology is the time of the unusual veterinary crises in 1962 near London, England, where the mysterious turkey X disease was linked to peanut meal contaminated with secondary metabolites, aflatoxins, from *Aspergillus flavus*.[16,20] This disease was the start for immense research on mycotoxins and mycotoxicoses.

1.2. Secondary Metabolites

Secondary metabolites are low-molecular-weight metabolites that can have potent physiological activities,[21] but are not necessary for normal growth or development of the organism.[22] They are usually produced at restricted parts of a life cycle, with production being often correlated to a specific stage of morphological differentiation.[21] However, their role in the biology of fungi is still poorly understood. Most likely their production is advantageous for the survival of an organism in its ecological niche, where a diverse array of competing organisms and predators is present.[22] An example of the anti-predator theory is an experiment that showed how springtails (fungivore arthropods) exhibit a distinct preference for feeding on a soil mold *Aspergillus nidulans* mutant that lacked a gene responsible for the regulation of the production of many secondary metabolites, including mycotoxins, over the wild-type mold.[23]

Fungal secondary metabolites can also be produced in the context of host–pathogen interactions; fungi producing secondary metabolites as virulence factors and infecting the host to promote the spreading of the pathogen. As an example, it was demonstrated that in the absence of production of trichothecene mycotoxins, the fungus *Fusarium graminearum* could not move into the rachis of wheat plants.[24]

Mycotoxins could also be produced as a response to oxidative stress. During colonization and infection, fungi can be exposed to host metabolites that are produced as a consequence of their presence. Some of these metabolites (e.g., reactive oxygen species (ROS)) can trigger response pathways in fungi that include the production of mycotoxins. For instance, it has been demonstrated that the mycotoxin deoxynivalenol (DON) accumulates in liquid cultures of *F. graminearum* under oxidative stress by H_2O_2.[25] Another example is increased accumulation of the mycotoxin sterigmatocystin in the fungus *A. nidulans* after treatment with oxidant *tert*-butyl hydroperoxide.[26]

As a result of various biological activities (e.g., antifungal, antibacterial, antitumor), fungal secondary metabolites have had an extraordinary impact on human life during many years. They have therefore been classified according to their impact on human interests: pharmaceuticals (e.g., penicillin), plant growth regulators (e.g., gibberellins), pigments (e.g., carotenoids, melanin), or mycotoxins (e.g., fumonisins, aflatoxins, trichothecenes).[21,27] Even though they can be chemically very diverse, all of the fungal secondary metabolites arise from a limited number of precursors from primary metabolism.[21] Therefore, another, more biochemically-rational way to classify fungal secondary metabolites is based on the enzyme class that synthesizes their basic

chemical structure.[21] The largest groups are: polyketides, non-ribosomal peptides, alkaloids and terpenes.

1.2.1. Polyketides

Polyketides are the most abundant fungal secondary metabolites synthesized by type I polyketide synthases (PKS), multidomain proteins.[21] Polyketides are derived by the repetitive condensation of acetate units or other short carboxylic acids (from acetylCoA, malonylCoA), through an enzymatic mechanism similar to fatty acid synthesis.[28] There are three main domains in fungal PKS: acyl carrier, acetyltransferase and ketoacyl CoA synthase. The diversity of polyketides is achieved by varying the repetition reactions, the number of reduction reactions, type of extender units used and a variety of post-polyketide synthesis modifications.[21]

There are many examples of fungal polyketides, such as lovastatin,[29] which is a commercially available cholesterol-lowering agent, or strobilurins,[30] a group of compounds used in agriculture as fungicides. Many classes of mycotoxins that are of importance in agriculture and food industries, including aflatoxins, fumonisins, ochratoxins, zearalenone, are also polyketides.[28]

1.2.1.1. Aflatoxins

Aflatoxins are a group of roughly 20 related toxic fungal polyketides that are especially known for their carcinogenic properties.[31] They are produced by several species of soil-borne *Aspergillus*, responsible for decomposition of plant materials.[32] The most common *Aspergillus* contaminants in agriculture are species *A. flavus* and *Aspergillus parasiticus*.[20] Warm temperatures and humidity favor their growth, making aflatoxin food contamination a common problem in tropical and subtropical regions of the world. Aflatoxin-contaminated food (Figure 4) includes cereals (maize, sorghum, rice, wheat), oilseeds (peanut, soybean, sunflower, cotton), spices (chilies, black pepper, coriander), tree nuts (almonds, pistachio, walnut, coconut) and milk products.[32]

Figure 4. Aflatoxin infected peanuts (left) and maize (right).[33]

Based on their chemical structures, aflatoxins belong to a group of difuranocoumarins that are divided into two subgroups: difuranocoumarocyclopentenones (AFB$_1$, AFB$_2$, AFM$_1$, AFM$_2$) and difuranocoumarolactones (AFG$_1$, AFG$_2$) (Figure 5).[32] The major aflatoxins were named based on their fluorescence under the UV light (blue or green) and relative chromatographic mobility during thin-layer chromatography (TLC) (e.g., B$_1$ and B$_2$, and G$_1$ and G$_2$). Aflatoxins with M designation are products from hepatic animal metabolism first isolated from milk. When cows consume contaminated feeds, they metabolize AFB$_1$ the a hydroxylated form AFM$_1$, making milk products as an indirect source of aflatoxins.[20]
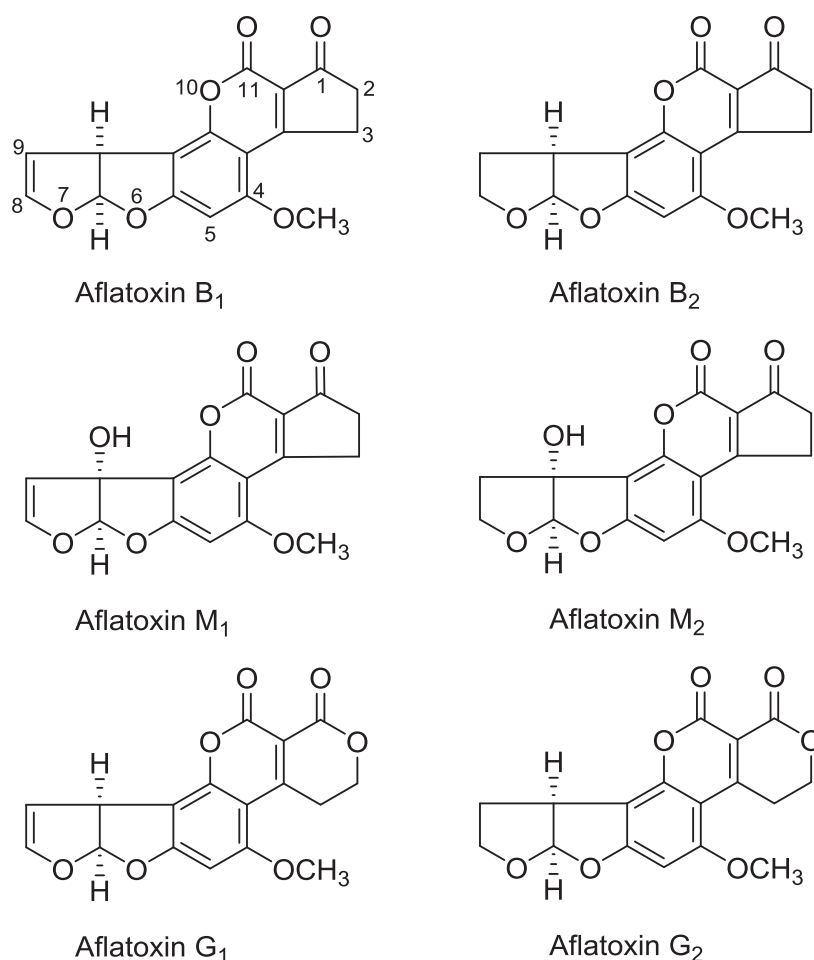
Figure 5. Chemical structures of aflatoxins.[34]

Since aflatoxins are highly liposoluble, they are readily absorbed through the gastrointestinal and respiratory tracts into the blood stream.[32] They are metabolized by cytochrome P450 enzymes into 8,9-epoxides that possess the ability to bind to proteins, as well as with purines and purine

nucleosides to form DNA and RNA adducts, which is the chemical basis for their cancer causing potential.[35]AFB$_1$, AFG$_1$ and AFM$_1$ are the most toxic naturally-occurring carcinogens known. Aflatoxins are also responsible for the suppression of both humoral and cell-mediated immunity, causing susceptibility to infectious diseases.[32]

1.2.1.2. Fumonisins

Fumonisins are a group of mycotoxins produced by several agriculturally important fungi, primarily *Fusarium verticillioides* and *Fusarium proliferatum*.[16,20] Recently, it was found that *Aspergillus niger* could also produce some types of fumonisins.[28] The major commodity affected by this group of toxins is corn, but there are some reports on their occurrence in rice and sorghum.[28] Structurally, they have a long-chain hydrocarbon unit, similar to sphingosine and sphinganine. This structural similarity is the reason for their toxicity, which is based on interference with sphingolipid metabolism.[15,20] Fumonisins are classified into four groups—A, B, C and P (Figure 6). The A group differs from the B group by the presence of an *N*-acetyl amide group instead of an amine group at the C-2 position. The C group of fumonisins is chemically similar to the B group, except the fact that C-1 terminal methyl group is not present in the C series of fumonisins. The P series contains a 3-hydroxypyridinium moiety at the C-2 position in the backbone instead of the amine found in the B series of fumonisins.[36] Two new nominated fumonisins have recently been reported from cultures *A.welwitschiae* isolated from grapes grown in wine producing regions of Canada.[37,38] Fumonisins from the B-group are the most abundant, and fumonisin B$_1$ (FB$_1$) makes up 70% of the total fumonisins content.[28] FB$_1$ has been shown to be the most toxic fumonisin, causing leukoencephalomalacia in equines and rabbits, pulmonary edema and hydrothorax in swine and apoptosis in the rat liver.[15] Fumonisin consumption has also been associated with esophageal cancer in humans, and because FB1 reduces the folate uptake in different cell lines, it has been implicated in neural tube defects in human babies.[20]

O COOH
COOH
R₂OH

O $COOH$

$COOH$

R_2OH

19   16   14   12   10   7   6   5   3   2 R_4

CH_3 O CH_3 R_1 R_3

$COOH$

O $COOH$
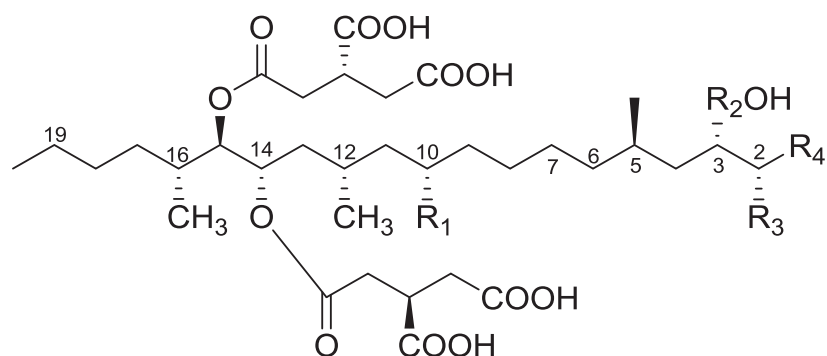
Fumonisins	Group	Empirical formula	Molecular weight	R_1	R_2	R_3	R_4
Fumonisin A₁	A	$C_{36}H_{61}NO_{16}$	763	OH	OH	$NHCOCH_3$	CH_3
Fumonisin A₂	A	$C_{36}H_{61}NO_{15}$	747	H	OH	$NHCOCH_3$	CH_3
Fumonisin A₃	A	$C_{36}H_{61}NO_{15}$	747	OH	H	$NHCOCH_3$	CH_3
Fumonisin B₁	B	$C_{34}H_{59}NO_{15}$	721	OH	OH	NH_2	CH_3
Fumonisin B₂	B	$C_{34}H_{59}NO_{14}$	705	H	OH	NH_2	CH_3
Fumonisin B₃	B	$C_{34}H_{59}NO_{14}$	705	OH	H	NH_2	CH_3
Fumonisin C₁	C	$C_{33}H_{57}NO_{15}$	707	OH	OH	NH_2	H

Figure 6. Chemical structures of fumonisins.[36]

1.2.1.3. Ochratoxins

Ochratoxins are nephrotoxic and carcinogenic mycotoxins produced by several *Aspergillus* and *Penicillium* species and are found in cereals, coffee, wine, beer and spices.[28] There are three types of ochratoxins produced by different fungi: ochratoxin A (OTA), ochratoxin B (OTB) and ochratoxin C (OTC). Their structures consist of a pentaketide dihydroisocoumarin moiety linked with phenylalanine through an amide bond (Figure 7).[39] Furthermore, OTA and OTC (the ethyl ester of OTA) are chlorinated, which is rather unusual for terrestrial natural products. Of the three ochratoxin analogues, OTA is the most common and most toxic.[40] OTA and OTB can also exist in an lactone-opened form.[28] OTA is a nephrotoxin in all animal species studied to date and it is most likely toxic to humans. It has also been reported to be a liver toxin, an immune suppressant, a potent teratogen and carcinogen.[15]
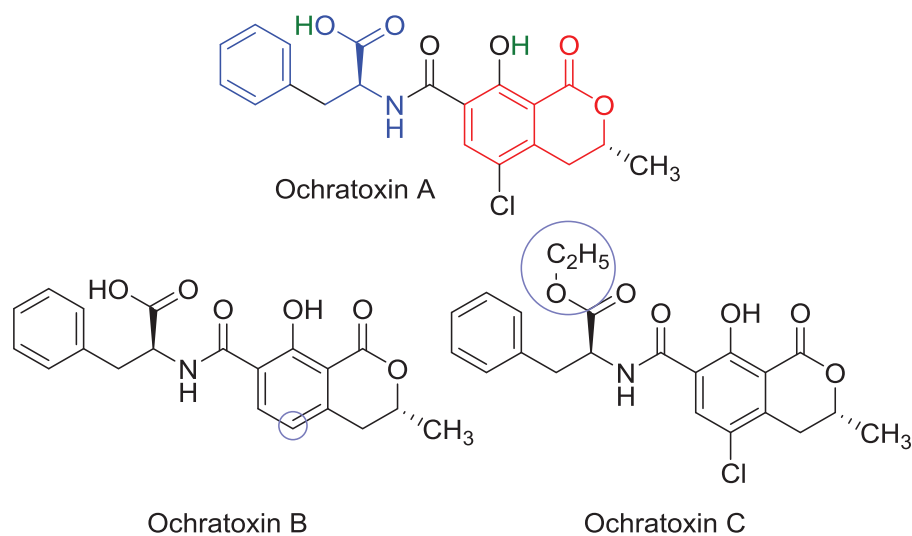
Figure 7. Chemical structures of Ochratoxin A (dark blue: phenylalanine part, red: dihydroisocoumarin ring, green: acidic hydrogens), B, and C. Highlighted structural features are characteristic to the three different ochratoxin molecules (light blue circles).[39]

1.2.1.4. Zearalenone

Zearalenone (ZEN) is a secondary metabolite produced by *F. graminearum* (teleomorph *Gibberella zeae*) and other *Fusarium* molds (*Fusarium culmorum, Fusarium equiseti, Fusarium crookwellense*) contaminating crops (e.g. corn, wheat, barley, oats, sorghum).[15,20] Grains infected with these *Fusarium* species may exhibit the pink color associated with the production of a pink pigment, simultaneously with ZEA (Figure 8).[16]
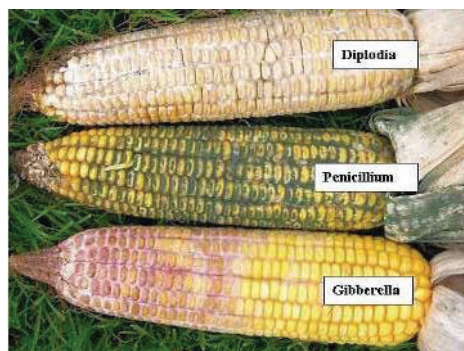
Figure 8. Three common ear molds: *Diplodia* sp. (white, on top), *Penicillium* sp. (green, middle) and *F. graminearum* (teleomorph *G. zeae*) ear rot (pink color).[41]

ZEN has a resorcinol (*m*-benzenediol) moiety fused to a 14-member macrocyclic lactone (Figure 9).[28] The trivial name zearalenone was made as a combination of *G. zeae*, resorcylic acid lactone, -ene (for the presence of the C-11 to C-12 double bond), and -one, for the C-7 ketone. In mammals, the keto group at C-7 is reduced to two stereoisomeric metabolites of ZEN, α- and β-zearalenol (ZOL) (Figure 9). These metabolites are also produced by fungi, but at much lower concentrations than ZEN [42]

Zearalenone (ZEN)

Zearalanone

α-zearalenol (α-ZOL)

α–zearalanol

β–zearalenol (β-ZOL)

β-zearalanol
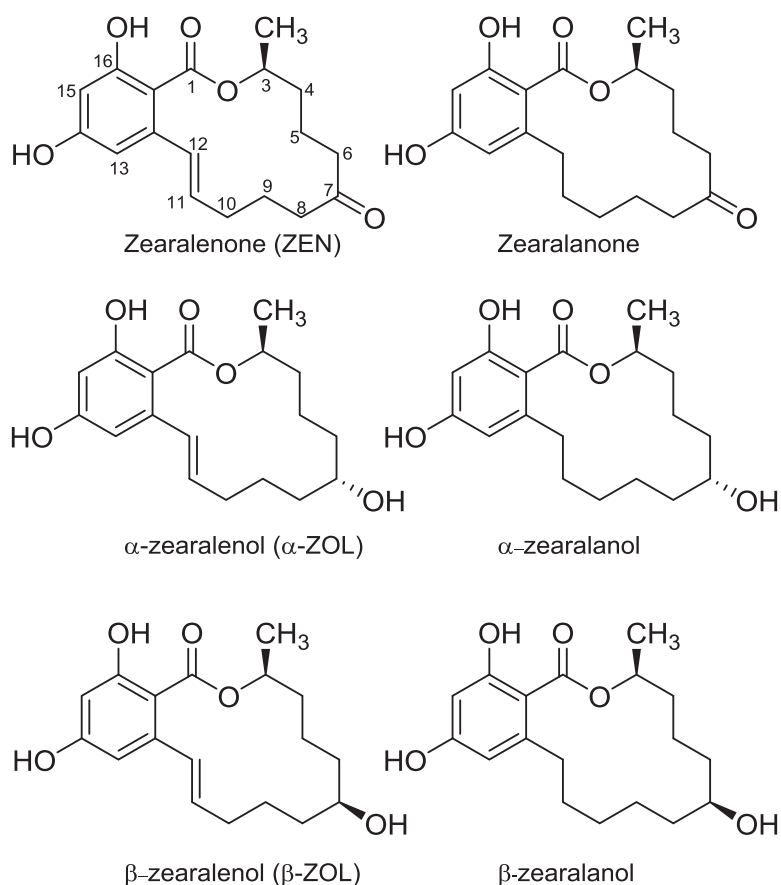
Figure 9. Chemical structures and numbering system of ZEA and its derivatives.[43]

ZEN and the reduced forms resemble 17β-estradiol, the principal hormone produced by the human ovary, which allows them to bind to estrogen receptors in mammalian cells. α-ZOL was found to be 73 times more estrogenic than ZEN, while β-ZOL exhibited about half of the activity of ZEN.[43] Morphological changes in animals that have been exposed to ZEN or ZOLs are precocious development of mammae and prepucial enlargement in young barrows.[16] Another often observed morphological change following exposure with these mycotoxins includes increase of genital organs in gilts as shown in Figure 10.
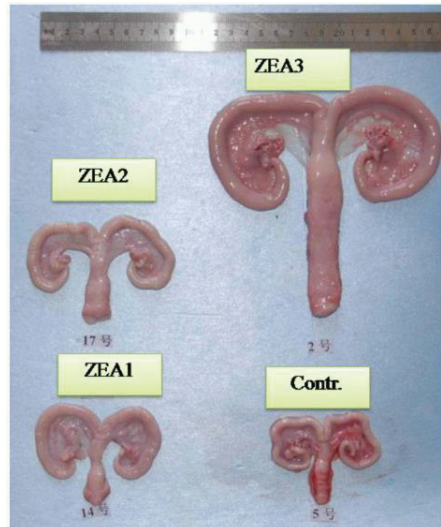
Figure 10. Effects of different levels of zearalenone on genital organs (ovary, cornu uteri, vagina-vestibule) of gilts. Zearalenone was not detectable in control diet; ZEA1, ZEA2, or ZEA3 represents control diet with addition of 1.1, 2.0, or 3.2 mg/kg zearalenone.[44] Reprinted with journal permission.

While biologically potent, ZEN is of low acute toxicity. The 50% lethal dose in female rats is higher than 10,000 mg/kg of bodyweight, in female guinea pigs it is 5,000 mg/kg,[45] while 1 µg/kg is enough to elicit a uterogenic response in female swine[15]. It is therefore appropriate to describe ZEN as an estrogenic mycotoxin.

1.2.2. Non-ribosomal peptides (NRPs)

Non-ribosomal peptides (NRPs) are synthesized by large multidomain, multimodular enzymes called non-ribosomal peptide synthases (NRPS). In contrast to genetically encoded peptides synthesized at ribosomes, NRPs contain both proteinogenic and non-proteinogenic amino acids,[46] giving them wide structural diversity. Other factors contributing to their diversity are chemical modifications, the length of produced peptides, and whether the peptide is cyclized or not.[21] NRPS encoding genes are plentiful in fungi and bacteria, but not in animals and plants.[47] The natural function of many NRPs is still unknown, but it has been clear that they play role in fungal reproductive and pathogenic development, morphology, cell surface properties, stress management, and nutrient procurement, as well as their known role as mycotoxins involved in plant or animal pathogenesis.[47] NRPs include a number of widely used antibiotics (e.g. penicillin and cephalosporin) and immunosuppressive drugs (e.g. cyclosporine).[48,49]
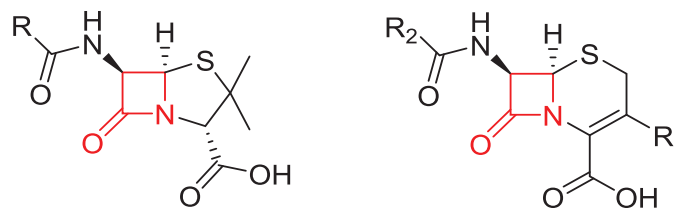
Figure 11. Core chemical structures of penicillins (left) and cephalosporins (right). The β-lactam ring is shown in red.[50]

Penicillin and cephalosporin are β-lactam antibiotics (Figure 11), produced by fungi from the genera *Penicillium, Cephalosporium*, and *Aspergillus*.[49] Their mechanism of action is disruption of the peptoglycan synthesis.[51] Peptoglycans are constituents of the cell wall of most bacteria. Cyclosporins are undecapeptides produced by the fungal species *Tolypocladium inflatum*,[49] and are used as immunosuppressive drug in treatment of patients after organ-transplant surgery.[21] Cyclosporin A contains the non-proteinogenic amino acid D-alanine.[49]

1.2.3.   Alkaloids

Alkaloids are secondary metabolites that contain nitrogen in a heterocycle usually originating from an amino acid.[52] Unlike polyketides or non-ribosomal peptides, their biosynthesis is not dependent on a specific enzyme class. Among the most studied fungal alkaloids are the ergot and loline alkaloids,[48] produced by *Claviceps* and *Epichloë* species (anamorph *Neotyphodium*), which are grass pathogens and endophytes of the family Clavicipitaceae.[52] Loline alkaloids are deterrent and toxic to insects,[53] and ergot alkaloids cause ergotism, in humans and other animal mammals like cattle, sheep, pigs and chickens. Clinical symptoms of ergotism are gangrene, abortion, convulsions, suppression of lactation , hypersensitivity and ataxia.[15] Ergot alkaloids are a class of indole-derived mycotoxins. They are usually derived from tryptophan and dimethylallyl pyrophosphate, although amino acids other than tryptophan could be used as precursors.[21] The first step of the pathway is the isoprenylation of tryptophan to 4-dimethylallyltryptophan (Figure 12) by the enzyme dimethylallyl tryptophan synthase.[52] There is a series of cyclization, isomerization and oxidation steps through agroclavine to lysergic acid, a precursor of a wide range of ergoline alkaloids (Figure 12).[21]
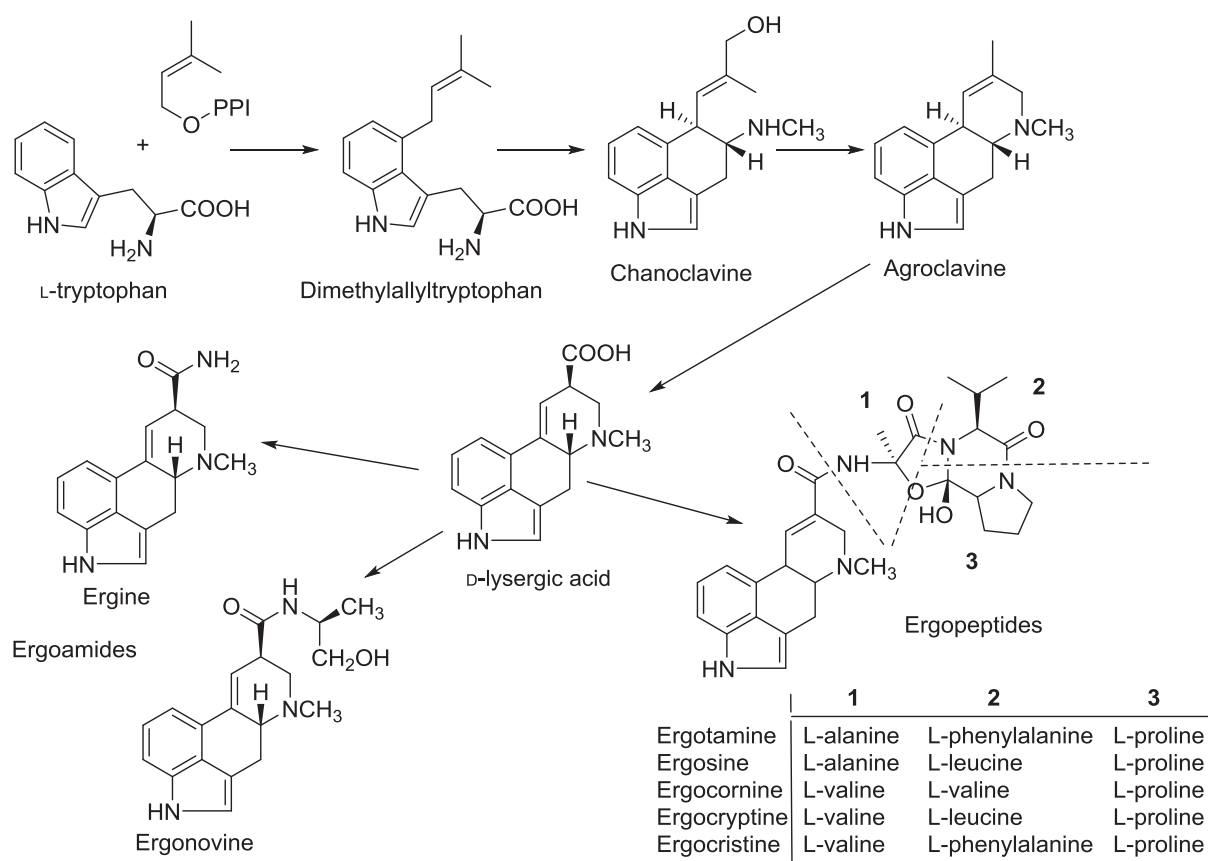
Figure 12. Ergot alkaloids produced clavicipitaceous fungi in infected plants. Ergotamine, ergosine, ergocornine, ergocryptine and ergocristine are examples of ergopeptides commonly found in ergots of *Claviceps purpurea* but commonly not in *Epichloë* species.[53]

Their wide range of biological activities engaged the interest of physicians and pharmacologists. Hoffman combined different amines via an amide linkage with lysergic acid to produce ergobasine (also known as ergometrine and ergonovine). By varying the amino alcohol constituent, he obtained Methergine, a prescription drug used to control hemorrhage after childbirth. Hoffman continued to synthetize new lysergic acid derivatives, and in his series he made D-lysergic acid diethylamide, popularly known as LSD, the famous hallucinogenic drug.[15,21] Other therapeutic uses of ergot alkaloids are as prolactin inhibitors, in the treatment of Parkinsonism and in migraine treatment.[15]

1.2.4. Terpenes

Terpenes are a large class of organic compounds derived from activated forms of isoprene (2-methyl-1,3-butadiene, C_5H_8) (Figure 13). Isoprene consists of five carbon atoms, so the carbon number in terpenes is usually a multiple of five.[52] However, isoprene itself does not occur naturally, and thus is not used directly for biosynthesis, but rather isopentenyl pyrophosphate.[54] "Terpene" commonly refers to C_{10} compounds, terpene homologues containing 15 carbon atoms are known as sesquiterpens, those containing 20 and 30 carbon atoms as diterpenes and triterpenes, respectively, and so on.[54] Terpenes modified by oxidation or rearrangement of the carbon skeleton are called terpenoids or isoprenoids.
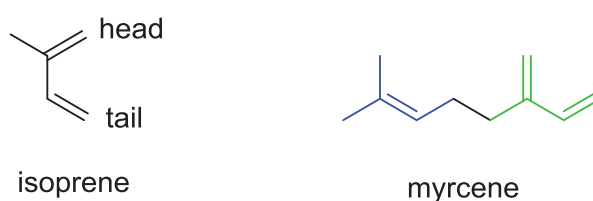
Figure 13. Chemical structure of an isoprene unit (left), and molecule of a simple terpene myrcene (right) where two isoprene units are connected "head to tail".[55]

Terpenes are present in many groups of organisms, and do not only include secondary metabolites, but also molecules like sterols or carotenoids. Typical fungal terpenoids include gibberellins, aristolochene, indole–diterpenes and trichothecenes.[21] Gibberellins are diterpenes and plant growth hormones produced by phytopatogens like *Gibberella fujikuroi* (anamorph: *F. verticilloides*) causing bakanae disease of rice.[48] Aristolochene is a bicyclic sesquiterpene produced by several fungi, including *Penicillium roqueforti*, a fungus used to make blue cheeses.[56] Aristolochene is also a precursor of the mycotoxin PR-toxin.[57] Indole–diterpenoides are a large, structurally diverse group of a mixed biosynthesis—indole unit is tryptophan-derived, in addition to diterpenoid moiety. They cause tremorgenicity in mammals, and are produced by species of *Penicillium*, *Aspergillus* and *Claviceps*.[58]

1.2.4.1. Trichothecenes

Trichothecenes are a major class of mycotoxins, produced by a range of fungi from the order Hypocreales, including the genera *Fusarium*, *Myrothecium*, *Verticimonosporium*, *Stachybotrys*, *Trichoderma*, *Trichothecium*, *Cephalosporium*, and *Cylindrocarpon*.[59] These fungi are adapted for growth and colonization of substrates with a wide range of moisture availability and nutrient content, making them widespread across the world.[27] Genera most frequently associated with crop infection in temperate climates are *Fusarium* and *Stachybotrys*. From an economic

perspective, the most important trichothecene producers are species within the *Fusarium* genus.[60] They are important plant pathogens causing diseases like *Fusarium* head blight (FHB), crown rot in barley, wheat, rye etc.[59]; and *Fusarium* wilt of solanaceous crops like potatoes, tobacco[61] and tomatoes.[62] Their occurrence in important agricultural crops consequently has an impact on human and livestock health, causing a range of acute and chronic symptoms.

Presently, there are approximately 200 known trichothecenes.[27] They are a large group of sesquiterpenoids that share a rigid tetracyclic (12,13-epoxytrichothec-9-ene) ring system (Figure 14) consisting of cyclohexene ring (A) with a double bond between C-9 and C-10, a tetrahydropyranyl ring (B), a cyclopentyl (C) ring and the epoxide ring at C-12.[27,59] The A-ring is in the half-chair conformation, and the B-ring is in the chair conformation, making the molecule rigid, with the exception when C-4 and C-15 are linked by an ether bridge, making the boat conformation preferred for the (B) ring.[63]

Trichothecenes have been divided into two main classes—simple trichothecenes (Types A–C) and macrocyclic trichothecenes (Type D) (Figures 14 and 15).[64] Types A–C may be differentiated based on the substitution at C-8 (Figures 14 and 15).[27,59] Type A trichothecenes are the simplest group, including compounds that are hydroxylated (e.g. neosolaniol), esterified (e.g. T-2 toxin) or not substituted at all (e.g. trichodermin) at the C-8 position. Type B trichothecenes contain a keto (carbonyl) function at C-8 (e.g. nivalenol (NIV), deoxynivalenol (DON)). The Type B trichothecenes produced by *Fusarium* spp. also contain a hydroxyl group at C-7, which is a structural feature not present in trichothecenes from other genera.[27] Type C trichothecenes are not as common as type A and B, and are distinguished by an additional epoxide ring at C-7/C-8 (e.g. crotocin). Type D trichothecenes, or macrocyclic trichothecenes, have an additional cyclic diester or triester linkage between C-4 and C-15 (e.g. roridin A, verrucarin A, satratoxin H). However, there are some exceptions that cannot be grouped accurately using this classification system and several other classification systems for trichothecenes have been proposed. Ueno added two more groups: Type E and Type F. Type E is represented by the macrocyclic trichothecenes in which the macrocyclic ring is opened, and Type F is represented by verrucarin K in which 12,13-epoxide is changed to vinyl group.[65] Tamm divided trichothecenes in a simpler manner—into three groups. The simple sesquiterpenes being either alcohols or simple esters, the trichoverroids, which are esters with one or two more complex C_6- or C_8-carboxylic acids, and the macrocyclic di- and triesters.[66]

Type A trichothecenes are generally more acutely toxic than the Type B analogues, with decreasing order of toxicity with isovaleryl>hydrogen>hydroxyl substitution at the C-8 position.[67] Thus, the biotransformation product T-2 tetraol is less toxic than the parent T-2 toxin.[68] In Type B trichothecenes, the presence of a C-4 hydroxyl in NIV versus hydrogen in DON increases the toxicity 10-fold, while lymphotoxicity in the group decreases in the order acetoxy>hydroxyl>hydrogen at C-4.[67]
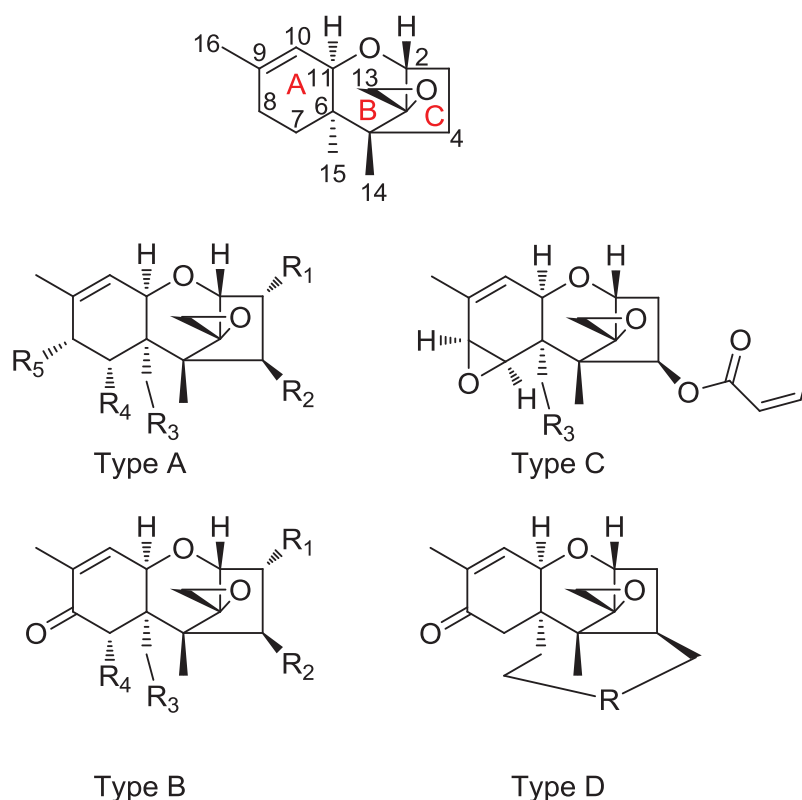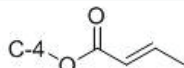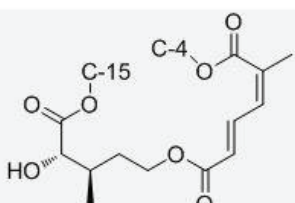
Figure 14. Classification of trichothecenes based on their chemical structures. They all share a rigid tetracyclic (12,13-epoxytrichothec-9-ene) ring system (top).[27]

A general feature of the trichothecenes is that they inhibit eukaryotic protein synthesis by preventing peptide bond formation at the A-site of the peptidyl transferase center of the 60S ribosomal subunit.[69] This makes tissues comprising of rapidly growing and dividing cells the most affected. They also inhibit mitochondrial protein synthesis,[70] interact with protein thiol groups,[71] and produce oxidative stress due to generation of the free radicals.[72] Exposure to trichothecenes also causes feed refusal, vomiting, skin dermatitis, immunological problems, growth retardation, reduced ovarian function, reproductive disorders, and hemorrhagic lesions.[27,73] Trichothecenes show different levels of toxicities in different organisms. As an example, T-2 toxin is among the most toxic trichothecenes in mammals and *Arabidopsis*, but in wheat for example, DON is more phytotoxic than T-2 toxin.[74,59] DON displayed higher toxicity in *Arabidopsis* in comparison to NIV, but NIV has been shown to be more toxic in mammals.[74]

Because fungi are capable of producing several toxins simultaneously, it is often difficult to assess what the net toxicity of such a mixture is.[75] For example, *F. graminearum* may produce NIV, fusaranon-X (FX), DON, acetyl–DONs and ZEN, as well as a range of secondary metabolites with unknown biological effects.[75]

Toxin name	Type	R_1	R_2	R_3	R_4	R_5	R
T-2 toxin	A	OH	OAc	OAc	H	$OCOCH_2CH(CH_3)_2$	
T-2 triol	A	OH	OH	OH	H	$OCOCH_2CH(CH_3)_2$	
T-2 tetraol	A	OH	OH	OH	H	OH	
Neosolaniol (NEO)	A	OH	OAc	OAc	H	OH	
HT-2 toxin	A	OH	OH	OAc	H	$OCOCH_2CH(CH_3)_2$	
Fusarenon X (FX)	B	OH	OAc	OH	OH	=O	
Deoxynivalenol (DON)	B	OH	H	OH	OH	=O	
3-acetyl DON	B	OAc	H	OH	OH	=O	
15-acetyl DON	B	OH	H	OAc	OH	=O	
Nivalenol (NIV)	B	OH	OH	OH	OH	=O	
Trichodermin	B	H	OAc	H	H	H	
Crotocin	C	H	C-4–O–CO–CH=CH–CH₃	-		7,8-epoxide	
Verrucarin A	D	H		H	H	H	

Figure 15. Chemical structures of some common trichothecenes. This figure was adapted from Wu et al.[74] and Shank et al.[59]

1.2.4.1.1. 4-Deoxynivalenol (DON, vomitoxin)

Deoxynivalenol (IUPAC name 12,13-epoxy-3α,7α,15-trihydroxytrichothec-9-en-8-one) is a mycotoxin belonging to Type B trichothecenes (Figure 16). It is produced mainly by fungal plant pathogens *F. graminearum* (sexual stage: *G. zeae*) and in some geographical areas by *F. culmorum*.[76,77] It is often the most prevalent among *Fusarium* mycotoxins encountered in grain fields.[78] DON is found in different grains, such as wheat, rye, barley and oats.[77] In the 2013 report from the European Food Safety Authority (EFSA), a total of 26,613 independent analytical results were available for DON and its derivatives (3-acetyl deoxynivalenol (3ADON) and 15-acetyl deoxynivalenol (15ADON)) and a plant biotransformation product (deoxynivalenol 3-

glucoside (DON-3-Glc)).[78] The data were collected by 21 EU member states and Norway between 2007 and 2012, and DON was found in 44.6%, 43.5% and 75.2% of unprocessed grains of undefined end-use, food and feed samples, respectively. Even though not the most acutely toxic mycotoxin, it is considered to be the most economically important. Simulations have shown that in the USA alone, annual costs for DON to be 637 million US$ in crop losses of wheat and corn and 18 million US$ in feed losses.[78,79] DON is highly stable and can survive various food processing methods like milling and powdering.[79] The chemical detoxification of DON in solution and in contaminated grains has been successful (by ozone, ammonia, chlorine, hydrogen peroxide, sodium bisulfite, sodium carbonate and chlorine dioxide), but large scale application has been prevented due to either costs, safety concerns, or negative impact on grain quality.[60]
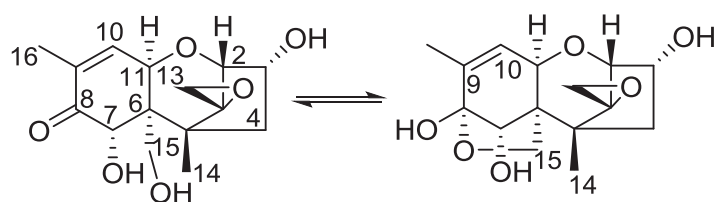
Figure 16. Chemical structure of the mycotoxin deoxynivalenol and equilibrating hemiketal form.

DON is also known as vomitoxin due to its strong emetic effects after consumption as it is transported into the brain and binding to dopaminergic receptors.[80] The ingestion of DON with contaminated feed or food leads to reduced immunity, anemia, headache, nausea, abdominal pain, feed refusal and growth retardation.[60]

DON exerts multiple toxic effects on eukaryotic cells. Although a complete mechanism is still not clear, recent research showed that, with other trichothecenes, DON binds to the A-site of the peptidyl transferase center of the 60S subunit of ribosomes in eukaryotic cells, interfering with protein translation.[69] In mammalian cells, DON targets the innate immune system and activates ribotoxic stress, resulting in upregulation of cytokine gene expression.[81] In plants DON is causes oxidative stress damage, as it increases reactive oxygen species (ROS) levels.[82] Infusion of wheat leaves with DON induced hydrogen peroxide production, followed by cell death,[83] and it has been shown that hydrogen peroxide enhances DON production by *Fusarium*.[84] The formation of polyamines in plants, that becomes a part of the nitrogen metabolism in plants upon the infection with *F. graminearum*, also seems to induce DON production.[78,85]

The toxicity of DON is naturally connected with its chemical structure. It is a polar organic compound, with the molecular formula $C_{15}H_{20}O_6$ and molar mass 296.32 g/mol. It is soluble in polar organic solvents (e.g. aqueous methanol, ethanol, chloroform, acetonitrile and ethyl acetate) and water.[80] DON possesses many structural features that could potentially give rise to chemical

reactivity. One of the characteristic features is an epoxide on C-12,13 (Figure 16). In the 1970s, researchers concluded that the epoxide group in trichothecenes is necessary for the inhibition of the protein biosynthesis.[86,87] The epoxide group is stable under neutral and slightly acidic conditions, and it survives boiling, baking, and steaming at 135 °C, as well as extrusion at 150 °C.[60] DON can be deepoxidized and reduced to an olefin by rumen microflora.[88] Even though its toxicity is closely related with a presence of the epoxide ring, additional molecular features, as the presence of the α,β-unsaturated system, which makes DON prone to Michael addition to the C-9,10 double bond, [84] are also important for their toxicity.[74,89] Fruhman et al., found that 2.1 µM DON reduced in vitro translation by 50%, but that 22.5 µM of the methanethiol Michael adduct of DON was needed in order to obtain the same effect.[89] Other important structural features of DON are C-3 and C-15 hydroxyl groups that can undergo glycosylation or acetylation. It was shown that a DON-3-Glc conjugate does not inhibit *in vitro* translation of the proteins in wheat ribosomes.[74] 3-OH acetylation reduced phytotoxicity of specific trichothecenes in *Arabidopsis*, *Chlamydomonas*, tobacco and rice, but DON and 3ADON demonstrated generally equal phytotoxicity in wheat seedling germination and coleoptile growth inhibition studies.[59] In plate growth tests with yeast, it has been shown that 15ADON demonstrated significant growth inhibition, in contrast to 3ADON.[90] In proliferation experiments on human colon cancer Caco-2 cells, 3ADON was 2-fold less toxic than DON and 15ADON.[91] Because of the proximity of the C-15 hydroxyl group to the C-8 carbonyl group, there is a possibility of intramolecular cyclization to a hemiketal.[63] Hemiketal DON cannot undergo Michael addition of nucleophiles to the 9,10-double bond. Different side groups in DON, their size, polarity and conformation could all affect uptake metabolism and overall biological activity. The structure–activity relationships have been shown to be complex[74] and toxicity in living systems is affected by multiple interactions, as well as intrinsic activity, and the range of toxicity can vary depending on the model system used.

1.3. Xenobiotic transformation – Phase I, Phase II and Phase III metabolism

All organisms are continuously exposed to potentially toxic or adverse chemicals from the environment. Whenever such substances are not naturally produced by the organism itself, or are not expected to be within the organism, they are called xenobiotics. Xenobiotics are mostly of no nutritional value and have no metabolic function. Before they may effectively be excreted, most xenobiotics undergo biotransformation. Generally, there are two types of biochemical biotransformation reactions known as phase I and phase II reactions (Figure 17), according to a concept introduced in 1947 by Roger Williams.[92] Even though the aim of biotransforming xenobiotics is detoxification and elimination, it can also lead to an increase in toxicity. An example is aflatoxin B1 that is activated by phase I enzymes to AFB1-8,9-*exo*-epoxide and AFB1-8,9-*endo*-epoxide.[93] The *exo*-epoxide binds to DNA forming an adduct, and makes the metabolite mutagenic and carcinogenic.[35,93]

Phase I metabolism is present in both animals and plants. It is also called the transformation or functionalization phase, as it usually involves oxidation and reduction reactions, as well as hydrolysis reactions. Most frequent are oxidations of carbon, redox reactions involving carbonyl compounds as products or substrates (oxidation of alcohols and aldehydes, reduction of aldehydes and ketones), oxidation and/or oxygenation of nitrogen atoms, oxidations/reductions at sulfur atoms, and hydrolysis reactions of esters, lactones, amides, lactams, or peptide hydrolysis, as well as hydration of epoxides.[94] These are called "activating" reactions as they may introduce reactive functions on the xenobiotic molecules that could undergo further conjugation, which is part of phase II metabolism.[95,96] Drug metabolizing enzymes (DMEs) play a central role in the elimination and detoxification of xenobiotics. Phase I DMEs consist of many isoenzymes (several hundred variations have been identified), but primarily of the hemoprotein cytochrome P450 family (CYP). It is a superfamily of microsomal mixed function oxidases, abundant in liver, gastrointestinal tract, lung and kidneys.[97,98] They are widely distributed across species and have an extremely broad range of substrate specificities.

If the molecule already contains a functional group (e.g. –COOH, –OH, –NH$_2$, -SH) suitable for phase II metabolism, then the conjugation may proceed without phase I functionalization. Many conjugation processes involve S$_N$2 reaction between an electrophilic nucleoside-containing cofactor (such as acetyl coenzyme A (acetyl–CoA), 3′-phosphate-5′-phosphosulfate (PAPS), uridine diphosphate glucuronic acid (UDP-glucuronic acid), or S-adenosyl methionine) and a nucleophilic functional group (e.g., –OH or –NH$_2$) in the xenobiotic. Phase II reactions are important for transforming xenobiotics to more water-soluble and thus more easily excretable forms.[99] Animals and plants have similar xenobiotic-metabolizing enzymes, but there are also some that are plant-specific.[100] Examples of phase II conjugation reactions include glucuronidation, glucosylation, sulfation, acetylation, methylation, and conjugation with amino acids (such as glycine, glutamic acid, and taurine) as well as glutathione conjugation.

Glucuronidation is the most frequent conjugation reaction in mammals.[101] The glucuronyl donor is UDP-glucuronic acid, and glucuronosyltransferases that are present in the endoplasmic reticulum and cytosol catalyze the conjugation reaction. The glucuronic acid moiety may be attached to oxygen, nitrogen or sulfur groups of the substrates.[102] In plants and insects, the most common conjugation reaction is *glucosylation*, where the glucose donor is UDP-glucose, and the reaction is catalyzed by glucosyl transferases. The conjugated products are usually in the β-configuration.[103]

Sulfation is catalyzed by a family of enzymes called sulfotransferases (SULTs). There are two classes of SULTs that have been identified—the membrane-bound SULTs located at the Golgi apparatus in cells, responsible for sulfation in cells, and the cytosolic SULTs responsible for the metabolism of xenobiotics and small endogenous substrates.[104] The sulfate donor in biological sulfation reactions is adenosine PAPS.[102]

Acetylation reactions are characterized by the transfer of an acetyl moiety, where the donor or the active acetate is acetyl–CoA. The acetyl functional group is introduced to the chemical compound via *N*- or *O*- acetylation.[99] These reactions are catalyzed by acetyltransferases present

in the cytosol of various tissues, in humans particularly in the liver.[102] *N-* or *O-*acetyltransferases catalyze the synthesis of secondary plant metabolites and could also participate in detoxification of xenobiotis.[100] In higher plants, xenobiotic glucosides can undergo further transformation by *malonylation*. This is catalyzed by malonyltransferases that use malonyl-CoA as a donor catalyzing transacylation in a range of phenolic and naphthol glucosides.[100]

Methylation is a common, but generally minor pathway for xenobiotic biotransformations. It is a more often observed biotransformation pathway for small endogenous compounds, but also plays a role in the metabolism of macromolecules like nucleic acids. Compounds can undergo *N-*, *O-*, *S-* and arsenic methylation catalyzed by enzymes called methyltransferases, employing *S-*adenosylmethionine as the methyl donor.[99,102]

Amino acid conjugation reactions are a route of metabolism of xenobiotic carboxylic acids. The enzymes of conjugation reside in mitochondria. Mechanistically, it differs from the other conjugation reactions. It involves initial activation of the carboxylic acid moiety with ATP, generating an acyl adenylate and pyrophosphate. Bound acyl adenylate reacts with coenzyme A (CoASH) to yield a high energy xenobiotic-CoA thioester intermediate that will link the activated acyl group to the amino group of the acceptor amino acid with regeneration of CoASH.[105]

Glutathione conjugation involves conjugation of the tripeptide glutathione with a xenobiotic that is enzymatically catalyzed by glutathione transferases. The detoxification pathway of xenobiotics via glutathione is discussed in more detail below.
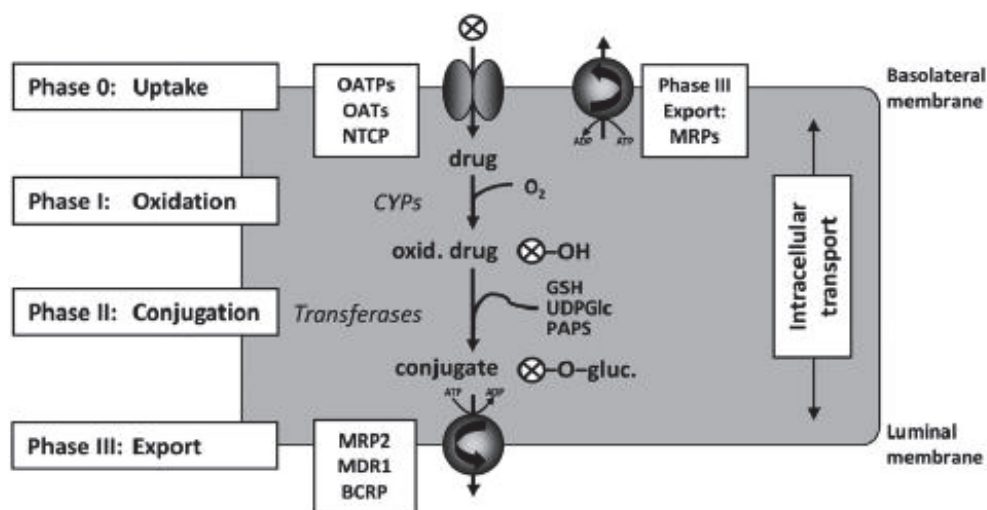
Figure 17. Sequential steps in xenobiotic elimination by metabolism and membrane transport in the liver.[106] Reprinted with journal permission.

The biologically inactivated, water-soluble conjugates formed during phase II biotransformation are not able to penetrate the phospholipid membrane barrier and have to be exported from the

cytosol by membrane-located transport proteins. This process is known as phase III biotransformation, also called the compartmentation phase in plants.[96] In this process, conjugated metabolites are stored in the vacuole or further modified and deposited in the cell wall.[95] The only mechanism that allows plants to excrete the metabolites efficiently into the environment is root exudation, but it is rather unlikely that toxins produced in shoots would be transported to the roots and exuded.[107] Phase III transporters in humans are expressed in many tissues, including the liver, intestines, kidneys, lungs and brain, providing a barrier against xenobiotic penetration, acting as the major determinants of the systemic bioavailability of many xenobiotics.[108] Phase III transporters belong to a main cluster of transporter families—the ATP binding cassette (ABC) carriers that operate as pumps at the expense of ATP splitting. They perform the final step of xenobiotic excretion into fluids, such as feces, urine and bile.[106] Some of the most important transporters are the GS-X pumps, named multidrug resistance-associated protein 1 (MRP1), transferring mostly glutathione and glucuronide conjugates,[109] and P-glycoprotein 1 (P-gp) with broad substrate specificity, largely contributing to the blood–brain barrier.[110]

1.3.1. Glutathione, its role in detoxification and metabolism of xenobiotics in plants and animals
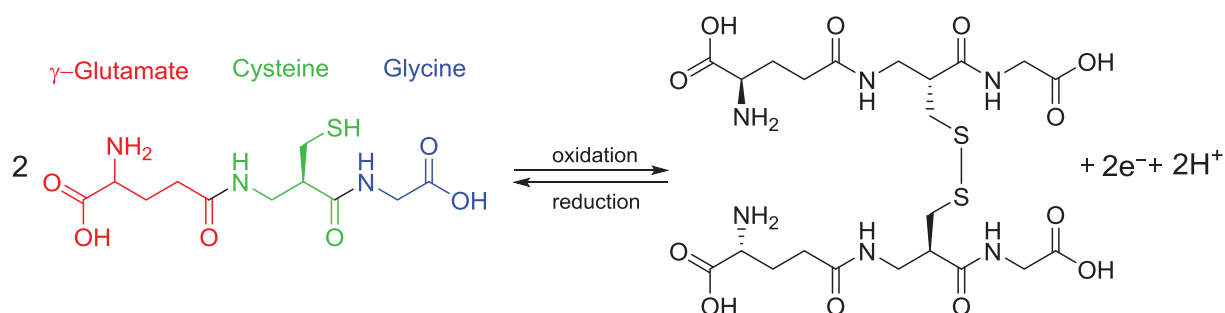
Figure 18. Chemical structure of glutathione and its oxidized form, glutathione disulfide (GSSG).

Glutathione (γ-glutamyl-cysteinyl-glycine) (Figure 18) is a tripeptide and the most abundant thiol in almost all aerobic species, occurring at intracellular concentrations of 0.5 to 10 mM, and 3-4 orders of magnitude lower extracellularly.[111] Some plant taxa contain glutathione homologues in which glycine is exchanged by a different amino acid at the C-terminal residue (like homoglutathione, γ-glutamyl-cysteinyl-β-alanine, which is found in many legumes, or hydroxymethylGSH; γ-glutamyl-cysteinyl-serine found in cereals).[112]

In both plants and animals, GSH is synthesized from the three amino acid precursors in an ATP-dependent two step reaction.[111,112] While the synthesis in animals happens only in the cytosol,[111] the first step of synthesis in plants takes place in plastids and the second step occurs in the cytosol.[112]

GSH possesses a variety of important physiological and metabolic functions in all mammalian and plant cells, probably the most important being the detoxification of free radicals via redox reactions and of electrophilic compounds via conjugation reactions.[111] GSH can be oxidized to GSSG (Figure 18). In its reduced state, the thiol group in GSH donates an electron (in the presence of the enzyme GSH peroxidase) to unstable molecules such as reactive oxygen species, thereby reacting with another molecule of GSH and forming the oxidized form glutathione disulfide (GSSG).[111]

Xenobiotics that are especially harmful to all organisms are those containing electrophilic sites, as they can exert toxic effects by covalent binding to nucleophiles. Different electrophilic reagents react preferentially with different nucleophilic sites. A qualitative way of describing the ease of polarization of the electrophilic/nucleophilic center can be explained by the concept of hard and soft electrophiles/nucleophiles. Hardness and softness are described in terms of polarizability, i.e., the ease with which electron density can be displaced and delocalized to form new covalent bonds. Soft electrophiles/nucleophiles can be polarized with a low positive/negative charge, and hard electrophiles/nucleophiles are highly polarized and have high positive/negative charge in the electrophilic/nucleophilic center. Sulfur has a large atomic radius so that its valence electrons are relatively far from the nucleus and, as such, are highly polarizable. Upon ionization of the thiol, the consequent expansion of the anionic cloud yields the relatively soft thiolate nucleophile. Toxic electrophiles react preferentially with biological targets of similar hardness or softness. The α,β-unsaturated carbonyls can be viewed as soft electrophiles that cause cytotoxicity by selectively forming adducts with soft nucleophilic anionic thiolates.[96,113] The softest cellular nucleophilic site is the non-bonded pair of electrons in the sulfur atom of cysteine residues. As shown in Figure 19, conjugation between GSH and soft electrophiles can be spontaneous or undergo glutathione S-transferase (GST) catalysis. In contrast, the reaction with hard electrophiles requires GST catalysis.[96]
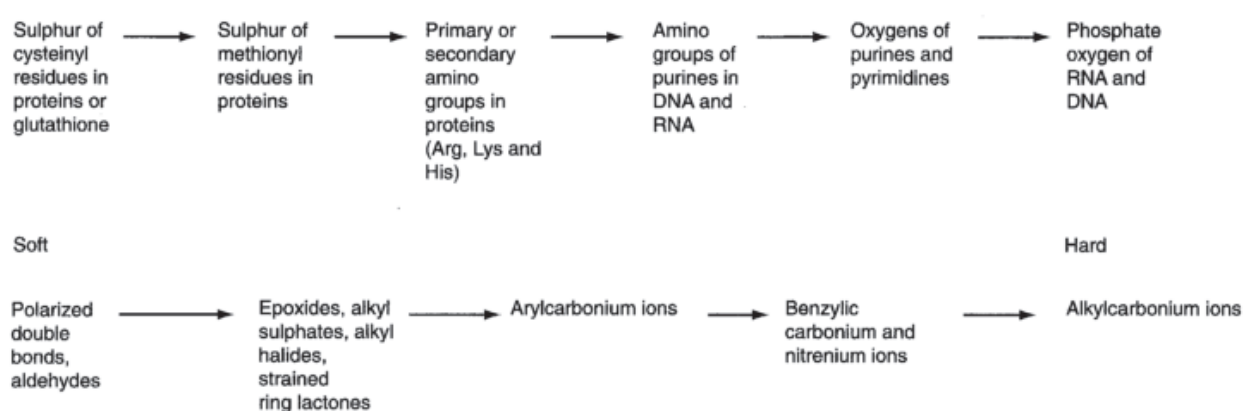
Figure 19. Diagram summarizing nucleophilic sites in cellular macromolecules (top) and electrophilic sites in xenobiotics (bottom) arranged in order of increasing hardness.[96] Reprinted with journal permission.

Biodegradation of glutathione conjugates differs in animals and plants. In animals (Figure 20) the biodegradation occurs extracellularly. The *N*-terminal cysteinyl moiety in GSH is *γ*-linked to the carboxyl group of glutamate instead of the more common *α*-carboxyl peptide linkage, making GSH resistant to intracellular degradation. The membrane-bound enzyme γ-glutamyl transpeptidase (γGT) is the only enzyme that removes the γ-glutamyl moiety from the GSH under physiological conditions. The first sequential breakdown products of GSH-conjugates are glutamate, then glycine, which is removed by dipeptidases. Both of the amino acids can later on be used for GSH synthesis.[111] The corresponding cysteine-conjugates can either be acetylated intracellularly at the amino group by *N*-acetyltransferases to form mercapturic acids (*N*-acetylcysteine *S*-conjugates) or cleaved by β-lyase (usually present in liver and kidneys) to a mercaptan.[114]
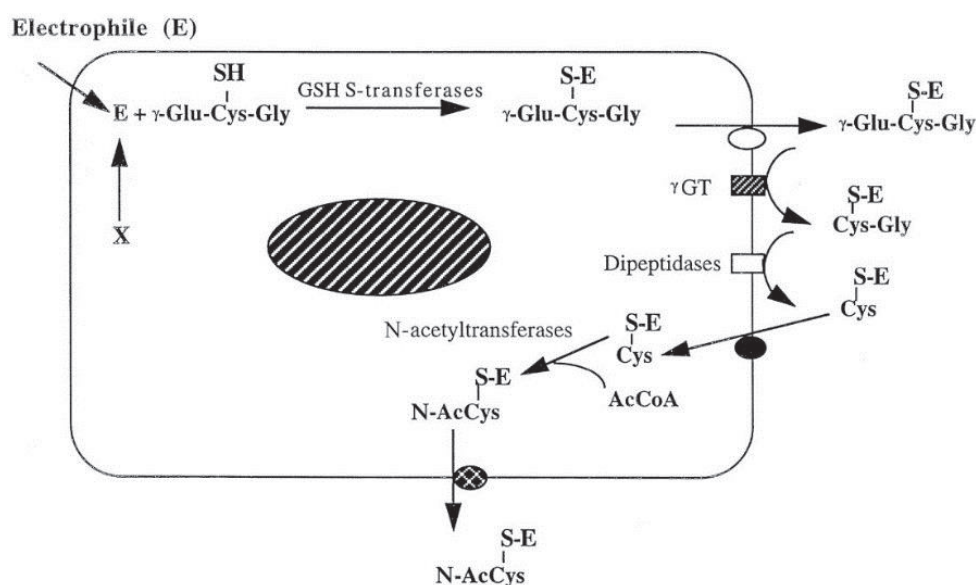
Figure 20. Metabolic reactions and transport steps in mercapturic acid biosynthesis in mammals. The GSH-conjugate is made intracellularly and then transported out of the cell for subsequent degradation. The resulting Cys-conjugate is transported back into the cell and *N*-acetylated to form mercapturic acid. Ac, acetyl; CoA, coenzyme A; Cys, cysteine; E, electrophile; Glu, glutamate; Gly, glycine; S-E, thiol-conjugated electrophile; SH, sulfhydryl group.[111] Reprinted with journal permission.

In plants, GSH conjugation happens in the cytosol followed by transport into the vacuoles via ATP-dependent transporters (Figure 21). There, the conjugates are metabolized to Cys-conjugates, whose further fate is species- and xenobiotic-dependent and may include cleavage to a mercaptan by β-lyase or formation of *N*-malonylcysteine conjugates.[115] *N*-malonyl conjugates can possibly undergo further decarboxylation to *N*-acetylcysteine conjugates, and although rare, a second *S*-glutathionylation.[116] Other enzymes, e.g. *N*-acetyltransferases or *O*-acetyltransferases,

catalyzing synthesis of secondary plant metabolites, could also participate in detoxification of xenobiotics in plants, but no direct evidence has been found so far.[100]
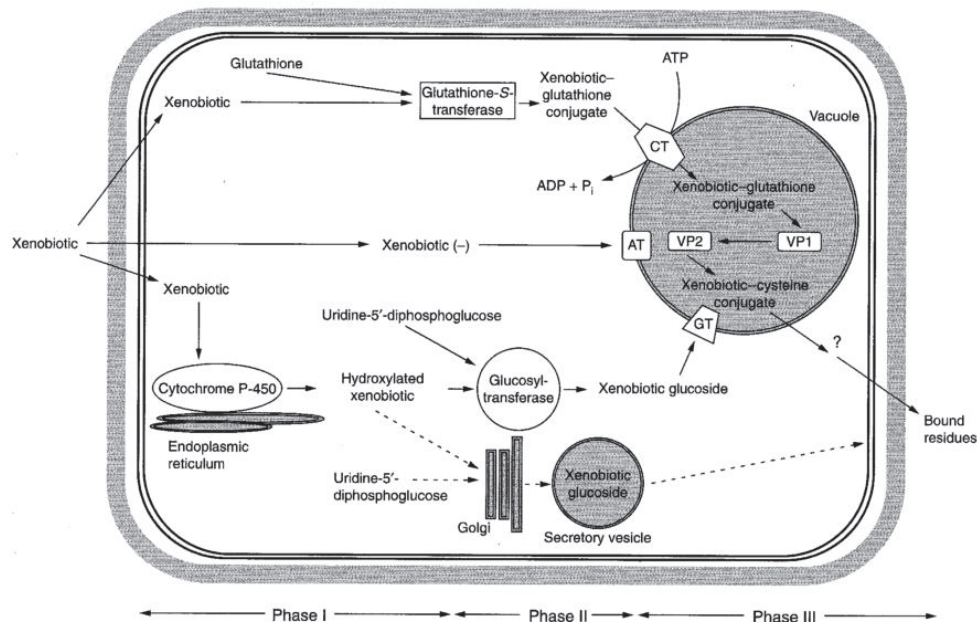
Figure 21. The formation of GSH–xenobiotic conjugates in plants happens in the cytosol. Conjugates are subsequently transported into vacuoles where they are further degraded.[96] Reprinted with journal permission.

1.3.2. Glutathione *S*-transferases (GSTs)

Glutathione *S*-transferases are a family of multifunctional proteins that play important roles in cellular protection against oxidative stress and xenobiotic metabolism. GSTs catalyze a large number of reactions including nucleophilic aromatic substitutions, Michael additions, isomerations, reduction of hydroperoxides, and conjugation of many hydrophobic and electrophilic compounds with reduced glutathione.[99] In animals, GSTs in the liver and other organs play a well-documented role in detoxifying toxins, oxidative stress response and an essential role in biosynthesis of inflammatory mediators-leukotrienes. In plants, these roles are not that clear, i.e. next to detoxifying toxins by conjugation, some classes of GSTs play a role in the transport of flavonoids to vacuoles as well as in stress metabolism, where GSTs act as a glutathione peroxidase, or in primary metabolism where it isomerases maleylacetoacetate.[117] In mammals, GSTs have mostly been described in the cytoplasm, but they are also present in mitochondria and peroxisomes.[99] Biochemical and immunological investigations in plants also

localize GSTs mostly in cytoplasm, but there are some classes of GSTs present in plastid or mitochondria, and a limited number of reports discuss nuclear and extracellular GST.[118]

GSTs have been divided into eight classes: tau, phi, theta, zeta, lambda, EF1Bγ, dehydroascorbate reductase (DHAR), and tetrachlorohydroquinone dehalogenase. Among these, phi, tau, DHAR, and lambda GSTs are specific to plants.[119]

GSTs are soluble proteins structurally composed of two polypeptide units, with typical molecular masses of around 50 kD and an isoelectric point in the pH range 4–5.[117] Each subunit contains a part called H-site that is structurally variable responsible for accepting a wide range of hydrophobic cosubstrates of diverse chemistries. Another site is the G-site, an independent catalytic site specific for GSH formed from a conserved group of amino-acid residues indicating that the binding and correct orientation of glutathione is of central importance. The G site also facilitates the ionization of the thiol group of GSH to produce a more reactive thiolate anion through hydrogen bonding with adjacent hydroxyl groups. The effect of hydrogen bonding is to reduce the dissociation constant (pK_a) of the thiol. In mammalian alpha, pi and mu GSTs this function is performed by tyrosine residues and by serine residues in plants.[117]

1.4. Masked mycotoxins

Agriculturally relevant plants, either in the field or after the harvest and during storage, are often exposed to mycotoxin-producing fungi. Those mycotoxins may be biotransformed by plant metabolism, especially in highly metabolically active field plants.[120] *Fusarium* fungi are field fungi, in contrast to fungi of the genera *Aspergillus* and *Penicillium*,[121] and their mycotoxins (e.g. NIV, DON, ZEN, T2-toxin, HT-2 toxin, fumonisins) are the most prominent targets for conjugation.[120] However, the biotransformation of other mycotoxins (ochratoxin A, patulin) in plants has also been described. The purpose of such biotransformation in plants is the biological inactivation of toxic foreign compounds, often by conjugation reactions. However, such toxin conjugates could potentially be released from the plant matrix or deconjugated in the digestive tract of mammals.[120] Furthermore, food processing, as well as microorganisms used in fermentation processes in manufacturing of beer, wine, fermented sausages or mixed pickles can also chemically alter mycotoxins.[107] Mycotoxins may also covalently or non-covalently bind to polymeric carbohydrate or protein matrices.[122]

The major problems arising from the presence of such conjugated or bound mycotoxins is the present lack of data on their occurrence and toxicity as well as the fact that these conjugates or modified forms are not detected with conventional analytical methods. For those reasons, they are often referred to as "masked mycotoxins". The attribute "masked" was originally referring merely to analytical issues, and no underlying structures or origins were supposed. The problem is that the term "masked" and several different terms like "hidden", "conjugated" and "bound"

are used ambiguously in the literature. In 2011, the International Life Science Institute (ILSI) adopted the definition of masked mycotoxins as *derivatives whose structure has been changed in plants and are not detectable by conventional analytical methods*.[123] Berthiller et al. tried to further differentiate masked mycotoxins into extractable and bound (non-extractable) and the latter group further into covalently and non-covalently attached to polymeric carbohydrate or protein matrices.[107] However, analytical methods evolved rapidly and nowadays some masked mycotoxins are detected in routine analyses and are no longer "masked" according to definition. Rychlik et al. proposed a new, systematic definition based on hierarchic levels.[123] The first level would be modified mycotoxins. The second level of categorization is based on the way they were modified: biologically and chemically modified mycotoxins. The third level of biologically modified is to functionalized (phase I-metabolites) and conjugated (phase II-metabolites), and third level of chemically modified is differently, thermally and non-thermally formed. The fourth level is merely dividing conjugated forms according to where the conjugation happened – in animals, fungi or plants. Masked mycotoxin is now a term used exclusively for plant conjugates.[123]

The most commonly used analytical methods in mycotoxin determination vary from chromatographic methods, which nowadays are frequently combined with mass spectrometers (MS), to immunochemical methods. Depending on the cross-reactivity of the antibodies with different mycotoxin conjugates, immunochemical methods may recognize modified mycotoxins together with the parent mycotoxin, unlike chromatographic methods that are ideally supposed to resolve each compound.[107]

1.4.1. Masked and modified DON

The scientific interest in masked mycotoxins began after several mysterious cases of mycotoxicoses in the 1980s in which symptoms in affected animals did not correspond to the low mycotoxin content detected in their feed.[120] In 1983, Miller and Young proposed metabolic biotransformation of DON to less toxic derivatives in field corn inoculated with *F. graminearum*, as the concentration of DON increased and then declined.[124] It was speculated for some time that the main plant metabolite of DON is a DON-glucoside, but the discovery of deoxynivalenol-3-β-D-glucopyranoside (DON-3-Glc) lasted until 1992, when Sewald et al. isolated the molecule as a main biotransformation product in maize cells after DON treatment.[125] DON-3-Glc was later shown to occur in naturally contaminated cereals,[126] and a correlation between the susceptibility of field grain to *Fusarium* head blight (FHB) and the DON-3-Glc /DON ratio in agricultural crops was found.[127] Once DON-3-Glc became commercially available as analytical standard, its concurrent presence with DON in cereals has been manifested.[128-130] *In vitro* studies that examined the metabolism of DON and DON-3-Glc by human intestinal microbiota showed that DON can be released from its glycosylated form.[131,132]

Glycosylation is a major detoxification pathway in plants; however, DON conjugates of other polar substances have also been identified. *In vitro* formation of DON–GSH conjugates and upregulation of gene transcripts encoding GSH-*S*-transferase and cysteine synthases in DON-treated barley were reported.[133] Flowering wheat ears were inoculated with a mixture of DON and ^{13}C labelled DON and untargeted screening using liquid chromatography high resolution mass spectrometry revealed eight new biotransformation products tentatively identified as: DON–GSH, DON–Cys, DON–CysGly, "DON−2H"-*S*-glutathione (lacking two protons relative to DON–GSH), DON–dihexoside, 15-acetyl DON-3-*O*- β-D-glucoside and DON malonyl-glucoside.[134,135] Other recently found conjugated forms in wheat are DON-3- and -15-sulfates.[136]

Modified forms of DON can also be found in the producing fungi themselves. Most relevant fungal conjugates of DON are 3-acetyldeoxynivalenol (3ADON) and 15-acetyldeoxynivalenol (15ADON) (Figure 22). They both arise from a common precursor (3,15-diacetyldeoxynivalenol) and are both biosynthetic precursors of DON.[122] The route to specific product is dependent on genetic or environmental conditions. The chemotype distribution is changing, and recent studies showed that in North America and the Russian Far East, the 3ADON chemotype has been increasing and substituting the 15ADON type.[90] Depending on the allele of the carboxylesterase Tri8, either the C-15 or C-3 acetyl group is removed from the precursor.[137]

In several animal species, the intestinal biota may hydrolyze DON-acetates and reduce the epoxy-group in DON. Deepoxy-DON (Figure 22), which is a nontoxic metabolite of DON, was found in feces of cow,[138] sheep,[139] pig[140] and rat.[141] A deepoxy metabolite has also been identified in rat urine as the result of the metabolism of gut micro-organisms.[142] However, analysis of rat urine samples showed that DON-glucuronide was the major metabolite of DON.[143] Rats were given a single dose of [^{14}C]DON, and the distribution of DON in body fluids was followed over 72 h. A total of 37% of the administered DON was found in the urine after treatment with β-glucuronidase. In the same study, DON was for the first time reported as a urinary biomarker for DON-exposure, as it was detected after enzyme treatment of urine samples collected from female inhabitants in China.[143] In later metabolism studies of DON, Turner et al.[144] examined urinary metabolite profiles in 34 UK adults. Urine samples were previously analyzed for total DON, and were subsequently re-analyzed following enzymatic hydrolysis to indirectly determine the amount of DON-glucuronide to be in the range 85–98% of total DON. It was at that time not known which isomers of DON-glucuronides were formed, as there was one major metabolite detected in human urine, and two in rat urine using LC–MS/MS.[142] The major products from the incubation of DON with rat and human liver microsomes later identified DON-3-*O*-β-D-glucuronide and DON-15-*O*-β-D-glucuronide (Figure 22) as the most important conjugation products in these two species, respectively.[145] The chemical structure of a third minor isomer detected in rat liver microsomes was identified as DON-8-*O*-β-D-glucuronide in ketal form (Figure 22).[145] Because of the high excretion rate of DON in urine (average 72%), it can be concluded that excretion via feces is not the main detoxification route in humans.[146]

Schwartz et al. reported high recoveries of DON-, deepoxy-DON- and DON-3-Glc-sulfonates in feces and relatively low recoveries in urine of rats exposed to DON and DON-3-Glc, suggesting the formation of sulfonate conjugates of DON in the gastrointestinal tract.[147] Analysis of excreta and chyme samples in feeding trials with turkeys, chickens, pullets and roosters identified DON-3-sulfate (Figure 22) as the major DON metabolite in studied poultry species.[148] DON-sulfates were also recently detected in a human urine as a minor biotransformation product.[149]
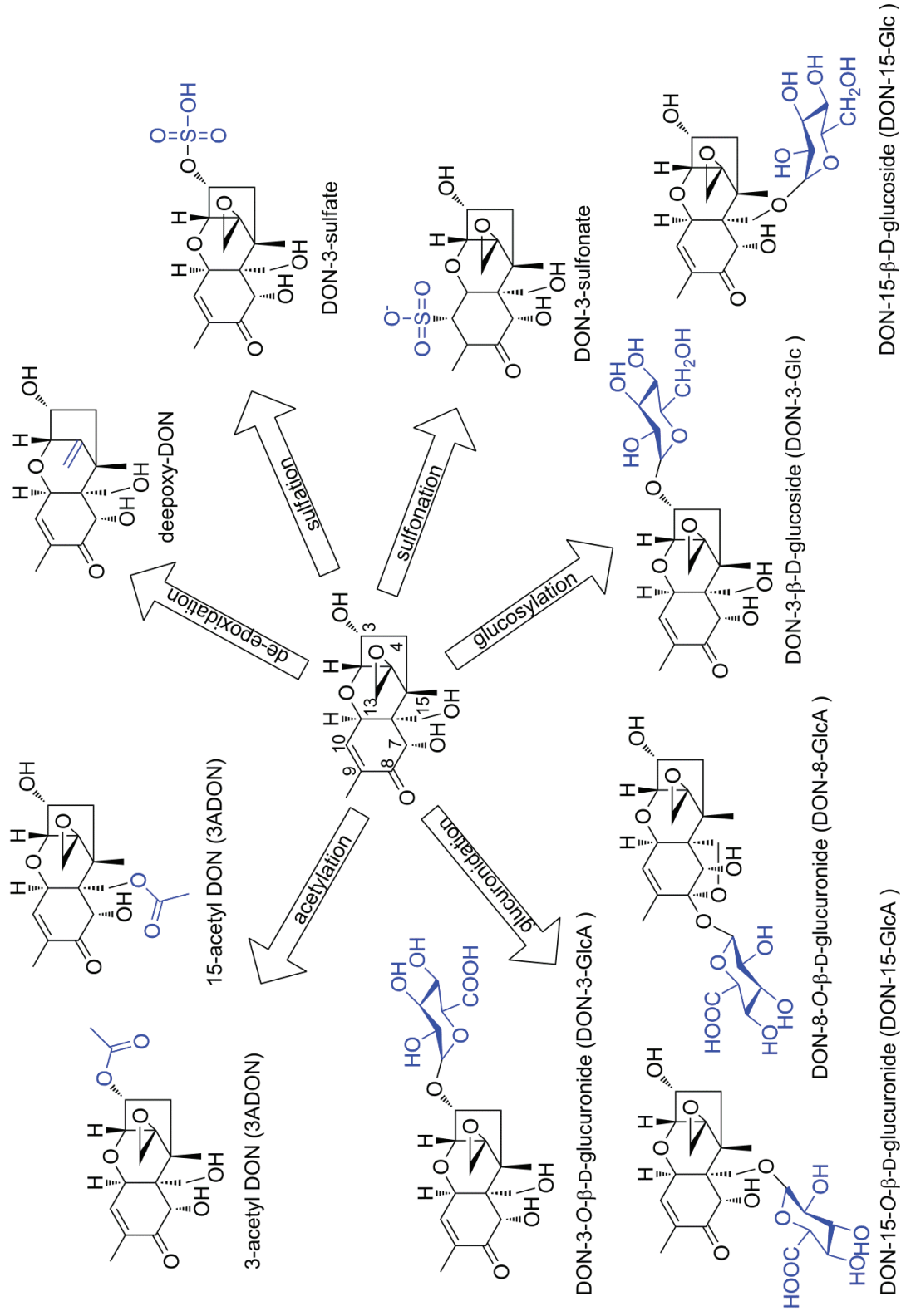
Figure 22. Chemical structures of some DON-conjugates. Adapted from Ran et al.[150]

30

The distribution constant, log D, of DON is −0.97 at pH 7, suggesting a polar behavior.[151] The presence of an acetyl moiety (3ADON and 15ADON) or the absence of an oxygen atom (like in deepoxy-DON), results in the decrease in the polarity (log D values are less negative compared to DON). On the other hand, the presence of a glucoside or a glucuronide moiety, DON-3-Glc, DON-3-GlcA, deoxynivalenol 15-glucuronide (DON-15-GlcA) leads to a polarity increase compared to DON. This increase or decrease in the polarity of DON metabolites may affect the ability to enter cells and be absorbed by the intestine and cause cell toxicity.[151]

Food processing, such as heating or fermentation, can also alter the chemical structure of DON. Bretz et al.[152] heated DON at various temperatures with several model compounds simulating typical food constituents. The degradation products were purified and characterized (Figure 23). Various cereal-based food samples were subsequently analyzed for those compounds and they were detected in 29–66% of the samples. Another study investigating the fate of *Fusarium* toxins, including DON, during malting of barley and brewing demonstrated a significant increase in DON and DON-3-Glc.[130] This was explained either by growth of *Fusarium* micromycetes from spores or from hyphae invading the kernels thereby causing the production of additional mycotoxins, or enzymatic degradation of cell walls, membrane-bound proteins and starch depots in kernels during mashing of malt resulting in the, release of DON-3-Glc from insoluble forms. In one of the studies also oligoglycosylated DON with up to four bound hexose units was detected in cereal-based products like malt, beer and breadstuffs.[153]
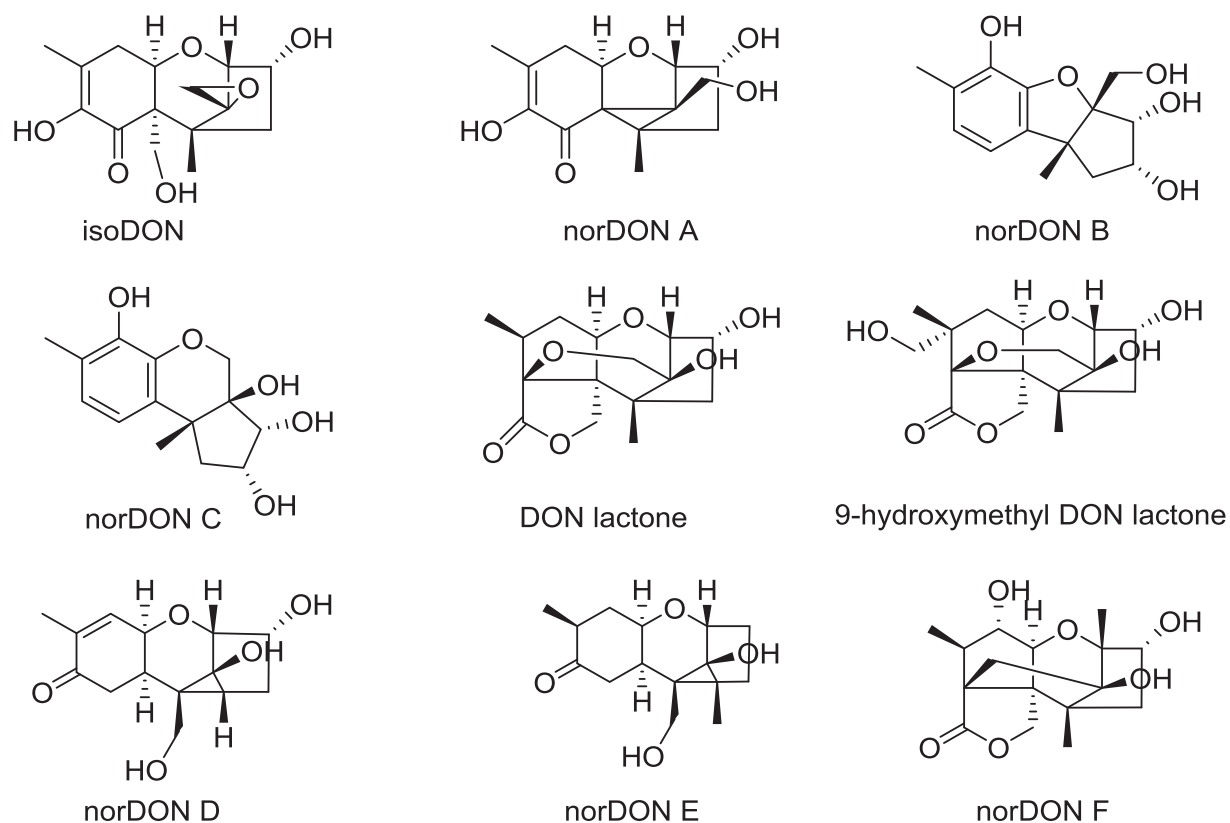
Figure 23. Chemical structures of degradation products of mycotoxin DON in base (norDON A, B and C and DON lactone) and under thermal food processing conditions (all).[152]

Following subchapters (1.5.–1.8.) are included in the current thesis to summarize the knowledge of several general organic chemistry topics that are necessary for better understanding of the observed chemical behavior in the reaction between DON and thiols.

1.5. The chemistry of thiols

Thiols are organosulfur compounds that contain at least one sulfhydryl group (–SH) bound to a carbon. They are also named as mercaptans from Latin *mercurium captāns*, meaning "captures mercury", referring to the fact that thiols readily form heavy-metal derivatives. Most thiols, especially those of low molecular weight, have a strong and repulsive odor. Examples are the defensive secretion of skunks, that contains mostly low-molecular-weight thiols and derivatives,[154] in addition to (*R, S*)-3-methyl-3-sulfanylhexan-1-ol, or specific human volatile thiol, present as a major component in human sweat.[155] Thiols are sulfur analogues of alcohol, but the smaller difference in electronegativity between the sulfur atom and the hydrogen atom

makes the S–H bond less polarized than the O–H bond, leading to diminished propensity to form hydrogen bonds.[156]

Sulfur is found in multiple oxidation states ranging from −2 to +6. This is because it can accommodate more than eight valance electrons due to the additional five unoccupied $3d$ orbitals of relatively low energy that could be used for p-d bonding in a fashion similar to p-p (π) bonding. Sulfur can thus expand its valence shell octet by two (as in sulfoxides) or four (as in sulfones) electrons. Oxidation of a thiol, unlike an oxidation of an alcohol, occurs at the sulfur (Figure 24). Sulfur analogs of aldehydes, ketones and carboxylic acids are known, but they are not simply obtained from oxidation reactions. The most commonly occurring oxidation products of thiols are disulfides and sulfonic acids (RSO_3H). Many thiols spontaneously oxidize to disulfides (RS–SR) merely on standing in air (O_2). When thiols are present together with disulfides in the same solution, they can react with disulfides (RS–SR) through reversible thiol-disulfide exchange reactions. These reactions are occurring alone at appreciable rates, or they can be catalyzed in the living systems by enzymes of the thioredoxin family. Thiols have a high biological relevance due to its wide redox versatility and the fact that many enzymes possessing essential functions contain thiol groups.[157,158] Furthermore, disulfide bonds in proteins help to stabilize their three-dimensional structures. Thiols can react with two-electron oxidants such as hydroperoxides or hypohalous acids yielding sulfenic acids (RSOH). As they are typically unstable, they decay, usually by reaction with another thiol, yielding disulfides. Thiols form highly reactive thiyl radicals (RS$^\bullet$) in single-electron oxidation reactions. The RS$^\bullet$ radicals react with themselves, again forming disulfides or disulfide radical anion (RSSR$^{\bullet -}$) from reaction with another thiol. Thiyl radicals can reduce oxygen to a superoxide radical ($O_2^{\bullet -}$) or react with oxygen to yield peroxyl radicals (RSOO$^\bullet$) that can form oxyacids such as sulfenic, sulfinic (RSO_2H) and sulfonic acids.[159]
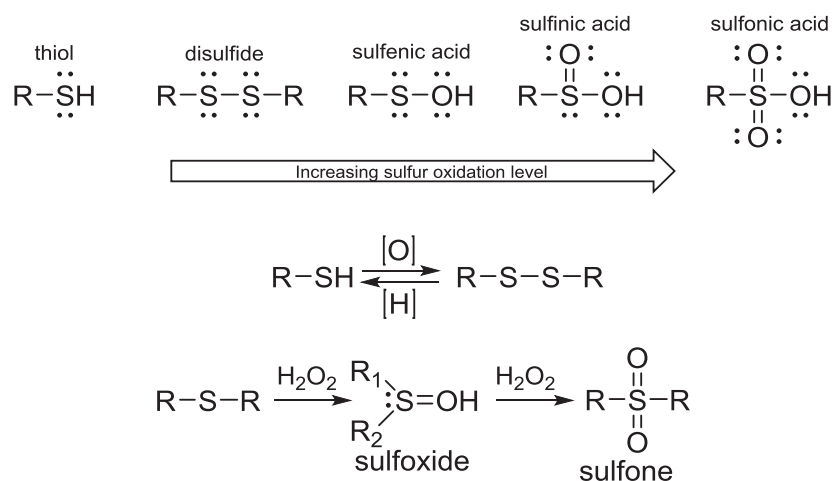
Figure 24. Oxidation of sulfur species.[160]

Many and enzymatic reactions of thiols involve the nucleophilic attack of the ionized thiolate ion (RS⁻) on an electrophile. The protonated form, RSH, and deprotonated form, RS⁻, are in acid–base equilibrium that can be described with the acid dissociation constant, K_a. The value of K_a, that is usually expressed in a logarithmic form, pK_a, is a measure of the acid strength relative to water. The larger the pK_a value, the smaller the extent of dissociation is at the given pH (the weaker the acid is). The pK_a of the acid is the pH where the acid is exactly half dissociated.[161] At the pH that is the pK_a of a thiol, 50% is in the thiolate form (RS⁻) and 50% is in protonated RSH form. The availability of thiolate at a fixed pH depends on the pK_a of the corresponding thiol.[158] The finding by Noda et al.[162] that butyl mercaptans absorb ultraviolet light in a strongly alkaline solution, but not in a strongly acidic solution, suggested a means of measuring the concentration of the RS⁻ form spectrophotometrically. The pK_a of a thiol thus could be determined by plotting the UV absorbance as a function of pH. The dissociation constants of individual thiols vary over a wide range (pK_a 6.5–10).[163] As a general rule, the observed rate constants for nucleophilic reactions involving thiols increase with increasing pH because relatively more thiolate is available at a higher pH.[159] The thiolate group can participate in reactions with electrophilic reactive species either via nucleophilic substitution or addition reactions to form covalent adducts.[158] The pK_a values of the important natural thiols cysteine and glutathione have been determined to be 8.2 and 9.1, respectively.[156] In general, thiols are considered as weak acids, but the protein microenvironment can dramatically influence their pK_a values. The presence of a positively charged residue, such as lysine or arginine, as well as the formation of a hydrogen bond, may increase thiol acidity by 3–4 orders of magnitude. In cysteines, a thiolate side chain becomes a stronger nucleophile and readily reacts with oxidants and electrophilic species, although interactions with specific residues or metals can also stabilize the thiolate form. The cysteine thiol group plays a key biological role in catalysis and serves as an important site for many posttranslational modifications.[156]

1.6. α,β-unsaturated carbonyl and Michael addition

The conjugated arrangement of C=C and C=O bonds endows α,β-unsaturated carbonyl compounds with unique reactivity.[160] Conjugation of a double bond to a carbonyl group transmits the electrophilic character of the carbonyl carbon to the β-carbon of the double bond (Figure 25).
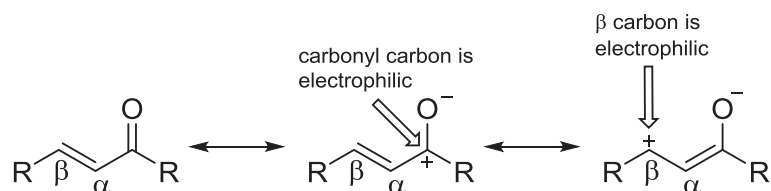
Figure 25. Resonance structure of an α,β-unsaturated carbonyl compound. Carbonyl group and β-carbon have a positive charge, making them susceptible for the nucleophilic attack.[164]

If the nucleophilic attack happens to the double bond in an α,β-unsaturated carbonyl compounds it gives a resonance-stabilized enolate ion intermediate (Figure 26) that can be protonated on either oxygen or carbon.
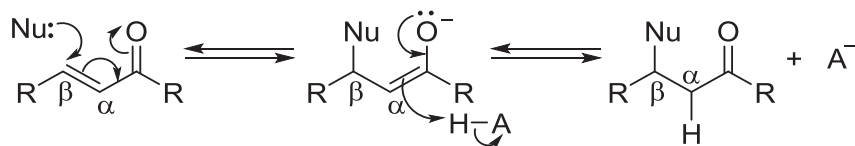
Figure 26. Nucleophilic attack at the β-carbon producing an enolate intermediate. The intermediate collapses and the α-carbon gets protonated. This type of reaction is called conjugate addition or Michael addition.[164]

In either case, the carbonyl group is eventually regenerated and the overall result of the reaction is net addition to the double bond. This type of reaction is called conjugate addition or a Michael addition. A nucleophile is also called a "Michael donor" and an activated electrophilic olefin is the "Michael acceptor", and the product is a "Michael adduct". The Michael addition is generally considered as addition of enolate nucleophiles to activated olefins, but a wide range of functional groups, such as amines, thiols, and phosphines, possess sufficient nucleophilicity to perform as Michael donors.[165]

If the nucleophile is a weak base, Michael addition is a reversible reaction. The reverse reaction is called β-elimination (Figure 27), and the mechanism is called E1cb, where "E" stands for elimination, the numeral "1" refers to the fact it is a stepwise reaction with first order kinetics, and "cb" refers to the intermediate, which is the conjugate base of the starting compound.[160]
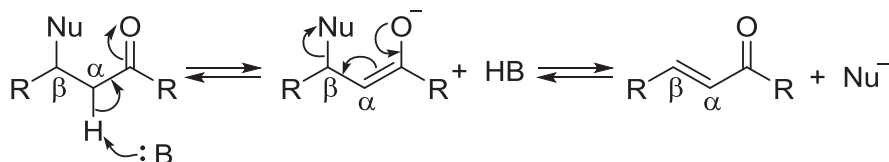
Figure 27. The mechanism of β-elimination.[164]

Because both the addition and the elimination reactions proceed through a resonance-stabilized carbanion intermediate, the carbonyl group has to be located in an appropriate position.

Any Michael addition reaction is competing with the addition to the carbonyl group. Relatively weak bases that give reversible carbonyl-addition reactions with ordinary aldehydes and ketones tend to give conjugate addition with α,β-unsaturated aldehydes and ketones. Michael addition is observed with these nucleophiles because the products are more stable than the carbonyl-addition products. Even if reversible carbonyl addition occurs more rapidly, the conjugate addition can

drain the carbonyl compound from the addition equilibrium and the Michael adduct is formed ultimately. This is a case of kinetic versus thermodynamic control of a reaction. The Michael adduct is thermodynamically favored and the more stable reaction product. This can be explained by considering the bond energies of the C=C double bond versus the C=O bond. The Michael adduct retains a carbonyl group at the expense of a carbon–carbon double bond, and the carbonyl addition retains a carbon–carbon double bond at the expense of a carbonyl group. Because a C=O bond is considerably stronger than a C=C bond, the Michael adduct will be the more stable product. However, if the nucleophile is a stronger base, an irreversible addition to the carbonyl will occur.[160]

1.7. Epoxides and epoxide nucleophilic substitution reactions

An epoxide is a heterocyclic compound with a three-membered ring ether linkage. They are also referred to as oxiranes, α- or 1,2-epoxides.[166] Epoxides possess significant bond angle strain (around 60 degrees, instead of the ideal 109.5 degrees) that causes bonds to be weaker and more easily broken than in ordinary ethers. The strain energy is calculated to be 13 kcal/mole.[166] Therefore, opening of an epoxide ring is a favorable reaction; but the structure of the resulting product depends on the reaction conditions, since both carbons in an epoxide group are electrophilic.

Under acidic conditions, the first step in opening of the epoxide is protonation of the epoxide oxygen. A protonated epoxide is expected to behave similarly to a tertiary carbocation. (Figure 28). The tertiary carbon bears about 0.7 of a positive charge and has a nearly trigonal planar geometry, indicating that there is almost no steric hindrance for the nucleophile.[160] The bond between the tertiary carbon and the epoxide oxygen is unusually long and weak (Figure 28). The protonated oxygen blocks the front side of the carbocation, so that nucleophilic attack must occur from the backside with an inversion of stereochemistry. Thus, this reaction follows an S_N1 reaction mechanism. In unsymmetrical epoxides, with secondary or primary carbons, there is much less carbocation character at either carbon of the protonated epoxide, so acid-catalyzed ring-opening reactions tends to give mixtures of the products.[160]
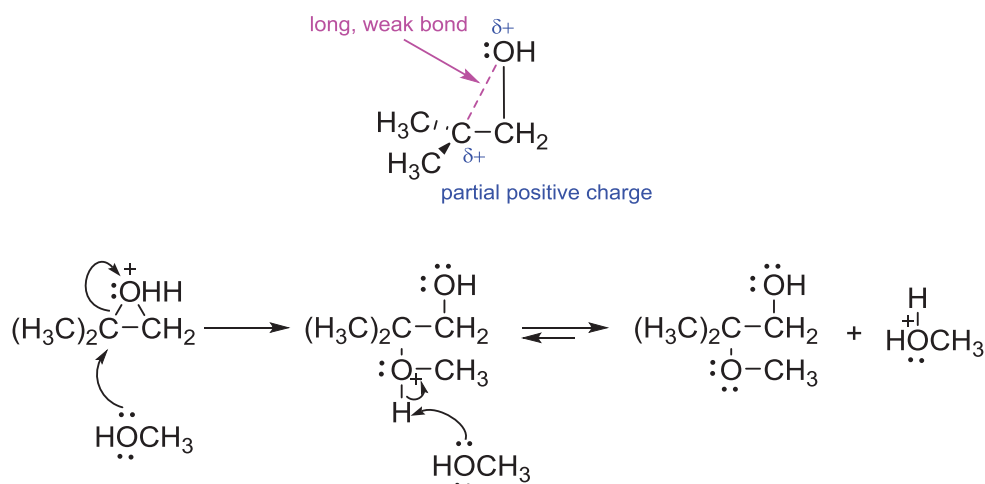
Figure 28. S$_N$1 reaction mechanism of epoxide-ring opening under acidic conditions.[160]

Under basic conditions, the epoxide ring-opening follows an S$_N$2 reaction mechanism with backside addition of a nucleophile on the epoxide carbon. The nucleophile will simply attack the least sterically hindered epoxide carbon (i.e. the one with fewer alkyl substituents). As the bond between carbon and the nucleophile forms, the bond between carbon and the leaving group breaks. In the transition state of the reaction, there are partial bonds between carbon and nucleophile and carbon and the leaving group. The epoxide is opened to form an alkoxide, which then reacts in a Brønsted acid–base reaction with a proton source to give an alcohol (Figure 29).
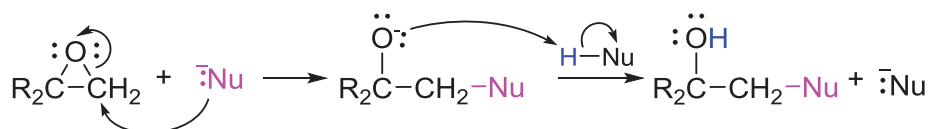
Figure 29. S$_N$2 reaction mechanism of the epoxide-ring opening under basic conditions.[160]

There are several ways to synthetize epoxides, but one common approach involves the direct oxidation of alkenes with peroxycarboxylic acids such as *meta*-chloroperoxybenzoic acid (mCPBA).

1.8. Hemiacetals/acetals and hemiketals/ketals

Hemiacetals and hemiketals are compounds made by the nucleophilic addition of an alcohol nucleophile to a carbonyl group. When an alcohol adds to an aldehyde, the product is called hemiacetal, and when an alcohol adds to a ketone, the product is a hemiketal (Figure 30).
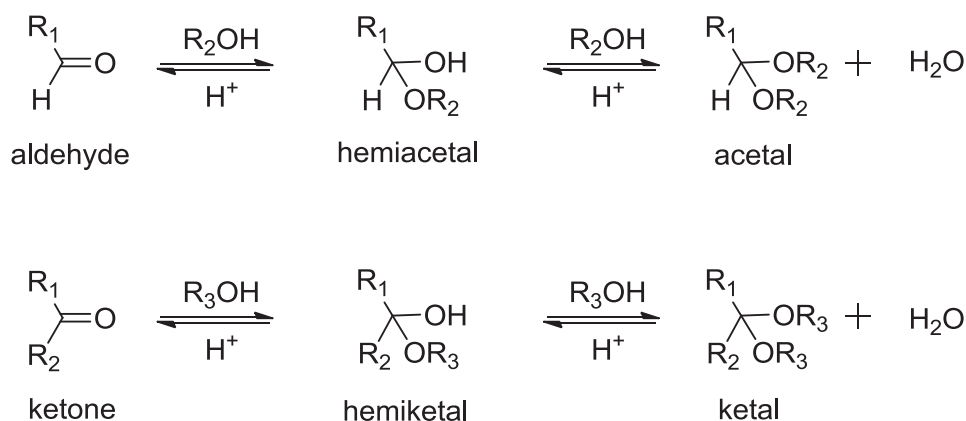
Figure 30. Acetal and ketal formation from aldehydes and ketones.[167]

Hemiacetals and hemiketals may be thought of intermediates in the formation of acetals and ketals. *Hemi* means half, and thus one of the oxygen atoms of the deoxygenated carbon atoms is a hydroxyl, while the other one is an alkoxy group (Figure 29). Acetals and ketals are compounds where two alkoxy groups are linked to the same carbon (geminal-diether derivatives). They are formed when the hydroxyl group of hemiacetals/hemiketals becomes protonated and lost as water. The carbocation that is produced is rapidly attacked by a molecule of alcohol, forming another –OR group on the carbon.[160,161]

Both, hemiacetal/hemiketal and acetal/ketal formation are reversible reactions. The reactions are driven to the products either by the use of excess alcohol or by removal of water. The formation of hemiacetals/hemiketals is catalyzed by both acids and bases. Acidic conditions are increasing the electrophilicity of the carbonyl group via protonation (Figure 31 (top)), while basic conditions work by increasing the nucleophilicity of the alcohol by removing the OH proton before it attacks the carbonyl group. (Figure 31 (bottom)).[161]
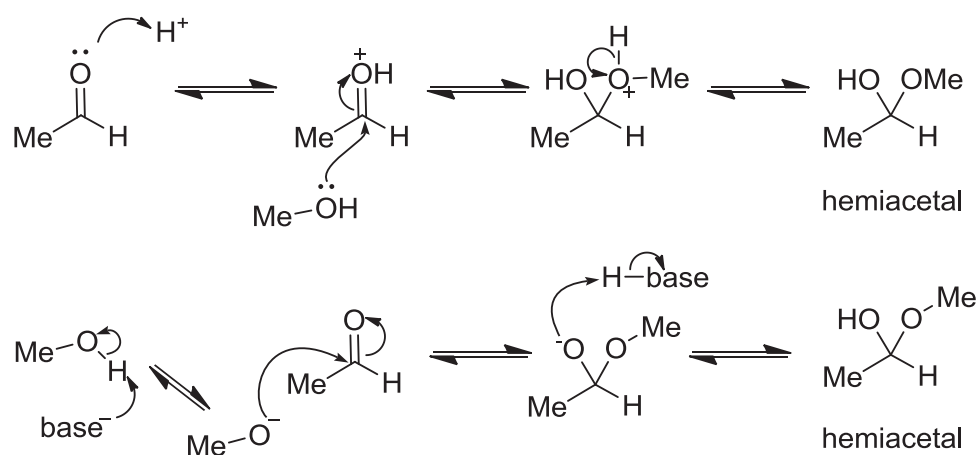
Figure 31. Mechanism of acid-catalysed (top) and base-catalyzed (bottom) hemiacetal formation.[161]

The conversion of hemiacetals/hemiketals into acetals/ketals is only catalyzed by acids. It is important to note that acid can also catalyze decomposition of these compounds, meaning that acid and base catalysts only increase the rate of the approach to equilibrium, but do not change its position.[161]

The hydrolysis of hemiacetals/hemiketals to aldehydes/ketones is catalyzed by acid bases (Figure 32), but the hydrolysis of acetals/ketals to hemiacetals/hemiketals is catalyzed by acids only, making acetals/ketals stable in basic and neutral solution. The reason for the hemi-form to be unstable in base is the fact that base deprotonates the –OH group, allowing the alkoxide to leave. Hemiacetals/hemiketals, in most cases cannot be isolated because they either react further to yield acetals (in alcohol solution under acidic conditions) or decompose to aldehydes or ketones and an alcohol.[161]
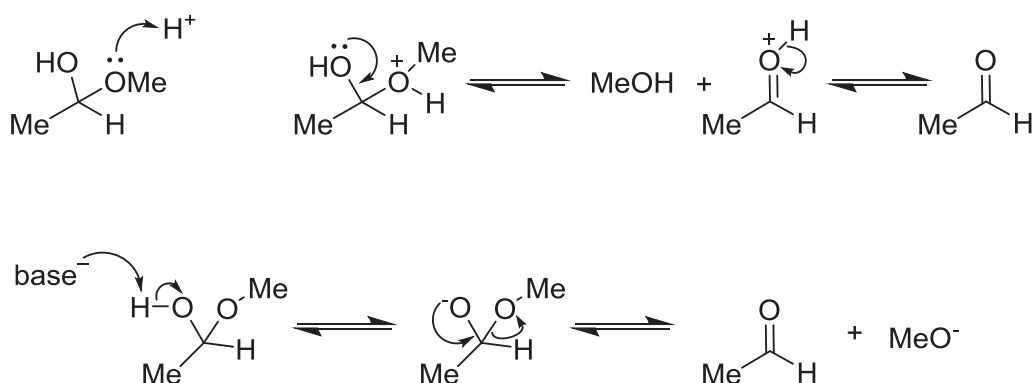
Figure 32. Mechanism of acid-catalysed (top) and base-catalyzed (bottom) hemiacetal decomposition.[161]

When aldehydes or ketones contain a hydroxyl group, they occasionally form intramolecular cyclic hemiacetals or hemiketals. A well-known example of such an intramolecular hemiacetal formation is glucose and other sugars. In aqueous solution, 99% of glucose exists as a cyclic hemiacetal.[168] Cyclic hemiacetals/hemiketals are generally stable, especially if they make a five- or six-membered ring, which implies relatively little strain. Their stability could also partly be explained by entropy, as the formation of an acyclic hemiacetal/hemiketal results in a decrease in entropy, as two molecules are consumed for every one produced.[169]

2. AIMS OF THE STUDY

The biotransformation of the mycotoxin deoxynivalenol (DON) via the glutathione pathway had been reported in DON-treated wheat lines. In these reports, the DON–glutathione (DON–GSH) conjugate and its degradation products DON–cysteinylglycine (DON–CysGly) and DON-cysteine (DON–Cys) were tentatively identified by LC-HRMS/MS. However, DON has several potential reactive sites where thia-addition may occur.

Therefore, the main goals of this study were to:

1. Investigate and gain better understanding of the reaction between DON and model thiols (**Paper I**)

2. Optimize the reaction conditions (**Paper I**)

3. Isolate the products and identify the structures (NMR, HRMS^2) (**Papers I, II, III**)

4. Apply optimized conditions to synthetize biological thiol adducts (**Paper II** and **III**)

5. Quantify the samples and produce analytical standards (**Papers II** and **III**)

6. Investigate the toxicity of the thiol adducts (**Papers I** and **II**)

7. Test if the GSH addition to DON is an enzymatic reaction (**Paper III**)

8. Develop and apply suitable analytical LC–MS methods for thiol adducts of DON (**Papers I, II, III** and **IV**)

9. Investigate occurrence in nature (**Paper IV**)

3. METHODOLOGY

In this research, a diversity of methods was used. Reaction between DON and thiols was monitored with liquid chromatography coupled to mass spectrometry (LC-MS), purification of the products was done using preparative LC-MS or solid-phase extraction (SPE). Products were characterized using LC–MS^n and LC–HRMS/HRMS^2, as well as NMR, and quantified using qNMR ERETIC experiments. The toxicity of the prepared conjugates was assessed in human monocytes using cell proliferation and viability assays and pro-inflammatory cytokine response in human macrophages. Another important step prior to the LC–MS analysis of the biological materials (cells and plant samples) was to determine how to carry out the sample preparation with the proper extraction steps.

Most of the relevant techniques are described below.

3.1. Preparation of the biological samples for LC–MS analysis

Today's modern methods can provide high resolution spectra of complex mixtures of almost every matrix (from gases to biological macromolecules) and detection limits down to femtograms and below, but a prerequisite to a good advanced analysis is a suitable sample preparation. The basic concept of it is to convert a real matrix into a sample in a format suitable for analysis by a separation or other analytical technique.[170] Also, removing the interfering matrix elements (phospholipids, salts, proteins, sugars, nucleic acids) prior to the analysis of biological material with the LC–MS is extremely important because these elements can alter the MS response (ion suppression or enhancement) or co-elute with a target analyte. Cleaner samples therefore not only reduced matrix effects, but also lower limits of detection, improved chromatography and column lifetime, and reduce instrument downtime.[171]

Extraction is one of the oldest sample preparation methods, where an analyte of interest is separated from a sample matrix by solvent (solvent extraction from solids and liquid–liquid extraction from solutions). Selectivity can be obtained by altering the temperature and pressure, by the choice of extraction solvent or liquid and the use of pH and additives.[170]

3.2. Liquid chromatography coupled to mass spectrometry (LC–MS)

Liquid chromatography coupled with mass spectrometry or tandem mass spectrometry (LC–MS/MS) is the most promising technique for simultaneously screening, identifying and measuring a large number of the mycotoxins.[172]

3.2.1. Basic principles of liquid chromatography

Chromatography is a method of separation. The components of a mixture are separated based on the components' relative ability to adsorb and/or partition between the mobile phase and the stationary phase. Depending upon the separation principle and mode of chromatography, the technique is classified into various types. While selecting the chromatographic method for mixture analysis, it is important to think about physical (polarity, molecular mass, density, viscosity) and chemical properties (pH, acidic and basic behavior) of the test substance. Chromatography is based on the partition of molecules or ions between two immiscible phases. In all the chromatographic techniques, the sample is dissolved in a mobile phase (liquid, gas or supercritical fluid). This mobile phase is allowed to run over the stationary phase which is fixed in place on a solid surface (with the exception of countercurrent chromatography). The components of the sample distribute themselves between the mobile and stationary phase to varying degrees—components weakly held by the stationary phase travel rapidly and elute first, and components strongly retained by the stationary phase move slowly and elute later.[173] The chromatographic technique is usually named after the mobile phase (gas chromatography (GC), liquid chromatography (LC), supercritical fluid chromatography). LC is the most commonly used separation technique coupled with mass spectrometry (MS), because unlike GC-MS, it is not limited to the analysis of volatile analytes, it is applicable to analytes with a wide variety of polarities and molecular masses, and derivatization is usually not necessary.[174]

There are several different LC modes: normal-phase liquid chromatography (NPLC), reversed-phase liquid chromatography (RPLC), ion-exchange liquid chromatography (IELC) and size exclusion chromatography (SELC). Except SELC, all of the separations in LC are the consequences of interactions developed between the functional groups of solute molecules, solvent molecules and the functional groups of stationary phase. These interactions could be hydrogen bonding, van der Waals forces and electrostatic forces. In NPLC, the stationary phase (particles of silica gel, alumina or carbon) is more polar than the mobile phase. Silica gel and carbon particles can also be modified covalently with polar groups like aminopropyl, cyanopropyl and diol functional groups. The mobile phase is composed of organic solvents (methanol, ethanol, hexane, ethyl acetate). Solutes are eluted in order of increasing polarity: the retention of solute molecules decreases with increasing polarity of the solvent in the mobile phase.[175]

RPLC is the most frequently used mode in LC. Stationary phases are nonpolar and hydrophobic packings where, most often, silica is covalently modified by octadecyl (C_{18}), octyl (C_8), hexyl (C_6), propyl (C_3), ethyl (C_2), methyl (C_1), phenyl or cyclohexyl functional groups. The mobile phase is more polar than the stationary phase; it is usually water and water-miscible organic solvents such as methanol or acetonitrile. The retention in RPLC arises because water in the mobile phase repels the nonpolar regions of solute molecules and facilitates their interaction with

the nonpolar functional groups of the stationary phase. Solute molecules are eluted in order of increasing hydrophobicity or decreasing polarity.[175]

3.2.1.1. Solid phase extraction (SPE)

SPE is one of the most widely used methods for extraction, changing of solvents, cleanup, desalting, concentration and fractionation of organic compounds from samples. SPE uses the same type of stationary phases as are used in LC columns. The phase is contained in a glass or plastic column above a frit or glass wool. The column might have a frit on top of the stationary phase and might also have a stopcock to control the solvent flow through the column.[176] Commercial SPE cartridges have 1–10 ml capacities and are discarded after use. It is usually used to clean up a sample before using a chromatographic or other analytical method to quantify the amount of analyte(s) in the sample.[176] The basic procedure consists of loading a solution onto a solid phase capable of retaining the target analytes, washing away undesired components and eluting the desired analytes with another solvents into a collection tube.[177]

3.2.2. Sample introduction and ion sources

Even though the analytical potential of combining separation methods like GC and LC with mass spectrometry (MS) was realized a long time ago, the main problem with combining them was the fact that GC and LC are at the atmospheric pressure, utilizing a mobile phase in which the analytes are carried, and MS is a vacuum-based technique. Interfacing LC with MS is more difficult than for GC, because a milliliter of most organic solvents produces ca 1000 milliliters of vapor on evaporation at standard temperature and pressure, which is incompatible with the vacuum requirements of mass spectrometers. Development of atmospheric pressure ionization (API) methods like atmospheric pressure chemical ionization (APCI) and electrospray ionization (ESI), where the solvent removal and sample ionization take place outside the vacuum chamber, finally allowed the coupling of the LC with the MS. Other important API ionization techniques are atmospheric pressure photo-ionization (APPI) and the newer surface ionization techniques, including desorption electrospray ionization (DESI) and direct analysis in real time (DART).[178]

3.2.3. Electrospray ionization (ESI)

All of the processes in a mass spectrometer (focusing, separation and detection) require charged species, ions, because electrically neutral molecules cannot be manipulated using electrical or magnetic fields. That is why after the sample introduction, it is important to convert molecules to ions. ESI is the dominant ionization method, from small molecules to biopolymers. It is a soft ionization technique where the energies involved are barely above those necessary to generate ions. Ions are formed in a charged, nebulized solution of the analyte that flows through a narrow steel tube where it is subjected to a positive or negative high voltage (2–5 kV) with the respect to

the vacuum chamber. The voltage removes ions of polarity opposite to that of the applied voltage, yielding a solution where there is only one charge type. An additional tube coaxial with the one carrying the liquid has a nitrogen flow and it acts as a sheath gas that nebulizes the eluate into a spray of charged droplets. As the droplets are desolvated, the density of the electric field of the droplets increases and they disintegrate, releasing ionized analytes into the gas phase. Disintegration happens when the repulsive Coulombic forces between like charges on the surface of the droplets exceed the forces of surface tension. The evaporation takes place at atmospheric pressure, outside the vacuum chamber and almost all gases derived from the liquid flow are removed outside the instrument.[178]

Ions formed using ESI depend on which and how many acid or basic groups are present in the analyte. Analytes with basic functional groups will be detected better in positive mode as predominantly protonated $[M+H]^+$, or $[M+alkali\ metal]^+$, with sodium being the most commonly observed.[178] Analytes with the acidic groups will be detected better in negative mode, most commonly observed as $[M+H]^-$. As the molecular mass of an analyte and the number of acid/base groups increases, the ionization often leads to the formation of multiply charged ions, $[M+nH]^{n+}$ in positive or $[M-nH]^{n-}$ in negative mode.[178] Depending on the mobile phase additives used for the LC (e.g. acetic or formic acids), formation of acetate ($[M+H]^-$) and formate ($[M+H]^-$) adducts is also common for the analytes that do not possess acidic or basic groups.

3.2.4. Mass analyzers

After the created ions enter the spectrometer, the mass analyzer separates them according to their mass-to-charge ratio (m/z), and to focus and transfer them onto a detector, or into a collision cell. There are several types of analyzers: quadrupole (Q), ion trap (linear (LIT) and cylindrical/quadrupole (QIT)), time-of-flight (TOF), magnetic sector (B), orbitrap and ion cyclotron resonance (ICR) cell. Orbitrap and ICR are so-called Fourier transform instruments. The choice of mass analyzer affects the aspects of data generated, such as mass resolution, mass measurement accuracy and available dynamic range. Analyzers separate ions in time (Q, QIT, LIT and B) or in space (TOF and Fourier transform). Scanning instruments are in-time systems, because the ions are collected successively over a period of time (milliseconds to seconds) and the electric (or magnetic) fields of the analyzer must be continuously varied. Scanning increases the versatility of an instrument, but the cost is reduced sensitivity when collecting spectra due to the limited amount of time spent analyzing a given mass during the collection of the entire spectrum. The in-space analyzers are non-scanning with all ions detected simultaneously (microsecond scale) and spectra obtained without altering the operating parameters of the analyzer. The in-space strategy improves sensitivity when collecting full spectra, but prevents the use of other important techniques (like selected reaction monitoring). However, analyzers can be combined to give tandem instruments (e.g., QqQ, QTOF) that can provide significantly more information than single analyzer systems. Tandem often implies that the instruments utilize like

analyzers, such as in the triple quadrupole (QqQ) system, whereas hybrid instruments combine dissimilar analyzers (LIT-orbitrap).[178]

The work in this thesis was carried out by using ESI as the ionization method, and depending on the type of data sought, different mass analyzers were used. Reaction monitoring was done on LIT, as well as multiple stage fragmentation experiments on the new products to gain some structural information. More information about the structure of the new products and their occurrence in the biological samples was gained from high-resolution mass spectrometry (HRMS/MS^2) experiments using an orbitrap, in a combination with hyperbolic quadrupole precursor selection. For the semipreparative work with LC-MS, QIT was used as the mass analyzer. All of the mass analyzers used are discussed below.

3.2.4.1. Quadrupole

A quadrupole consists of a set of four metal (molybdenum) or metal-coated ceramic rods with lengths of 10–20 cm and diameters up to 1 cm. The rods are placed parallel to each other in a square with the opposite pairs connected electrically. Their alignment must be precise to create the symmetrical electrical field necessary to separate ions with different m/z values.To obtain the ideal electrical field, the rods facing the center point should be hyberbolical, but cylindrical rods are also used. The voltage placed on one pair of the rods is comprised of a positive direct current (DC) in combination with an overlapping radio frequency (RF) voltage. The other pair of rods carries negative DC voltage with an RF component 180° out of phase with that on the first pair. The overlaid RF voltages are constantly oscillating between the positive and negative polarities. The mass separation is based on the fact that ions begin to oscillate upon entering the field produced by DC and RF voltages. However, only ions with one specific m/z value have a stable oscillatory trajectory along the axis of the quadrupole to the detector, while other ions develop unstable oscillation patterns perpendicular to the flight path and discharge onto the rods. The quadrupole is acting as a mass filter and this mode of operation is called selected ion monitoring (SIM) and it results in significantly increased sensitivity. By changing dc and rf progressively while keeping the ratio constant enables the scanning of a mass range yielding spectra comprised of the different m/z values.[178]

3.2.4.2. Three dimensional/cylindrical/quadrupole ion trap (QIT)

The QIT is a three-dimensional quadrupole that consists of a toroidal ring electrode and two end caps. Ions are produced externally and only a controlled number is allowed to enter the trap through one of the end caps by monitoring the ion current. A three-dimensional quadrupole field created by combined RF/DC field on the ring electrode and the grounded end caps causes the ions to cluster and remain close to the center of the cell where the electrical field is most symmetrical, resulting in the ions staying in their most stable orbits, that is also assisted by collisional cooling of the ions by helium. The combination of an amplified RF voltage on the ring

electrode with an RF voltage on the end caps ejects ions from the cell through the end cap where a detector is located. The combination of the RF voltages necessary to render an ion unstable is specific to each *m/z*. This is called resonance ejection and it is used to obtain mass spectra by ejecting ions sequentially according to their *m/z* values.

Ions with a specific *m/z* can be selected and kept in the trap with a stable trajectory, while the others are removed. The selected ions can be fragmented using collision-induced dissociation (CID) by introducing an additional pulse of gas into the trap. This isolation and fragmentation cycle can be repeated to provide MS^n spectra.[178]

Even though QIT can store ions and conduct MS^n experiments, it still suffers from several limitations. The limitation characteristic for all ion traps is the so-called one-third rule, which states that in CID MS^n it is not possible to detect product ions that are less than about one-third of the value of the precursor ion. Other limitation characteristic for ion traps is a low resolution.

If the number of the trapped ions in QIT is too high, the electrical field is overlapped by that ion cloud. This results in a drop in the performance of the instrument, particularly in mass resolution and linear response. To avoid that, a preliminary scan is performed and ionization time is optimized, confining the optimum number of ions inside the trap, which then limits the sensitivity of the instrument.[179]

3.2.4.3. Linear ion trap (LIT)

The LIT (Figure 33) has been developed to obtain a high injection and high ion storing efficiency. Ions oscillate in a linear fashion along the length of a quadrupole. Grids at each end of quadrupole, with voltages that can be manipulated, are used to allow ions to enter the LIT and to reflect and maintain the ions in the cell, and then enable their exit either onto a detector or into a second analyzer.[178] Even though the LIT has reduced space charge effects due to the increased ion storage volume and enhanced sensitivity for externally injected ions due to higher trapping efficiencies,[180] the limitations in resolution, mass accuracy and the one-third rule remain as for QIT.[179]
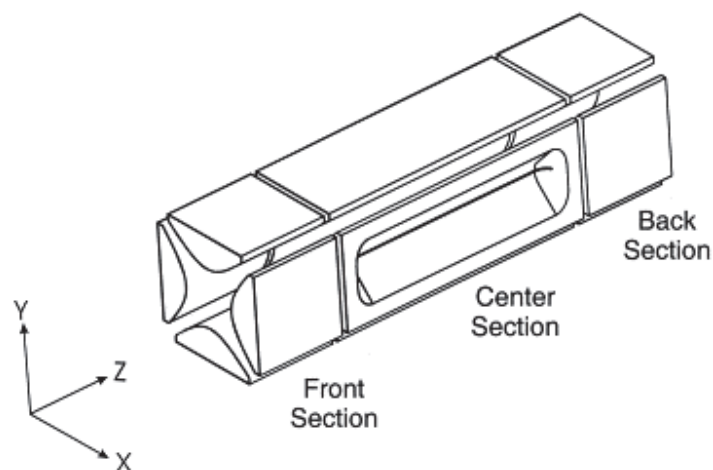
Figure 33. Basic design of the linear ion trap.[180]

3.2.4.4. Orbitrap

The orbitrap is the most recent commercial mass analyzer where the analytical cell of an FT instrument is also the detector, with the ions being recorded as an image current. The orbitrap is an electrostatic ion trap comprised of a spindle-shaped inner electrode and a split, barrel-like, outer electrode (Figure 34). Ions are collected in a specialized component called the C-trap and then injected into the orbitrap as high-speed pulses. The speed provides the ions with the centrifugal force necessary to counteract their attraction to the central electrode. When in the cell, the ions follow a complex trajectory composed of rotary motion around the inner electrode and an axial oscillation along the same electrode that is at the right angles to the rotary component. The oscillatory motion is the one inducing a current in the split outer electrode. The periodicity of the axial oscillation is proportional to the *m/z* of the component ions, and an image current is generated, recorded and then interpreted using Fourier-transformation (FT) analysis. One of the advantages of the orbitrap is a very high resolution and mass measurement with high accuracy. The disadvantage is that the number of the ions held in the trap is limited, and this might affect the detection of minor sample components.[178]
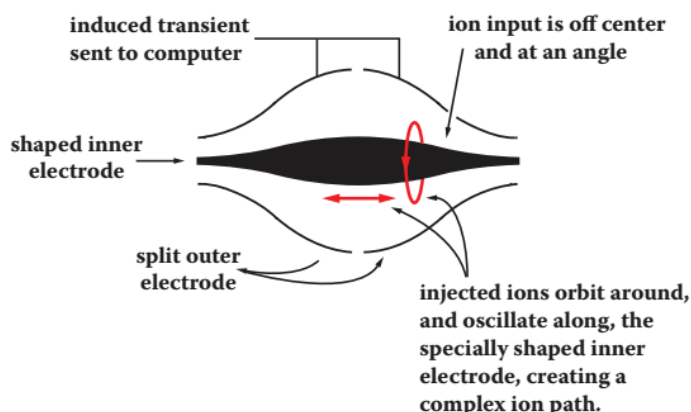
Figure 34. Orbitrap analyzer.[178]

3.3. Solution state nuclear magnetic resonance spectroscopy

3.3.1. Basic principles

Nuclear magnetic resonance (NMR) is a spectroscopic technique, an analytical tool for the structure elucidation of organic, biological and inorganic molecules by exploiting the intrinsic magnetic properties of atomic nuclei.[59] Like all spectroscopies, it uses a component of electromagnetic radiation (radio frequency waves) to promote the energy difference between two energy levels.[181] If an isotope contains an odd number of protons and neutrons, it possesses a non-zero spin. Spinning nuclei possesses angular momentum (P) and charge. The motion of this charge gives rise to an magnetic moment (μ).[182] Angular and magnetic momentum are correlated:

$$\mu = \gamma P \qquad (1)$$

Where γ, the gyromagnetic ratio—a measure of how "magnetic" a particular nuclide is, is a constant for any given nuclide. The most commonly studied nuclei are proton (^{1}H) and carbon (^{13}C), having gyromagnetic ratios 42.58 MHz/T and 10.71 MHz/T, respectively.[181] Based on the gyromagnetic ratio value, the ^{13}C nucleus is about 4 times less sensitive than ^{1}H, however the main cause of insensitivity in the NMR is the very low natural abundance of ^{13}C (1.1%). Acquisition time to acquire a good ^{13}C spectrum can take hours.

In the absence of an external magnetic field, nuclei (magnets) are randomly oriented. In the NMR experiments, an external magnetic field (B_0) is applied, and the spins of the nuclei align with (low energy, the α state or parallel state) or against (high energy, the β state, or antiparallel state) the external magnetic field and start precessing at the same frequency (ω_0) known as Larmor frequency. The Larmor frequency is characteristic for each type nucleus and is defined as:

$$\omega_0 = \gamma B_0 \qquad (2)$$

Subtle differences in the chemical environment in the molecule lead to a distortion of the magnetic field nucleus are experiencing, which leads to small differences in the precession frequency.

NMR occurs when the nucleus changes its spin state, driven by the absorption of a quantum of energy. This energy is applied as electromagnetic radiation, whose frequency must match that of the Larmor precession for the resonance condition to be satisfied, with the energy involved being given by:

$$\Delta E = \frac{h\gamma B_0}{2\pi} \qquad (3)$$

Where h is Planck's constant.

The relative population of a state is given by the Boltzman distribution:

$$\frac{N_\alpha}{N_\beta} = e^{\Delta E / k_B T} \qquad (4)$$

where $N_{\alpha,\beta}$ represents the number of nuclei in the spin orientation, k_B the Boltzmann constant and T the temperature. From equation (4) it can be seen that the population ratio of the states is affected by several factors. Nuclei with large gyromagnetic ratios are more sensitive in the NMR experiments. Sensitivity can be increased by increasing the strength of the external magnetic field. Since the energy difference between the two states is very small, the corresponding population differences are similarly small, making NMR very insensitive when compared to other spectroscopic techniques. However, the slight excess of the nuclei in the more favorable α-state generates so-called net magnetization.[181,182] To observe the net magnetization, as was mentioned, its thermal equilibrium needs to be disturbed with the additional external field generated by a radiofrequency (RF) pulse, which has a defined amplitude and duration. This irradiation imposes a torque to the bulk magnetic moment and it will rotate perpendicular to the pulse. A tilt angle for the bulk magnetization vector is adjusted by the length of the pulse.[181] If the applied pulse is a 90° pulse, the net magnetization is moved from the *z*-axis to the *x,y* plane (Figure 35).
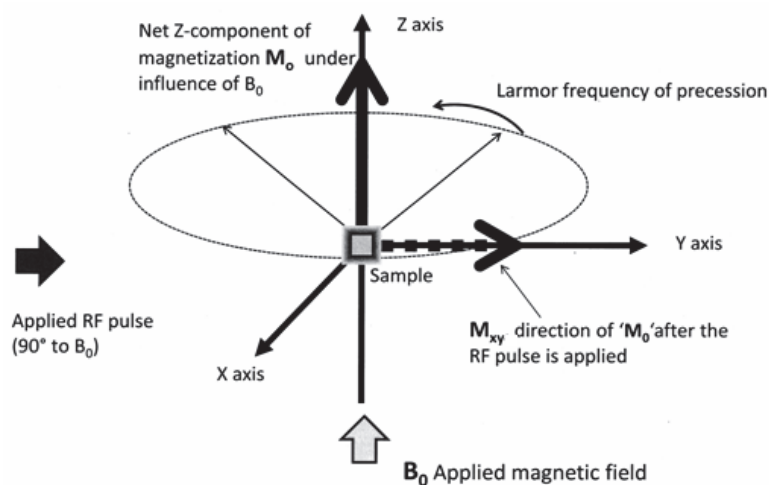
Figure 35. Net magnetization on the *z*-axis after applying the external B_0 magnetic field being "tipped over" to the direction in the *x,y* plane after applying 90° radio frequency pulse.[183]

After the RF pulse, the nuclei start relaxing and returning to the equilibrium position. The NMR technique monitors this relaxation process as a function of time. The rotating magnetization vector will produce a weak oscillating voltage in the coils that surround it, and the voltage is then detected. The relaxation of the bulk magnetization vector causes the oscillating voltage to disappear causing the decay of the NMR signal with time, producing the observed free induction decay (FID). Using Fourier transformation, the time domain of FID is turned into the corresponding frequency domain spectra (Figure 36).[181]
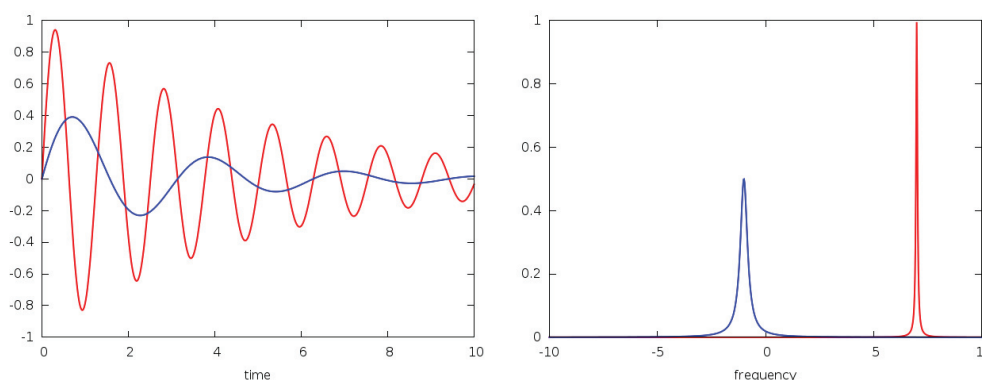
Figure 36. The left panel of the figure shows two exponentially decaying sine waves with different frequencies and decay rates. The blue sinusoid has a lower frequency and a faster decay rate than the red. As in the figure above, the lower frequency of the blue signal means that the peak obtained after Fourier transformation is closer to the zero frequency position than the red signal which has a higher frequency. The faster decay rate of the blue signal compared to the red translates into the blue peak being broader than the red after Fourier transformation.[184]

Differences in the chemical environment surrounding each individual atom in the molecule lead to a magnetic field distortion experienced by the nucleus. This effect is known as shielding and it results in specific frequency shift (chemical shift, δ expressed in ppm) for each nucleus. Distortions in the field also arise due to the magnetic moments of nearby nuclei and result in signal spin-spin splitting of the signal known as coupling (J, expressed in Hz).[59] The J coupling appears as an interaction mediated by the electrons participating in the bonds connecting the nuclei. The magnitude of J-coupling (scalar coupling) is typically larger when nuclei are separated by smaller number of bonds. It is typically observed for nuclei which are 2 (geminal) or 3 (vicinal) bonds apart, but longer range coupling can be observed in rigid or π–bonded systems. Information about the conformation can come from vicinal coupling constants. The Karplus equation describes the correlation between ^3J-coupling constants and dihedral torsion angle, with ^3J being smallest when the torsion angle is close to 90° and largest at angles 0 and 180°.[185]

In solution state NMR, the sample is usually dissolved in a deuterated solvent, as the resonance frequency of a deuteron (^2H) is very different from that of proton (^1H) and one can avoid the huge solvent absorption that would otherwise dominate the ^1H NMR spectrum due to high amounts of solvent. Modern NMR spectrometers also measure the deuterium absorption of the solvent to stabilize the magnetic field strength. As the observation frequency is field-dependent, the deuterium receiver notices a field fluctuation through a change of the observation frequency ("lock frequency") and can correct the field strength correspondingly. However, solvents are never 100% deuterated, and signals for the residual protons are still observed. A residual water peak is a common contaminant in NMR spectra. The chemical shift of the water peak depends on temperature, as well as on the presence of the potential hydrogen bond acceptors that tend to shift the water signal downfield.[186]

If the NMR sample contains solvent or remaining water peak that is causing a poor signal-to-noise for the peaks of interest, use of a solvent suppression technique is the best choice.[187] There are several solvent suppression techniques. In this research, the presaturation technique and excitation sculpting were used for signal suppression. The presaturation technique is based on applying a long, low power pulse during the relaxation delay at the frequency of the signal to be suppressed. In case of two undesirable resonances present in spectra, experiments with double presaturation on multiple frequencies simultaneously were chosen. The excitation sculpting is a technique that uses a simple echo sequence with a pulsed field gradient before and after the refocusing gradient. The pulse is tailored in a way that all the frequencies except those around the resonance solvent are excited.[188]

The shape and the chemical shift of exchangeable protons signals (–OH, –SH, –COOH etc.) is dependent on the degree of intermolecular and intramolecular hydrogen bonding. Those protons are not present in spectra of compounds run in deuterated protic solvents because they exchange with solvent deuteriums, which can be useful for their identification.[187]

3.3.2. NMR experiments

600 MHz and 800 MHz NMR instruments fitted with cryoprobes, and with the careful adjustment of the acquisition parameters (number of increments, repetition rate, number of scans), were sufficient for the successful structural elucidation with the 50–100 µg of material. For the complete determination of the chemical structure, there are several types of 1D and 2D NMR experiments needed.

3.3.2.1. One-Dimensional NMR Experiment

3.3.2.1.1. Standard 1D Proton (^{1}H) NMR experiment

Solving a problem of the structure of an organic chemical start with the acquisition of the ^{1}H spectrum, since it is the fastest experiment providing lots of information that are the foundations for further work. Regular 1D experiments usually consist of three stages: relaxation period (d1), pulse application (p1) and acquisition.[182] The pulse is most commonly set to a 90° or 30°. The latter one is used for faster experiments.
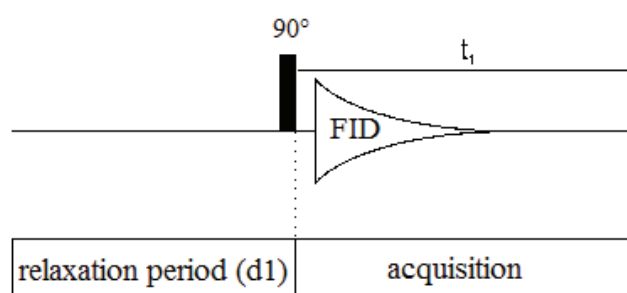
Figure 37. Pulse sequence and main elements of the single-pulse NMR experiment.[189]

3.3.2.1.2. 1D ^{13}C NMR experiments

3.3.2.1.2.1. Standard 1D ^{13}C NMR experiment

The 1D ^{13}C NMR experiment is much less sensitive than proton (^{1}H) because of the low natural abundance of ^{13}C. In the 1D ^{13}C NMR experiment, as in ^{1}H NMR experiment, a 30° or 90° pulse are most commonly applied. The experiment where a 30° pulse is applied is more common, as

the interpulse delay time can be set shorter than for the 90°. However, 90° pulse gives more detailed spectrum.

During the ^{13}C NMR experiment, broadband proton decoupling is usually applied to remove all ^{1}H–^{13}C couplings and to concentrate all the carbon resonance intensity into a single line. The continuous saturation of the proton spins provides further enhancement of the signal due to the Nuclear Overhauser Effect (NOE).[182] It is possible to see all the carbons, though quaternary carbons having no hydrogens are usually quite weak as the proton decoupling process gives rise to an NOE enhancement that quaternary carbons do not experience.

3.3.2.1.2.2. *J*-modulated spin-echo

This is a 1D ^{13}C experiment that is used to distinguish methine (CH) and methyl (CH$_3$) signals, that appear with the opposite phase from the quaternary (C) and methylene (CH$_2$) signals. It is based on applying a 90° pulse that would put the magnetization vector into the transverse plane, followed by a 180° pulse in the middle of the evolution period (spin-echo). In the decoupler-gated version of the experiment, the decoupler is off during the first evolution period in order to introduce *J*-modulation in the spectrum. Usually, the length of the evolution period is set $1/J_{CH}$ (125 Hz or 8 ms) and then, depending on the number of the couplings, magnetization is oriented either positive or negative. The pulsed variant of the experiment obtains the same result, but uses proton 180° pulses rather than by gating off the decoupler.[182]

3.3.2.1.2.3. DEPT (Distortionless Enhancement by Polarization Transfer)

The distortionless enhancement by polarization transfer (DEPT) experiment allows one to distinguish between carbons with different numbers of bonded protons. This method uses polarization transfer from ^{1}H to ^{13}C nuclei. As seen in the general DEPT sequence (Figure 38), the pulse Θ_y is variable.
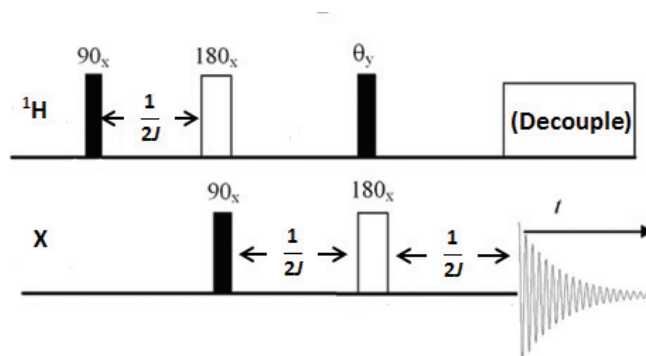
Figure 38. The DEPT sequence adapted from Claridge.[182]

Depending on the chosen tip angle Θ_y for the pulse, the intensities for the carbon signals will vary. For $\Theta_y = 45°$ all the peaks for CH, CH_2 and CH_3 will be positive. For $\Theta_y = 90°$ only CH will be observed and will give positive peaks. For $\Theta_y = 135°$ the peaks for CH and CH_3 will be positive and the peaks for CH_2 will be negative. Quaternary carbons should not be observed in any of these three experiments. Even though certain peaks should not be observed, if the pulse is not perfectly adjusted, they can still be present. Depending if the applied pulse is too long or too short, the unwanted peaks will appear in the spectrum according to Figure 39.[182]
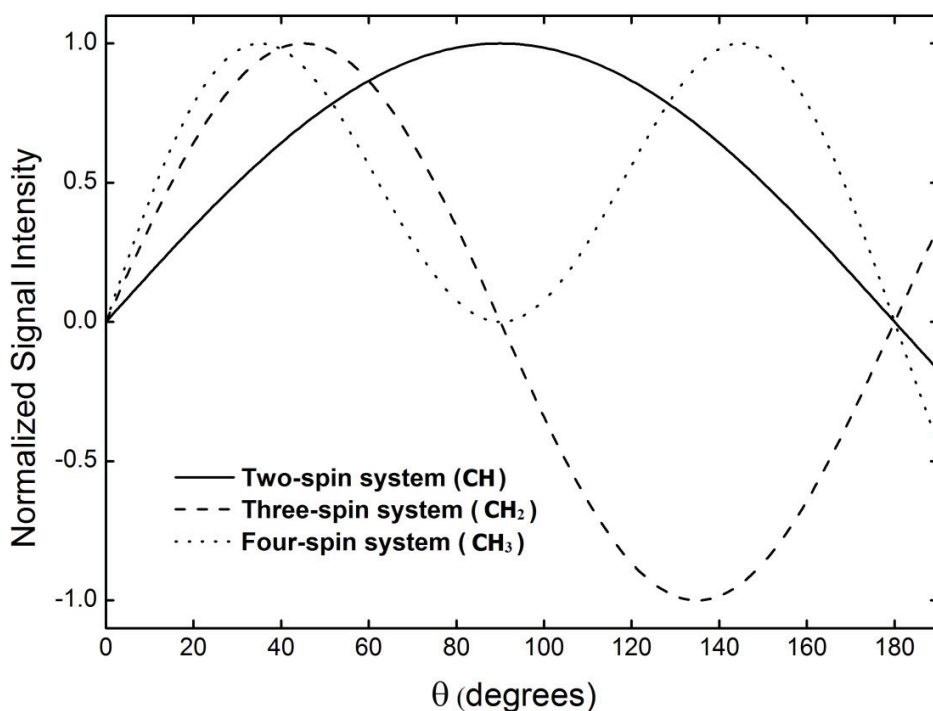
Figure 39: The variation of carbon signal intensities as a function of the angle Θy. Figure adapted from Hassan et al.[190]

3.3.2.2. Two-Dimensional Homonuclear NMR Experiments

In 2D NMR experiments, the two dimensions refer to two frequency dimensions. All of the 2D sequences are subdivided into preparation, evolution, mixing time and detection period (Figure 40). The preparation and mixing periods usually involve a pulse or a cluster of pulses. [182] The evolution time is what makes it different from 1D experiment, because there is a pulse at the beginning of the evolution time and then a wait before doing an acquisition pulse. If one varies

this by incrementing the waiting time for each successive cycle, one changes what one sees in the FID. Once data is acquired there are two "time domains"; one from the normal acquisition time and the other from the incremented delay.[187]
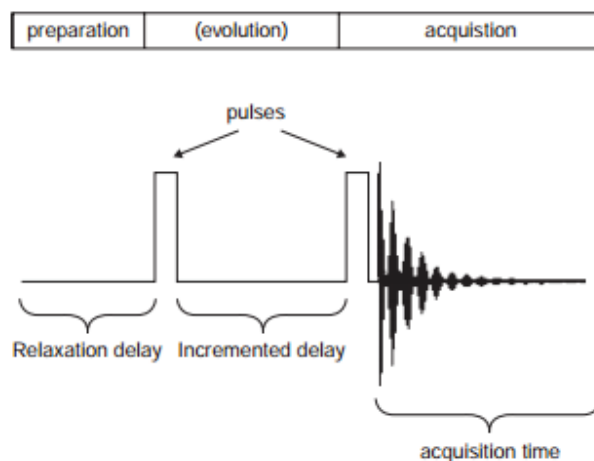
Figure 40. General scheme for any 2D experiment. Figure was taken from Richards and Hollerton.[187]

3.3.2.2.1. COSY (Correlation Spectroscopy) NMR experiment

COSY data identify short range connectivities (^2J and ^3J couplings).[191] COSY spectra show two types of peaks. Diagonal peaks have the same frequency coordinate on each axis and appear along the diagonal of the plot, while cross peaks have different values for each frequency coordinate and appear off the diagonal. Diagonal peaks correspond to the peaks in a 1D NMR experiment, while the cross peaks indicate couplings between pairs of nuclei (much as multiplet splitting indicates couplings in 1D NMR).[182] Because of the small quantities of toxin derivatives that we worked with, the residual water peak and solvent peak were very strong and were affecting the signal to noise. For this reason, COSY experiments with presaturation on the water peak or with double presaturation were most commonly used.

3.3.2.2.2. TOCSY (Total Correlation Spectroscopy) NMR experiment

As in COSY, observed cross peaks in TOCSY spectra come from coupled protons, but within a given spin system, not just between geminal or vicinal protons as in COSY. The TOCSY experiment can be optimized to detect short, medium and long range correlations by varying the spin-locked correlation (mixing) time. Mixing time in order 15 msec affords a COSY-like spectrum, but a long mixing time of 150 msec enables detection of connectivities of protons that are 5–6 bonds from each other.[191] Hetero-atoms (such as nitrogen or oxygen) and quaternary

carbons usually disrupt the TOCSY magnetization transfer and effectively isolate the protons from all the others in the molecule.[187]

3.3.2.2.3. NOESY (Nuclear Overhauser Effect correlation spectroscopy) NMR experiment

The NOESY experiment creates correlations between nuclei that are close to each other in space. The so called Nuclear Overhauser Effect (NOE) arises when the spin relaxation of nucleus A is felt by nearby nucleus B, stimulating a corresponding change in magnetization in B. In a typical NMR spectrum, the interference of electrons makes this coupling undetectable. However, a sample can be decoupled to "neutralize" the bond coupling through electrons, allowing the through-space coupling of the NOE to be detected.

A potential problem that can occur with larger molecules (typically MW higher than 600) is that the NOESY experiment is affected by the tumbling rate of molecules in solution. The larger the molecule, the slower it will tumble, and at certain point all expected enhancements will be nullified. This is also dependent on the viscosity of the solvent and the field strength of the spectrometer being used – a molecule giving positive NOE in a 400 MHz instrument may not give NOEs in a 600 MHz machine.[187]

3.3.2.2.4. ROESY (Rotating-frame Overhauser spectroscopy) NMR experiment

The ROESY experiment, along with the NOESY experiment, is used to determine which protons are close in space but not connected with chemical bonds. This technique is based on NOE in the rotating frame. The pulse sequence is almost identical as the one used for TOCSY, but to avoid TOCSY artefacts, the power used to achieve spin-lock is reduced. ROESY is especially useful for cases where NOESY signals are weak and near the transition between negative (for large molecule), positive (for small molecule) or null (if the correlation time happens to cancel the NOE). By convention, spectra should be phased in a way that the diagonal is always positive and ROE (NOE in the rotating frame) cross-peaks are negative. The ROESY experiment also yields cross peaks rising from chemical exchange. Exchange peaks and TOCSY type artefacts are always the same phase as the diagonal. Sensitivity of ROESY is increased by increasing the transverse relaxation time and by choosing a low viscosity solvent.[187]

3.3.2.3. The Two-Dimensional heteronuclear NMR experiments

2D heteronuclear correlation NMR experiments correlate the resonances from two different frequency regions belonging to the chemical shift ranges of different nuclei.[192]

3.3.2.3.1. HSQC (Hetero-nuclear Single-Quantum Correlation spectroscopy)

The HSQC experiment obtains a 2D heteronuclear chemical shift correlation map between directly-bonded ^{1}H and other nuclei (commonly, ^{13}C and ^{15}N). It is widely used because it is based on proton-detection, offering high sensitivity. ^{13}C magnetization prevails during the evolution period and is subsequently transferred to ^{1}H for detection. In both cases, the signals from protons not coupled to ^{13}C are suppressed so the HSQC detects only single-bond correlations between ^{1}H and ^{13}C, and signals from long-range couplings are missing.[192]

3.3.2.3.2. HMBC (Hetero-nuclear Multiple-Bond Correlation spectroscopy)

In this experiment, correlations are obtained between carbon atoms and protons that are separated by two and three bonds and sometimes, in conjugated systems, four bonds.[187] It is a particularly useful experiment for finding carbonyl or quaternary carbons when only small amounts of sample are available. Direct one-bond correlations are suppressed. The intensity of cross peaks depends on the coupling constant, which for three bond couplings follows the Karplus relationship. If the long range proton–carbon coupling is close to zero (like for dihedral angles near 90 degrees) then the signal will be absent from the spectrum. Thus, the absence of a cross peak does not confirm that proton–carbon pairs are many bonds apart.[182]

3.3.2.4. Selective 1D and 2D NMR experiments

3.3.2.4.1. Selective TOCSY/NOESY/ROESY 1D NMR experiments

Spectra obtained from these experiments are the selective 1D analogues of the non-selective 2D experiments. Advantages of the selective experiments compared to conventional 2D experiments are a greater proton signal resolution, making it possible to determine coupling constants, solvent and other impurity signals are effectively eliminated from the spectra, excitation of only a narrow region of the original ^{1}H NMR (5–30 Hz), and the reduction in the spectrometer time.[191]

The selected frequency is excited with a soft pulse, which is a single, low-amplitude radiofrequency of relatively long duration. Important characteristics of a soft pulse include its shape, amplitude, and length. The pulse shape may be correlated with the shape of the excitation profile, the pulse amplitude with the flip angle, and the pulse length with the pulse selectivity (the width of the excited spectral region).[193]

3.3.2.4.2. Band-Selective HMBC 2D NMR experiment

One limitation of HMBC is the difficulty in resolving correlations to closely neighbouring ^{13}C resonances when studying complex structures or those with especially crowded spectra, which can result in ambiguity in structural elucidation. The problem starts with potentially large ^{13}C shift range that needs to be acquired to provide the ^{13}C (F_1) frequency dimension of the final 2D spectrum. A larger shift range demands more t_1 increments and therefore a longer experiment

time. Many routine HMBC spectra are for these reasons acquired in relatively low F_1 resolution. In these cases, a semi-selective or band-selective HMBC experiments can be useful. It incorporates selective pulses on the ^{13}C channel to excite only a subset of all carbon nuclei and so focus the 2D correlation spectrum on these alone, thus increasing the resolution in the ^{13}C axis.[194]

3.3.2.5. Quantitative NMR (qNMR) – ERETIC (Electronic REference To access In-vivo Concentration) experiment

NMR spectroscopy is not only a powerful tool for structural elucidation, but also for quantitative analysis because of the direct proportionality of the ^{1}H signal intensity to the number of resonating nuclei.[195] Quantitative analysis requires a reference compound for analyte concentration calculation. If calculating the amount using an internal standard, the reference compound should be dissolved in a known volume of analyte solution and should fulfil several requirements: to be available in highly purified form, stable, chemically inert, non-volatile, non-hygroscopic and soluble in most of the common NMR solvents. The reference signal should be well separated from the analyte signals and preferably be a singlet.[196] Contamination of a valued analyte sample by the reference compound can be avoided with a qNMR experiment that uses an external standard.[197] There are three variations of the method with the external standard. The first variation uses a coaxial tube containing a reference standard inserted into an NMR tube containing the sample. The second variation is to have separate solutions of reference and the sample, and acquiring separate spectra.[198] The third variation is a method developed in 1999 by Akoka et al.[199] for quantification of analytes using an electronically-synthesized reference signal, called ERETIC. An RF signal at the observed proton frequency is electronically generated via very low power shaped pulse on a decoupler or second radio channel. That signal is directly introduced into the probe on a spare channel (typically ^{13}C) that is not necessarily tuned to the operating frequency during the acquisition. The proton coil that detects an NMR signal also detects the synthetic signal originating, in theory, from the ^{13}C-coil or channel. The ERETIC signal integral is then calibrated against a reference standard sample, and then the same signal is generated in the sample of unknown concentration (Figure 41).[200] However, there were reported inconsistencies when applying this method in a wider range of applications, due to experimental aspects: probes and samples. Samples that had similar dielectric properties as the concentration reference standard did well with the ERETIC technique, while those in different solvents or salt compositions gave large errors in quantitation.[200] A new, improved quantification experiment using PULCON (Pulse length based CONcentration determination) methodology was introduced by Wider at al.[201] It is based on the principle of reciprocity, where NMR signal intensity for a sample compound in a given coil is inversely proportional to the 90° or 360° pulse length. PULCON compensates signal intensities for losses in coil sensitivity due to sample-to-sample changes in dielectric properties (ionic strength) and does not require specialized equipment to be performed.[195]
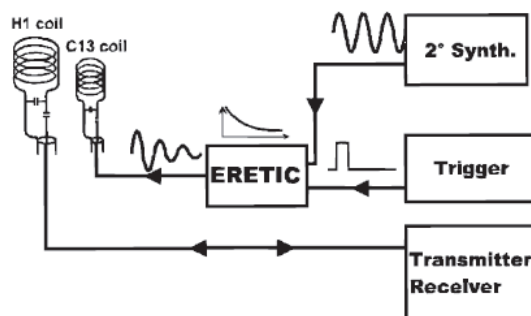
Figure 41. Configuration used for the ERETIC1 experiment by Akoka et al.[199] Reprinted with journal permission.

The module ERETIC2 that is available in the TopSpin software (version 3.0, Bruker Biospin) is based on PULCON and it only requires a 1D spectrum measured on a sample of known concentration under "quantitative" conditions: a tuned and matched probe, a calibrated 90° pulse, a relaxation delay time of at least five times as the spin-lattice relaxation time (T_1), acquisition time longer than spin–spin relaxation time (T_2) and sufficient signal-to-noise.[202]

The precision of the ERETIC was compared to the internal reference method and to the external reference method that employs reference material in separate solution from the sample. The internal reference method performed the best (precision 0.1%), but both external reference method (precision 0.3%) and ERETIC (precision 0.3%) yielded results that were only slightly less precise and accurate.[198]

3.4. Cell based bioassays

Cell-based bioassay is term used to refer to any assay based on some measurement of a living cell. Many aspects of living organisms are analyzed based on living cells studies: from cell signaling, proliferation, apoptosis, cellular genetics/morphology, cancer and more.[203] The desire to rapidly asses the toxicity of new compounds, together with the ethical consideration towards animals, and the fact that toxicity tests on mammals are expensive and require special laboratory facilities, has led to development of many different types of bioassays.[203,204] There are many types of primary and immortalized cell-lines that are commercially available, and each has advantages and disadvantages. Primary cells are taken directly from the living tissue and established for growth in vitro. Even though their response should represent a real cell response because they are not altered in any way, the downside is that they have a finite life span and can change in culture. On the other hand, immortalized cell lines' main advantage is that they are all genetically identical and can be grown indefinitely in culture, but the mutations that made them immortal can alter the biology of the cell.

Many different cell lines with different endpoints have been used in research related to *Fusarium* mycotoxins and they often have different sensitivities to different toxins.[205] The choice of the cell bioassay for the toxicity assessment of synthesized DON-conjugates in this thesis was made based on the knowledge of what kind of toxicity is displayed by DON.

4. LIST OF PAPERS

Paper I. Nucleophilic Addition of Thiols to Deoxynivalenol

Paper II. Preparation and Characterization of Cysteine Adducts of Deoxynivalenol

Paper III. Characterization of Deoxynivalenol-Glutathione Conjugates using Nuclear Magnetic Resonance Spectroscopy and Liquid Chromatography-High Resolution Mass Spectrometry

Paper IV. Glutathione-Conjugates of Deoxynivalenol in Naturally Contaminated Grain are Primarily Linked via the Epoxide Group

5. RESULTS AND DISCUSSION

5.1. Understanding the reaction and optimizing the reaction conditions

To gain an understanding of the chemistry behind the reaction of DON with thiols and the reaction dynamics, initial experiments used 2-mercaptoethanol as a model thiol (**Paper I**). The reaction of DON with 2-mercaptoethanol was followed at three different pH values for approximately one month using LC–MS. 2-mercaptoethanol was used as it is a liquid and thus easy to handle, as well as it is a simple, small molecule that was expected to give NMR spectra that were relatively simple to interpret. Like DON, it also lacks acidic or basic groups, so the DON–mercaptoethanol adducts were expected to ionize in a similar manner to DON (by forming formate/acetate adducts) and to have similar responses in the LC–MS. The *m/z* of the products that formed corresponded to single and double addition of mercaptoethanol to DON. The ratios of those products changed with time—three later eluting mono- and two di-mercaptoethanol adducts disappeared over time, until an earlier-eluting peak became prevalent and the only one left in the reaction mixture (Figure 42) (**Paper I**). It was anticipated that the products were most likely formed by reversible Michael addition to the 9,10-double bond of DON or by irreversible addition to the 12,13-epoxide ring (Figure 43). The reversible addition to the C-8 carbonyl was also considered as a possibility.

In order to test these hypotheses prior to the characterization of the reaction products, the reaction between 2-mercaptoethanol and the DON-analogues T-2 tetraol and deepoxy-DON (**Paper I**) was followed. T-2 tetraol (Figure 44) contains a hydroxyl group instead of the C-8 carbonyl, which means that the 9,10-double bond is no longer conjugated and Michael addition would not be possible. In deepoxy-DON (Figure 44) on the other hand the epoxide ring is reduced to an olefinic methylene, leaving a conjugated double bond the most feasible place for the addition.
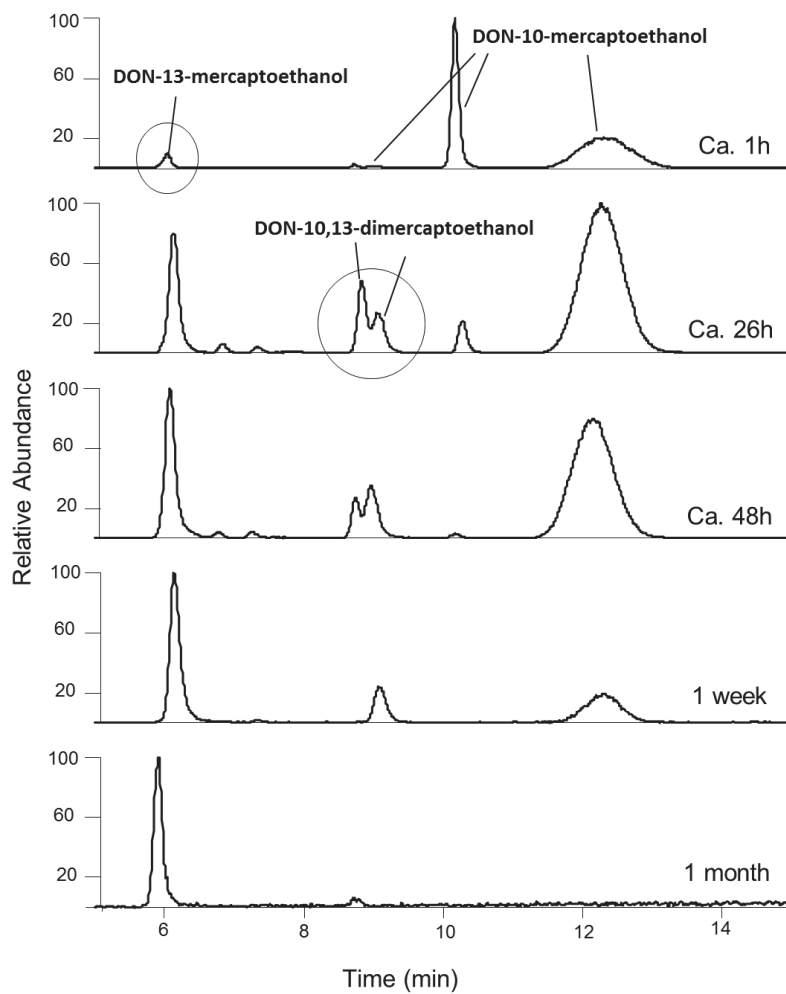
Figure 42. LC–MS extracted ion chromatograms (*m/z* 419 + *m/z* 497) from the reaction of DON with mercaptoethanol at pH 10.7. Circled peaks in the chromatogram are the ones that have been purified and identified by NMR. This figure was adapted from Paper I, Figure 2.
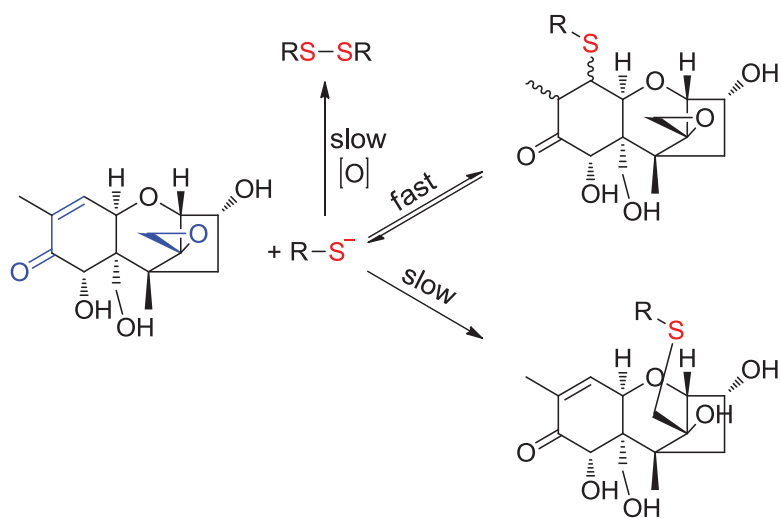
Figure 43. Scheme of possible reactions between the reactive thiolate ion and a molecule of DON. Blue color represents possible addition positions of the thiolate ion (red).

As expected, the LC–HRMS chromatograms of these reactions did not reveal any signal corresponding to double adducts. The LC–MS analyses of the reaction of 2-mercaptoethanol with deepoxy-DON revealed four peaks that changed in relative intensity over time. The peaks were due to reaction products affording ions with *m/z* of a single mercaptoethanol addition. These products almost completely disappeared after 10 days, leaving deepoxy-DON as the most intense peak in the chromatogram. This observation may be explained by the reversibility of the reaction, as the molecule undergoes β-elimination due to the presence of the electron-withdrawing carbonyl group together with the fact that the autoxidation of the thiol is moving the equilibrium towards the reactants. In contrast, the reaction between T-2 tetraol and mercaptoethanol revealed only one peak corresponding to a single mercaptoethanol addition that steadily grew in intensity throughout the analysis time. This is consistent with irreversible addition to the epoxide.
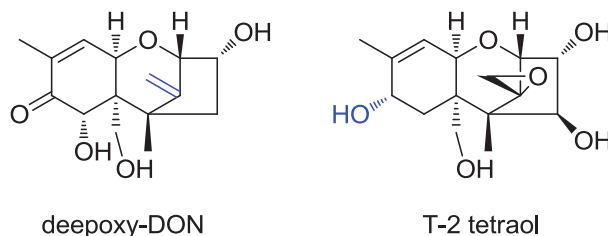
Figure 44. Chemical structures of the trichothecenes deepoxy-DON and T-2 tetraol. Blue color shows positions in the structure of deepoxy-DON and T-2 tetraol that differ from DON and are significant for the reaction with thiol.

The reaction of DON and 2-mercaptoethanol formed products that appeared to be identical, regardless of the pH of the reaction mixture. Several other products were detected in the reaction mixture, especially at the higher pH, that were not due to thiol-addition. The *m/z* of these products corresponded to previously identified DON degradation products[152] formed under basic conditions (Figure 23). Comparison of the LC–MS characteristics of standards (kindly obtained from Humpf et al., University of Münster) confirmed that these degradation products were norDON A, norDON B and norDON C. Because DON degradation is a competing reaction to thiol addition, for the preparative reactions it was desirable to use a large excess of thiol in respect to DON. Depletion of DON displayed a pseudo-first-order reaction kinetics behavior. The DON depletion rate increased with pH (**Paper I**) as there was relatively more of the reactive thiolate ion present. Eventually the DON depletion curve was flattening out. The reaction was more complex than initially expected, and several factors could be a cause of that, such as thiol autoxidation to disulfide, which reduces the thiol concentration with time, or several reversible reaction equilibria present in the mixture (reversible Michael addition, or, as was later confirmed by NMR analysis, hemiketal–ketone equilibrium).

An additional experiment was carried out at basic pH, where DON was reacted with several different thiols: 2-mercaptoethanol (Figure 45), 2-aminoethane thiol (Figure 45), sodium methanethiolate (Figure 45), sodium 2-mercaptoethanesulfonate (Figure 45), L–cysteine (Figure 45) and L–glutathione (Figure 45), and followed for 1 week using LC–MS (**Paper I**).
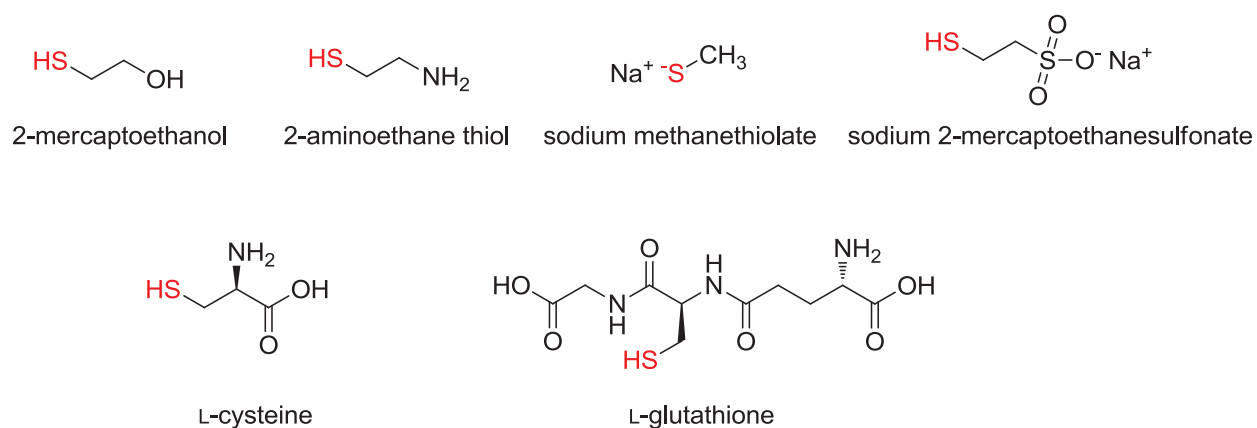
Figure 45. Chemical structures of thiols used in the reaction with DON (**Paper I**): 2-mercaptoethanol, 2-aminoethane thiol, sodium methanethiolate, sodium 2-mercaptoethanesulfonate, L–cysteine and L–glutathione

The product patterns in the chromatograms displayed many similarities to the DON-mercaptoethanol products, indicating a similar chemical behavior (**Paper I**). The chromatograms

always revealed several late-eluting peaks corresponding to the m/z of a single thiol addition to DON that changed in ratio with time. The smaller thiols (e.g. sodium methanethiolate) formed more isomers in a shorter time compared to bulkier thiols (e.g. glutathione), which could be due to steric hindrance. Double adducts were also detected in all the reaction mixtures. When mixtures were reanalyzed after 45 days, chromatograms revealed only the early eluting peak with m/z of a single thiol addition, which implied that this was most likely a product of irreversible addition to the epoxide ring

The preparative reactions, isolation of the DON-mercaptoethanol adducts (discussed in a section 5.2.) and NMR analysis (discussed in section 5.3.) finally identified the earliest eluting peak as the epoxide adduct, and confirmed that the double-adducts have a second thiol positioned at the 9,10-double bond. Based on these findings and similarities in the chromatograms of the reactions, we expected that all of the other early-eluting DON–thiol conjugates were epoxide-adduct analogous, and later-eluting single adducts were Michael adducts.

5.2. Synthesis and purification of thiol conjugates of DON and stability of the Michael adducts

For the synthetic reactions, basic conditions were used to increase the reaction rate, as well as high excess of thiols, so that the base catalyzed degradation of DON under the basic conditions (described in section 1.4.1) had no significant impact on the rate of the thiol addition reaction. These reaction conditions were optimized based on the observations from the initial experiments described in the section above. The goal was to first identify and confirm the place of the thiol addition by purifying the double adduct, and also the most stable adduct in the reaction mixture of DON and mercaptoethanol—the earliest eluting peak in the chromatogram with m/z corresponding to the single thiol addition. Two reactions were set up and followed with LC–MS until the desired products reached an optimum intensity in the chromatogram. The double adducts were not completely baseline-separated and were purified as a mixture. Reactions were stopped by desalting and fractionating the reaction mixtures on an SPE column, and purified with semi-preparative LC–MS (**Paper I**). Interestingly, the semi-preparative LC–MS of the double adduct revealed only one sharp peak corresponding to its m/z. However, the subsequent NMR analysis showed two compounds that were a pair of diastereoisomers (Figure 46).

DON-13-mercaptoethanol

DON-10,13-dimercaptoethanol diastereoisomers
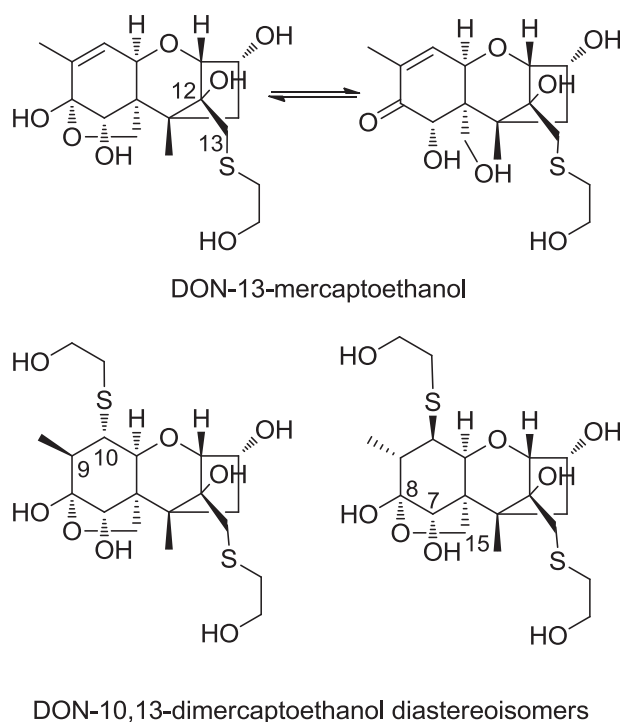
Figure 46. Structures of the products purified from the reaction of DON with mercaptoethanol. DON-13-mercaptoethanol, the earliest eluting peak in the chromatogram (Figure 42), is an equilibrating hemiketal–ketone pair, and DON-10,13-dimercaptoethanol are a hemiketal pair of diastereoisomers of the double addition of mercaptoethanol to DON.

Based on the observed reaction dynamics and identified model compounds (Figure 46), the next goal was to prepare, purify and identify DON conjugates of the biologically relevant thiols cysteine (**Paper II**) and glutathione (**Paper III**) (Figure 45). The main focus was on the synthesis of the epoxide adduct (the earliest eluting peak in the LC–MS chromatogram), and one of the Michael adducts (one of the later eluting peaks). Two parallel sets of reactions (1 mg of DON as a starting material) were set up and followed with LC–MS. Because the epoxide adduct is formed more slowly than the Michael adduct, but the reaction is irreversible (Figure 43), reactions for production of the epoxide-adducts were left to stand longer than the reactions for production of the Michael adduct (**Paper II**). In the case of the glutathione conjugate (**Paper III**), the reaction was incubated at 37 °C to increase the reaction rate. When the desired peaks for DON–Cys and DON–GSH conjugates reached the optimal intensity in the LC–MS chromatogram, the reaction mixture was fractionated by SPE (**Papers II** and **III**). Satisfactory purity for structural characterization was gained without the need for further purification. We predicted that the thiol might "fall off" from a Michael adduct after the purification step. Basic conditions that are used in the reaction increase the rate of reaching the equilibrium by creating more of the reactive thiolate ion, but once the thiol has been conjugated to the molecule, presence of the base leads to

the reverse reaction (E1cB-elimination), where the acidic proton on C-9 is abstracted by the base, causing the electrons from the neighboring bond to move and expelling the thiol from the molecule (Figure 47).
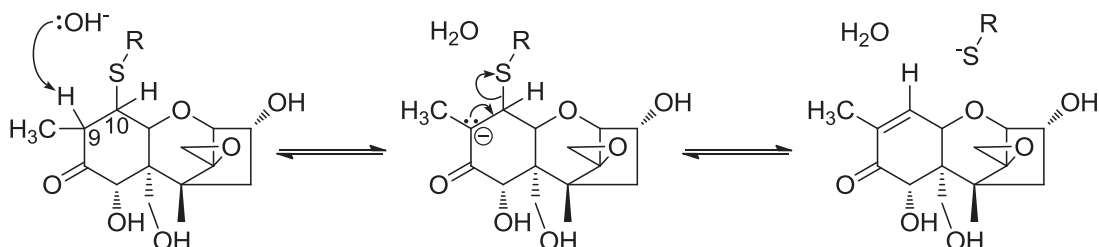
Figure 47. The E1cB-elimination of thiol from molecule of DON.

This equilibrium can be disturbed and moved toward the reactants by the change in the concentration of the reactants under alkaline conditions (DON degradation), autoxidation of the thiol, or by purifying adduct and removing the reactants from the system. It was anticipated that acidification of the reaction mixture would stabilize the Michael adduct and would stop the reversibility. Deconjugation was observed for DON–Cys Michael adducts, but not the epoxide adduct, in a mixture desalted from a buffer with SPE (**Paper II**). However, after acidifying an aliquot of the sample with acetic acid and following it with LC–MS by measuring the ratios between the two DON-10-Cys isomers and DON-13-Cys, it was shown that the rate of deconjugation became negligible (**Paper II**). Acid was therefore added after the purification step to stop the deconjugation of Michael adducts (**Papers II** and **III**). The understanding of this led to the successful preparation of stable analytical standards of DON-10-Cys and DON-10-GSH (**Papers II** and **III**).

Once samples were successfully purified, in order to interpret the LC–MS time course data, as well as the MS/MS data, it was necessary to determine the chemical structures of the major products of the reaction. To unambiguously identify the compounds, NMR spectroscopy and LC-HRMS/MS methods were employed.

5.3. Chemical characterization of DON conjugates (Papers I, II and III)

5.3.1. NMR spectroscopy

All of the analyzed DON-conjugates displayed some prominent features that distinguish the addition site. In ^{1}H NMR spectra of the epoxide adducts, where the C-9/C-10 double bound is intact, there were two singlet peaks with the upfield chemical shift (1-2 ppm), belonging to C-14 and C-16 methyl signals (Figure 48). H-14 methyl always appears as a sharp singlet (1.0-1.4 ppm), while H-16 methyl (1.7–2.0 ppm) in DON and DON-conjugates with preserved double bond appears broad due to the long-range coupling with H-10 and H-11, though with applied resolution enhancement they could be resolved as a triplet with small coupling constant (ca 1.5 Hz). The presence of the double bond between C-9 and C-10 moves the chemical shifts of nearby protons (H-10 and H-16) more downfield (3.0–3.5 ppm and 1.1–1.2 ppm). In the proton spectrum of Michael adducts, the H-16 methyl signal appears shifted upfield relative to the epoxide adduct and as a doublet, as it is being split by ^3J coupling to an added proton at C-9. Epoxide methylene protons H-13 are distinguishable doublets with a small ^2J coupling constant of about 3.5–3.8 Hz, which is usual for high ring-strain systems.[59] After thiol addition to C-13, the ring is open and the ^2J coupling constant is about 13.5 Hz for the H-13 methylene protons, which indicates the presence of the unstrained sp^3 methylene protons.

Full NMR assignments of DON-13-mercaptoethanol, DON-10,13-dimercaptoethanol, DON-10-Cys, DON-13-Cys, DON-10-GSH and DON-13-GSH were established by standard procedures and are discussed in detail in **Papers I**, **II** and **III**. COSY, TOCSY and 1D SELTOCSY were used to assign the spin-systems. ^{13}C NMR experiments, DEPT135 and J-modulated spin-echo experiments, helped with assigning the carbons with different numbers of attached protons. Final correlations were assigned and confirmed with HSQC and HMBC NMR experiments. The attachment positions of thiols were confirmed with HMBC experiments that identified correlations between protons and heteroatoms through bonds in the molecule. ROESY NMR experiments gave final stereochemical information and confirmation of assigned chemical shifts.

The ketone on the C-8 position under different solvent systems forms a hemiketal. Its presence can be confirmed by HMBC correlations from the H-16 methyl protons to C-8 at about 200 ppm for the ketone, and 105 ppm for the hemiketal isomer. DON and its mercaptoethanol conjugates were dissolved in acetonitrile-d_3 (**Paper I**), and to our knowledge it is a first time chemical shifts of DON were reported in deuterated acetonitrile. DON–GSH and DON–Cys conjugates were dissolved in D$_2$O, due to their low solubility in acetonitrile, with the addition of 0.9% of acetic acid-d_4 to prevent reverse Michael addition. In acetonitrile-d_3, DON had a hemiketal:ketone ratio of 5:95, the DON-13-mercaptoethanol adduct (Figure 46) had a ratio of 84:16, and DON-10,13-dimercaptoethanol adduct was fully in a hemiketal form (Figure 46). In D$_2$O with 0.9% acetic acid, the hemiketal:ketone ratio of DON was 9:89, while both DON-10-Cys and DON-10-GSH conjugates had a hemiketal:ketone ratio of ca 70:30, and the DON-13-Cys and DON-13-GSH conjugates had a ratio of 91:9 (**Papers II** and **III**). It appears that the degree of intramolecular cyclization is more favorable for adducts, especially the epoxide adduct, given that they are predominantly in the hemiketal form, in contrast to DON.

Correlations in the ROESY and NOESY spectra were results of the cross-relaxation, and include real cross-peaks caused by the nuclear Overhauser effect (NOE) between nearby protons, but also correlations caused by chemical or conformational change. Real NOE cross-peaks were in the opposite phase from the diagonal, so they were easily distinguished in ROESY spectra, but TOCSY spectra of DON–Cys and DON–GSH had some additional correlations detectable between protons of hemiketal and ketone spin systems. These additional cross-peaks most likely arise from a fast conformational exchange between the resonances of the hemiketal and ketone during the mixing time of the experiments due to the presence of acid in the solvent.[161,206]

ROESY and NOESY NMR experiments were used to determine the stereochemistry of the molecules and to confirm the chemical shifts assigned from the other NMR experiments. As Michael adducts (DON-10-thiol conjugates), have four possible diastereoisomers, most notable NOE correlation and a key in distinguishing between them is a correlation between β-oriented H-7 and H-9, H-10, H-15 and H-16 (as discussed in section 5.3.1.1.2.).

5.3.1.1. Step-by-step NMR elucidation of DON–Cys adducts (Paper II)

All the structures were established in a similar way (**Papers I–III**) and this section illustrates the approaches used for structural elucidation using DON–Cys conjugates as an example.

Structural elucidation using solution-state NMR for two of the purified DON–Cys conjugates started with a short 1D ^{1}H NMR experiment to get a cursory insight about where the signals are. Amounts of the compounds that were purified were in microgram range (DON-10-Cys, 70 µg; DON-13-Cys, 71 µg; DON-10-GSH, 143 µg; DON-13-GSH, 572 µg), and even though samples were freeze dried before being dissolved in deuterated solvent, the residual water peak dominated the spectra. In order to improve signal-to-noise, the next step was then to choose 1D ^{1}H NMR experiment that includes presaturation, to adjust the frequency that will be irradiated, and to optimize the power level of the pulse. Optimized values can also be transferred to 2D proton detected experiments that also use presaturation (e.g. COSY, TOCSY and NOESY/ROESY). Once a good ^{1}H NMR spectrum is obtained, to determine skeletal connectivity, the experiments are set in order—COSY (to determine geminal protons), TOCSY (to identify the spin-systems), HSQC (to identify each proton uniquely and the carbon that it is attached to), HMBC (to identify quaternary carbons, and carbons and protons that are three bonds away from each other, and to connect the spin systems) and ROESY/NOESY (to determine stereochemistry of the molecule based on the correlations between protons that are close in space). Last two experiments run are usually 1D ^{13}C experiments DEPT135 and J-modulated spin-echo or standard ^{13}C with a 70° flip angle.

^{1}H NMR of DON–Cys conjugates revealed that, even though there was one peak present in the LC–MS chromatogram for each of them, they were actually a mixture of two isomeric compounds (an equilibrium mixture of the hemiketal and ketone forms), as there were two sets of signals present in the NMR spectra, which was most obvious from the methyl peaks (Figure 48).

DON was analyzed in the same solvent as the DON–Cys adducts (D$_2$O+0.9% CD$_3$COOD) for signal comparison.
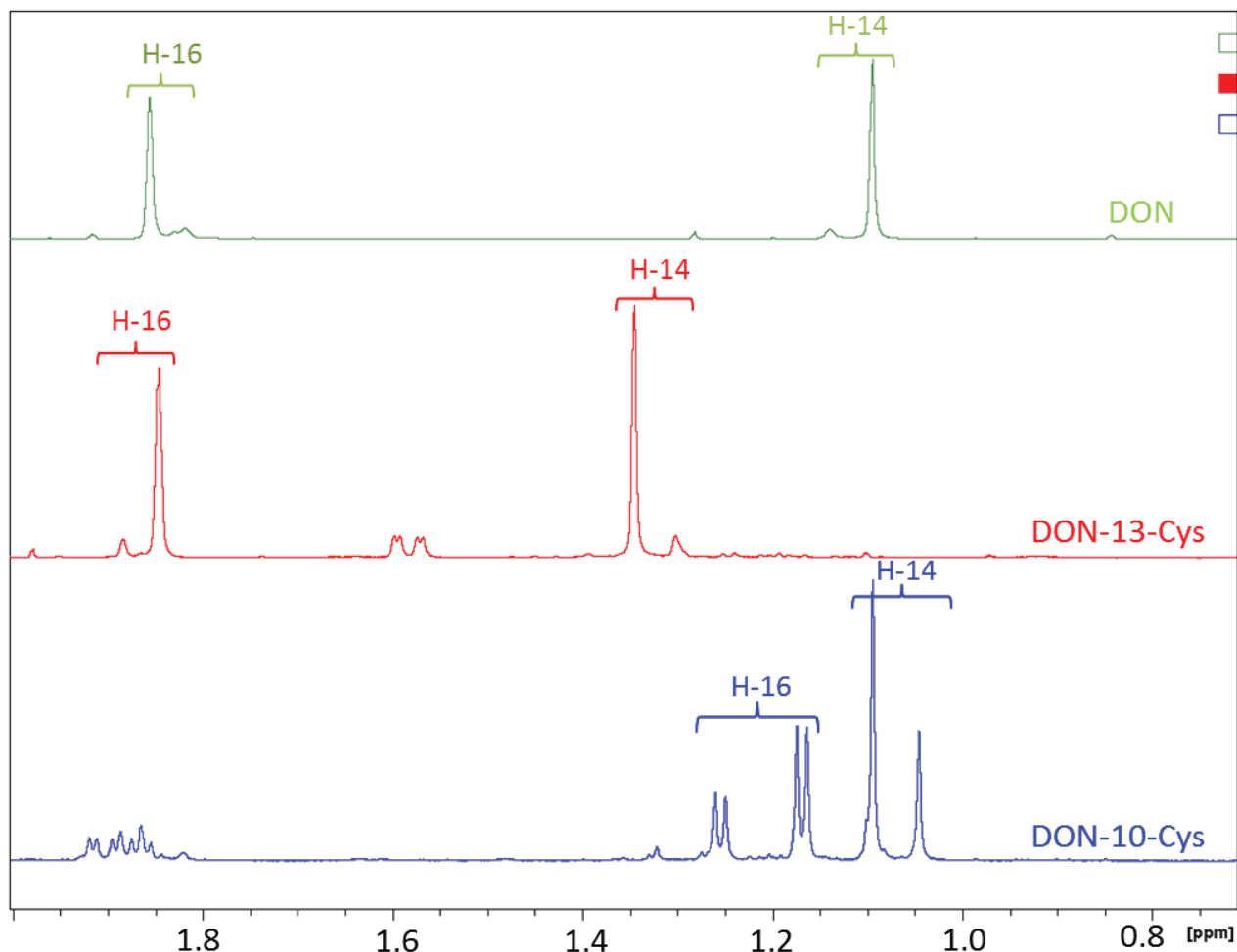
Figure 48. Comparison of the selected methyl region of 1D ^{1}H NMR spectra of DON, DON-13-Cys and DON-10-Cys in D$_2$O/CD$_3$COOD. Two methyl signal pairs show that the analyzed compounds were present as a mixture of isomers (hemiketal–ketone). Once Cys is added to DON, the hemiketal is more prefered over the ketone form (DON-10-Cys is in ca 70:30, and DON-13-Cys in 91:9 hemiketal:ketone ratio).

5.3.1.1.1. NMR spectroscopic analysis of DON-13-Cys

The discussion here is mainly related to the major isomer of DON-13-Cys, as the signal strength for some of the minor isomer signals was not sufficient for the full assignment. COSY and TOCSY NMR spectra of DON-13-Cys revealed six short spin systems. The best signal to start

the structural elucidation is the H-16 methyl singlet. TOCSY correlations from 1.90 ppm (H-16) were to a doublet of quartets at 5.65 ppm belonging to the olefinic proton (H-10), and to doublet at 4.96 ppm (H-11). The downfield chemical shifts of H-16 and H-10 in this adduct were almost the same as in DON, indicating that the double bond is preserved. The HSQC spectrum was used to assign the carbons that these protons were attached to. The chemical shift of C-10 (121.3 ppm) in DON-13-Cys was also similar to the chemical shift for C-10 in DON (122.0 ppm). The HMBC NMR spectrum showed correlations from H-16 to 121.3 ppm (C-10) and to a quaternary carbon 141.4 ppm (C-9). H-16 of the major isomer also showed an HMBC NMR correlation to 104.2 ppm (C-8), while the minor H-16 (1.95 ppm) showed a correlation to 201.4 ppm (Figure 50), as well to two olefinic carbons at 135.6 ppm (C-9) and 137.4 ppm (C-10). The C-8 carbon was assigned as a hemiketal (major) carbon and a ketone (minor) carbon, based on the chemical shifts typical for these carbons[207] and the HMBC correlations. The proton H-10 in the ketone form of DON has a chemical shift at 6.70 ppm, but in the hemiketal form, that signal shifts to 5.58 ppm. The minor isomer of DON-13-Cys showed COSY and TOCSY correlations from the minor H-16 methyl peak at 1.95 ppm to an olefinic proton at 6.68 ppm (H-10).
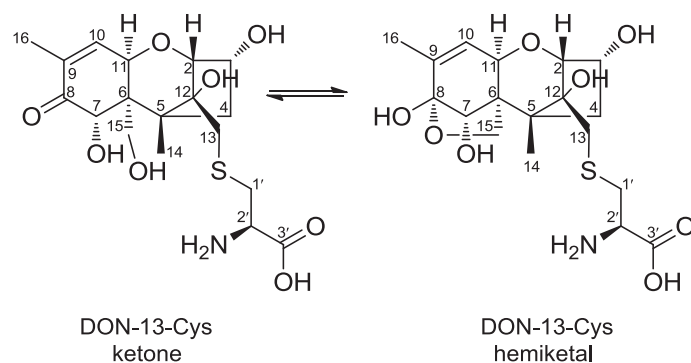
Figure 49. Structures of the DON-13-Cys ketone and hemiketal conjugate. The numbering used for the Cys side chain (**Paper II**) is not according to IUPAC standards and differs from the numbering used for DON–GSH analogs (**Paper III**).

Table 1. Observed multiplicities, coupling constants and correlations in COSY, TOCSY, HMBC and NOESY/ROESY NMR experiments from which the chemical shifts of DON-13-Cys were assigned.

atom	^{13}C	Type	^1H	Multiplicity, J(Hz)	COSY	TOCSY	HMBC ($^1H\to{}^{13}C$)	NOESY/ROESY
							DON-13-Cys (hemiketal)	
2	79.0	CH	4.18	d, 4.6	4.72 (H-3)	1.65 (H-4$_{pro\text{-}R}$) 2.21 (H-4$_{pro\text{-}S}$) 4.72 (H-3)	43.3 (C-4) 50.2 (C-5) 76.1 (C-11) 81.8 (C-12)	4.72 (H-3)
3	68.7	CH	4.72	dq, 10.5, 4.6	1.65 (H-4$_{pro\text{-}R}$) 2.21 (H-4$_{pro\text{-}S}$) 4.18 (H-2)	1.65 (H-4$_{pro\text{-}R}$) 2.21 (H-4$_{pro\text{-}S}$) 4.18 (H-2)	43.3 (C-4) 50.2 (C-5)	2.21 (H-4$_{pro\text{-}S}$) 4.18 (H-2)
4	43.3	CH$_2$	1.65	dd, 14.5, 4.6	2.21 (H-4$_{pro\text{-}S}$) 4.72 (H-3)	2.21 (H-4$_{pro\text{-}S}$) 4.18 (H-2) 4.72 (H-3)	50.6 (C-6) 68.7 (C-3) 81.8 (C-12)	2.21 (H-4$_{pro\text{-}S}$) 4.37 (H-15) 4.96 (H-11)
			2.21	dd, 14.5, 10.5	1.65 (H-4$_{pro\text{-}R}$) 4.72 (H-3)	1.65 (H-4$_{pro\text{-}R}$) 4.18 (H-2) 4.72 (H-3)	14.8 (C-14) 50.6 (C-6) 68.7 (C-3) 79.0 (C-2)	1.40 (H-14) 1.65 (H-4$_{pro\text{-}R}$) 4.72 (H-3)
5	50.2	C						
6	50.6	C						
7	75.5	CH	4.23	s	None	None	76.1 (C-11) 68.9 (C-15) 104.2 (C-8)	3.32 (H-13$_{pro\text{-}R}$) 3.61 (H-13$_{pro\text{-}S}$)
8	104.2	C						
9	141.4	C						
10	121.3	CH	5.65	dq, 5.4, 1.5	1.90 (H-16) 4.96 (H-11)	1.90 (H-16) 4.96 (H-11)	15.1 (C-16) 50.6 (C-6) 104.2 (C-8)	1.90 (H-16) 4.96 (H-11)
11	76.1	CH	4.96	d, 5.4	1.90 (H-16) 5.65 (H-10)	1.90 (H-16) 5.65 (H-10)	50.2 (C-5) 141.4 (C-9) 121.3 (C-10)	3.57 (H-15$_{pro\text{-}S}$) 4.37 (H-15$_{pro\text{-}R}$) 5.65 (H-10)
12	81.8	C						
13	34.7	CH$_2$	3.32	d, 13.5	3.61 (H-13$_{pro\text{-}S}$)	3.61 (H-13$_{pro\text{-}S}$)	33.6 (C-1') 81.8 (C-12)	3.61 (H-13$_{pro\text{-}S}$)
			3.61	d, 13.5	3.32 (H-13$_{pro\text{-}R}$)	3.32 (H-13$_{pro\text{-}R}$)	33.6 (C-1') 50.2 (C-5) 79.0 (C-2) 81.8 (C-12)	3.32 (H-13$_{pro\text{-}R}$) 4.23 (H-7)
14	14.8	CH$_3$	1.40	s	None	None	43.3 (C-4) 50.2 (C-5) 50.6 (C-6) 81.8 (C-12)	2.21 (H-4$_{pro\text{-}S}$) 3.32 (H-13$_{pro\text{-}R}$) 4.37 (H-15$_{pro\text{-}R}$)
15	68.9	CH$_2$	4.37	d, 9.3	3.57 (H-15$_{pro\text{-}S}$)	3.57 (H-15$_{pro\text{-}S}$)	50.6 (C-6) 76.1 (C-11) 104.2 (C-8)	1.40 (H-14) 1.65 (H-4$_{pro\text{-}R}$) 3.57 (H-15$_{pro\text{-}S}$) 4.96 (H-11)
			3.57	d, 9.3	4.37 (H-15$_{pro\text{-}R}$)	4.37 (H-15$_{pro\text{-}R}$)	50.2 (C-5) 76.1 (C-11) 104.2 (C-8)	1.40 (H-14) 1.65 (H-4$_{pro\text{-}R}$) 4.37 (H-15$_{pro\text{-}R}$) 4.96 (H-11)
16	15.1	CH$_3$	1.90	br s	4.96 (H-11) 5.65 (H-10)	4.96 (H-11) 5.65 (H-10)	104.2 (C-8) 121.3 (C-10) 141.4 (C-9)	4.96 (H-11) 5.65 (H-10)
1'	33.6	CH$_2$	3.30	(m)	4.09 (H-2')	4.09 (H-2')	34.7 (C-13) 53.5 (C-2') 172.5 (C-3')	4.09 (H-2')
2'	53.5	CH	4.09	br t, 5.0	3.30 (H-1')	3.30 (H-1')	33.6 (C-1') 172.5 (C-3')	3.30 (H-1')
3'	172.5	C						
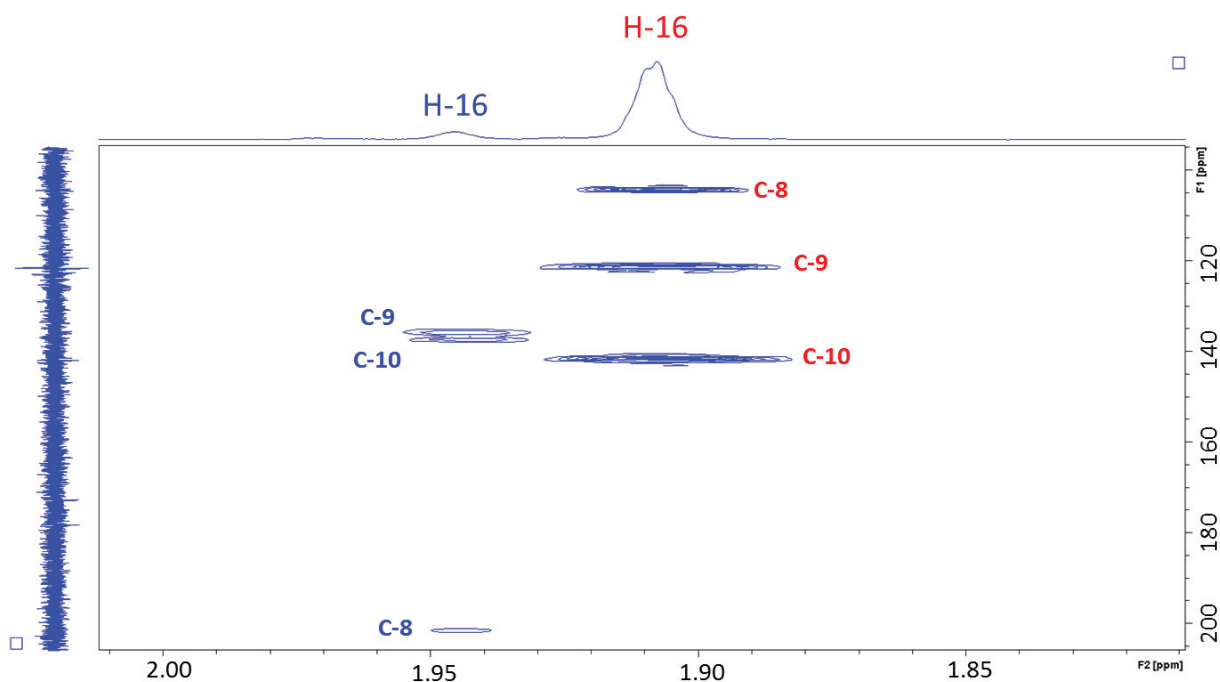
Figure 50. Selected region of the HMBC NMR spectrum of DON-13-Cys showing correlations from H-16 (1.90 ppm) of the major isomer (hemiketal, red) to 104.2 ppm (C-8), while the minor H-16 (1.95 ppm) showed a correlation to a carbonyl carbon at 201.4 ppm (C-8) of the minor isomer (ketone, blue).

The edited HSQC NMR spectrum differentiates between CH_3 and CH (positive phase) and CH_2 (negative phase). The HSQC NMR spectrum revealed the presence of four CH_2 groups for the major isomer. They belonged to H-4$_{\text{pro-}R}$/H-4$_{\text{pro-}S}$, H-13$_{\text{pro-}R}$/H-13$_{\text{pro-}S}$ and H-15$_{\text{pro-}R}$/H-15$_{\text{pro-}S}$ protons of DON, and one pair of signals from the H-1′ pair of the attached cysteine. The methylene protons, H-13$_{\text{pro-}R}$/H-13$_{\text{pro-}S}$ from the epoxy group in DON were two doublets at 3.28 ppm and 3.29 ppm, and J 3.7 Hz. In contrast, the corresponding methylene protons (H-13$_{\text{pro-}R}$/H-13$_{\text{pro-}S}$), in DON-13-Cys were doublets at 3.32 ppm and 3.61 ppm with J 13.5 Hz, indicating ring opening. Both of the H-13 doublets showed HMBC correlations to 33.6 ppm (C-1′) and 81.8 ppm (C-12), but only H-13$_{\text{pro-}R}$ showed additional correlations to 50.2 ppm (C-5) and 79.0 ppm (C-2) (Figure 51).
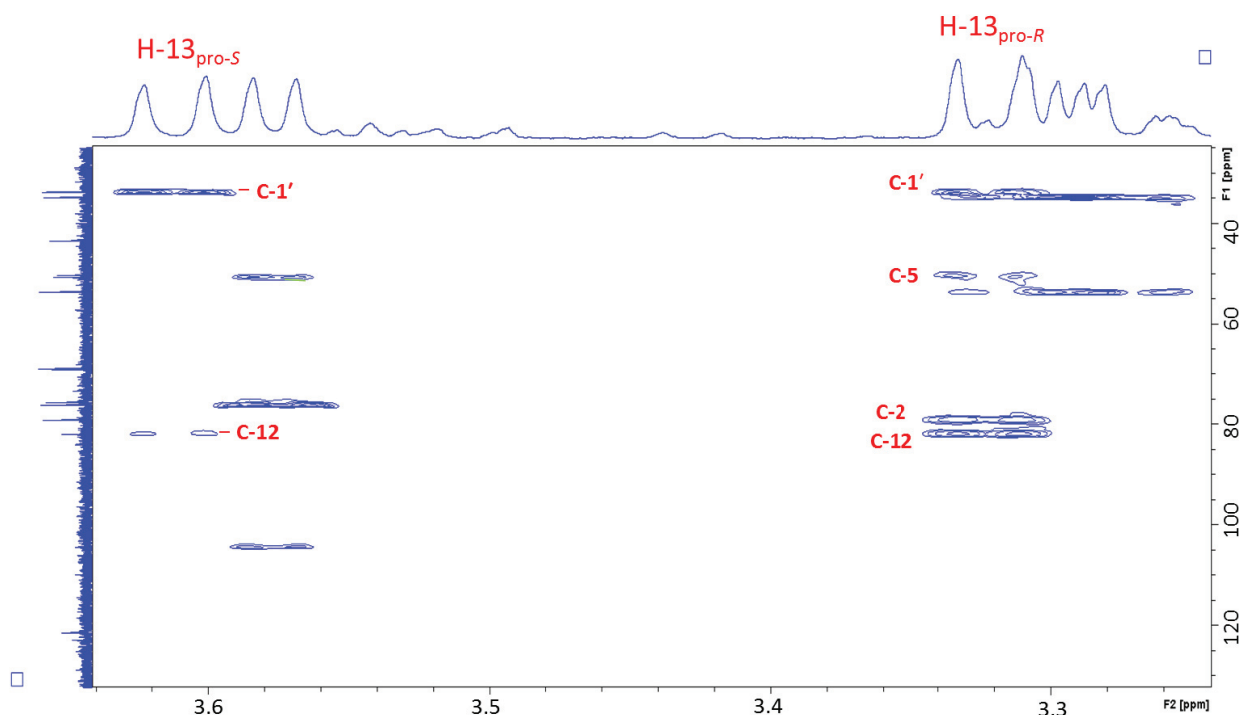
Figure 51. Selected HMBC area of DON-13-Cys showing correlations between H-13 protons and attached cysteine C-1′ carbon.

Cysteine protons at 3.30 ppm (H-1′), showed HMBC correlations to 53.5 ppm (C-2′) and 172.5 ppm (C-3′), but also to 34.7 ppm (C-13) which confirmed the attachment position of cysteine. Additionally, ROESY showed NOE correlations from 3.30 ppm (H-1′) to proton at 3.61ppm (H-13$_{pro-S}$), and to 4.09 ppm (H-2′), unambiguously placed the cysteine on the epoxide moiety.

Another useful signal to start the assignment of chemical shifts is the H-14 methyl signal (1.40 ppm). In DON-13-Cys this signal was shifted downfield compared to DON (1.09 ppm) (and DON-10-Cys, 1.08 ppm) (Figure 48). The HMBC correlations from H-14 (1.40 ppm) to three quaternary carbons at 50.2 ppm (C-5), 50.6 ppm (C-6), and 81.8 ppm (C-12), as well to 43.3 ppm (C-4) were useful for the assignment of the part of the molecule without protons.

Another small spin system in the major isomer confirmed with COSY/TOCSY spectra was H-15$_{pro-R}$/H-15$_{pro-S}$, two doublets at 4.37 ppm and 3.57 ppm with J 9.3 Hz. In ketone form of DON, chemical shifts of 15a/H-15b are 3.79 ppm and 3.86 ppm with J 12.6 Hz, and the change in the coupling constant indicated that there has been some change in the structure. The HMBC correlations from 15$_{pro-R}$/H-15$_{pro-S}$ of DON-13-Cys to 50.2 ppm (C-5), 50.6 ppm (C-6), 104.2 ppm (C-8) and 76.1 ppm (C-11) confirmed the major isomer as the hemiketal, as the HMBC correlations are showing carbons that are only 2–3 bonds away and hemiketal carbon C-8 is in that distance from the C-15 in hemiketal form. The NOE correlations showed that H-15$_{pro-R}$ at

76

4.37 ppm is closer to 1.40 ppm (H-14), and that H-15$_{pro-S}$ at 3.57 ppm is closer to 4.96 ppm (H-11), making it possible to sterically distinguish between those two methylene protons.

5.3.1.1.2. NMR spectroscopic analysis of DON-10-Cys

In contrast to DON and DON-13-Cys (Figure 48), DON-10-Cys (Figure 52) did not contain the olefinic proton at the 5.5-6.9 ppm and the downfield signal for H-16 methyl was shifted upfield and appeared as doublets with $J = 6.5$ Hz, indicating the attachment of a proton at C-9 that is splitting the methyl signal. Based on the two pairs of H-14 and H-16 signals, it is visible that the analysed sample is a mixture of two isomers (Figure 48). TOCSY and SELTOCSY NMR spectra showed coupling from H-16 methyl of the minor and major isomers (1.25/1.16 ppm) to 2.83/1.86 ppm (H-9), doublets of doublets at 3.48/3.05 ppm (H-10) and doublets at 4.77/4.59 ppm (H-11). Carbons of these protons were identified in the HSQC spectrum, and the HMBC NMR spectrum confirmed that the minor isomer is a ketone, and the major one is a hemiketal, based on the observed correlations from H-16 (1.25/1.16 ppm) to C-9 (44.1/43.0 ppm), C-10 (52.5/50.2 ppm) and C-8 (213.6/107.3 ppm) (Figure 53).
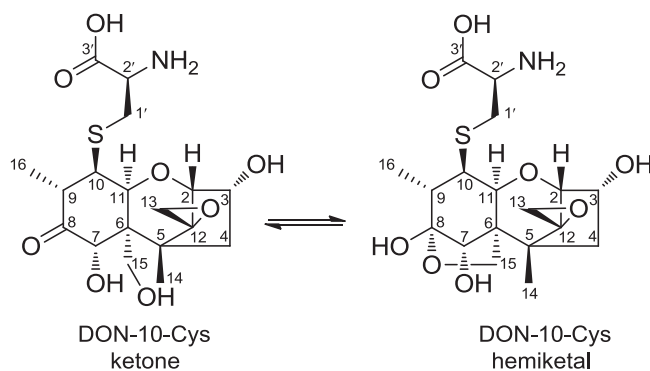

Figure 52. Structures of the ketone and hemiketal form of DON-10-Cys conjugate. The numbering used for Cys side chain (**Paper II**) is is not according to IUPAC standards and differs from the numbering used for DON–GSH analogs (**Paper III**).

Table 2. Observed multiplicities, coupling constants and correlations in COSY, TOCSY, HMBC and NOESY/ROESY NMR experiments from which the chemical shifts of hemiketal isomer of DON-10-Cys assignments were based on.

| atom	13C	Type	1H	Multiplicity, J(Hz)	COSY	TOCSY	HMBC (^{1}H→^{13}C)	NOESY/ROESY
							DON-10-Cys (hemiketal)	
2	82.4	CH	3.74	d, 4.5	4.52 (H-3)	1.89 (H-4$_{pro-R}$) 2.07 (H-4$_{pro-S}$) 4.52 (H-3)	44.4 (C-5) 68.4 (C-12) 75.5 (C-11)	3.27 (H-13$_{pro-S}$) 3.35 (H-13$_{pro-R}$) 4.52 (H-3)
3	69.53	CH	4.52	dt, 10.9, 4.5	1.89 (H-4$_{pro-R}$) 2.07 (H-4$_{pro-S}$) 3.74 (H-2)	1.89 (H-4$_{pro-R}$) 2.07 (H-4$_{pro-S}$) 3.74 (H-2)	44.9 (C-4) 82.4 (C-2)	1.89 (H-4$_{pro-R}$) 2.07 (H-4$_{pro-S}$) 3.74 (H-2)
4	44.9	CH$_2$	1.89	dd, 4.5, 14.5	2.07 (H-4$_{pro-S}$) 4.52 (H-3)	2.07 (H-4$_{pro-S}$) 3.74 (H-2) 4.52 (H-3)	44.4 (C-5) 56.6 (C-6) 69.53 (C-3)	2.07 (H-4$_{pro-S}$) 3.70 (H-15$_{pro-S}$) 4.59 (H-11)
			2.07	dd, 10.9, 14.5	1.89 (H-4$_{pro-R}$) 4.52 (H-3)	1.89 (H-4$_{pro-R}$) 3.74 (H-2) 4.52 (H-3)	44.4 (C-5) 56.6 (C-6) 69.53 (C-3) 82.4 (C-2)	1.08 (H-14) 1.89 (H-4$_{pro-R}$) 4.52 (H-3)
5	44.4	C						
6	56.6	C						
7	77.0	CH	3.99	s	None	None	43.0 (C-9) 56.6 (C-6) 68.5 (C-15) 75.5 (C-11) 107.3 (C-8)	1.86 (H-9) 3.35 (H-13$_{pro-R}$)
8	107.3	C						
9	43.0	CH	1.86	dq, 11.9, 6.5	1.16 (H-16) 3.05 (H-10)	1.16 (H-16) 3.05 (H-10)	13.1 (C-16) 50.2 (C-10) 77.0 (C-7) 107.3 (C-8)	1.16 (H-16) 3.05 (H-10) 3.99 (H-7)
10	50.2	CH	3.05	11.99, 5.8	1.86 (H-9) 4.59 (H-11)	1.16 (H-16) 1.86 (H-9) 4.59 (H-11)	13.1 (C-16) 32.0 (C-1') 43.0 (C-9)	1.16 (H-16) 1.86 (H-9) 3.70 (H-15$_{pro-S}$) 4.59 (H-11)
11	75.5	CH	4.59	d, 5.8	3.05 (H-10)	1.16 (H-16) 1.86 (H-9) 3.05 (H-10)	43.0 (C-9) 44.4 (C-5) 50.2 (C-10) 56.6 (C-6) 77.0 (C-7)	1.89 (H-4$_{pro-R}$) 3.05 (H-10) 3.46 (H-1'$_{pro-R}$) 3.70 (H-15$_{pro-S}$)
12	68.4	C						
13	49.2	CH$_2$	3.35	d, 3.8	3.27 (H-13$_{pro-S}$)	3.27 (H-13$_{pro-S}$)	44.4 (C-5) 68.4 (C-12) 82.4 (C-2)	1.08 (H-14) 3.99 (H-7)
			3.27	d, 3.8	3.35 (H-13$_{pro-R}$)	3.35 (H-13$_{pro-R}$)	44.4 (C-5) 68.4 (C-12) 82.4 (C-2)	3.74 (H-2) 3.99 (H-7)
14	15.2	CH$_3$	1.08	s	None	None	44.4 (C-5) 44.9 (C-4) 56.6 (C-6) 68.4 (C-12)	2.07 (H-4$_{pro-S}$) 4.23 (H-15$_{pro-R}$) 3.35 (H-13$_{pro-R}$)
15	68.5	CH$_2$	4.23	d, 8.5	3.70 (H-15 pro-S)	3.70 (H-15 pro-S)	44.4 (C-5) 56.6 (C-6) 75.5 (C-11)	1.08 (H-14) 3.70 (H-15$_{pro-S}$)
			3.70	d, 8.5	4.23 (H-15$_{pro-R}$)	4.23 (H-15$_{pro-R}$)	56.6 (C-6) 75.5 (C-11) 107.3 (C-8)	4.23 (H-15$_{pro-R}$) 4.59 (H-11)
16	13.1	CH$_3$	1.16	d, 6.5	1.86 (H-9)	1.86 (H-9) 3.05 (H-10) 4.59 (H-11)	43.0 (C-9) 50.2 (C-10) 107.3 (C-8)	1.86 (H-9) 3.05 (H-10)
1'	32.0	CH$_2$	3.46	dd, 14.8, 6.3	3.15 (H-1'$_{pro-S}$) 4.00 (H-2')	3.15 (H-1'$_{pro-S}$) 4.00 (H-2')	49.2 (C-13) 54.9 (C-2') 173.6 (C-3')	3.15 (H-1'$_{pro-S}$) 4.00 (H-2') 4.59 (H-11)
			3.15	dd, 14.8, 4.5	3.46 (H-1'$_{pro-R}$) 4.00 (H-2')	3.46 (H-1'$_{pro-R}$) 4.00 (H-2')	49.2 (C-13) 54.9 (C-2') 173.6 (C-3')	3.46 (H-1'$_{pro-R}$) 4.00 (H-2')
2'	54.9	CH	4.00	dd, 6.3, 4.5	3.15 (H-1'$_{pro-S}$) 3.46 (H-1'$_{pro-R}$)	3.15 (H-1'$_{pro-S}$) 3.46 (H-1'$_{pro-R}$)	32.0 (C-1') 173.6 (C-3')	3.15 (H-1'$_{pro-S}$) 3.46 (H-1'$_{pro-R}$)
3'	173.6	C						

Table 3. Observed multiplicities, coupling constants and correlations in COSY, TOCSY, HMBC and NOESY/ROESY NMR experiments from which the chemical shifts of ketone isomer of DON-10-Cys assignments were based on.

atom	13C	Type	1H	Multiplicity, J (Hz)	COSY	TOCSY	HMBC ($^1H{\rightarrow}^{13}C$)	NOESY/ROESY
						DON-10-Cys (ketone)		
2	81.5	CH	3.77	d, 4.5	4.52 (H-3)	2.09 (H-4$_{pro-S}$) 2.25 (H-4$_{pro-R}$) 4.52 (H-3)	46.9 (C-5) 67.9 (C-12) 76.2 (C-11)	3.32 (H-13$_{pro-R}$) 4.52 (H-3)
3	69.49	CH	4.52	m	2.09 (H-4$_{pro-S}$) 2.25 (H-4$_{pro-R}$) 3.77 (H-2)	2.07 (H-4$_{pro-S}$) 2.25 (H-4$_{pro-R}$) 3.77 (H-2)	44.0 (C-4) 81.5 (C-2)	2.09 (H-4$_{pro-S}$) 3.77 (H-2)
4	44.0	CH$_2$	2.25	dd, 14.8, 4.3	2.09 (H-4$_{pro-S}$) 4.52 (H-3)	2.09 (H-4$_{pro-S}$) 3.77 (H-2) 4.52 (H-3)	46.9 (C-5) 56.4 (C-6) 69.49 (C-3)	2.09 (H-4$_{pro-S}$) 4.77 (H-11)
			2.09	dd, 14.8, 11.5	2.25 (H-4$_{pro-R}$) 4.52 (H-3)	2.25 (H-4$_{pro-R}$) 3.77 (H-2) 4.52 (H-3)	44.3 (C-5) 56.4 (C-6) 69.49 (C-3) 81.5 (C-2)	1.03 (H-14) 2.25 (H-4$_{pro-R}$) 4.52 (H-3)
5	46.9	C						
6	56.4	C						
7	75.9	CH	4.80	d, 1.1	None	None	46.9 (C-5) 56.4 (C-6) 60.2 (C-15) 213.6 (C-8)	2.83 (H-9) 3.23 (H-13$_{pro-S}$) 3.32 (H-13$_{pro-R}$)
8	213.6	C						
9	44.1	CH	2.83	dq, 12.8, 6.5	1.25 (H-16) 3.48 (H-10)	1.25 (H-16) 3.48 (H-10)	13.0 (C-16) 52.5 (C-10) 213.6 (C-8)	1.25 (H-16) 3.48 (H-10) 4.80 (H-7)
10	52.5	CH	3.48	dd, 12.8, 3.4	2.83 (H-9) 4.77 (H-11)	1.25 (H-16) 2.83 (H-9) 4.77 (H-11)	33.0 (C-1')	1.25 (H-16) 2.83 (H-9) 4.77 (H-11)
11	76.2	CH	4.77	d, 5.3	3.48 (H-10)	1.25 (H-16) 2.83 (H-9) 3.48 (H-10)	44.1 (C-9) 52.5 (C-10) 76.2 (C-7)	2.25 (H-4$_{pro-R}$) 3.48 (H-10) 3.70 (H-15)
12	67.9	C						
13	49.5	CH$_2$	3.32	d, 3.8	3.23 (H-13$_{pro-S}$)	3.23 (H-13$_{pro-S}$)	46.9 (C-5) 67.9 (C-12) 81.5 (C-2)	3.77 (H-2) 4.80 (H-7)
			3.23	d, 3.8	3.32 (H-13$_{pro-R}$)	3.32 (H-13$_{pro-R}$)	68.5 (C-12) 82.6 (C-2)	1.03 (H-14) 4.80 (H-7)
14	14.3	CH$_3$	1.03	s	None	None	44.0 (C-4) 46.9 (C-5) 56.4 (C-6) 67.9 (C-12)	2.09 (H-4$_{pro-S}$) 3.23 (H-13$_{pro-S}$) 3.85 (H-15)
15	60.2	CH$_2$	3.70	d, 12.4	3.86 (H-15)	3.86 (H-15)	56.4 (C-6) 75.9 (C-7) 76.2 (C-11)	2.25 (H-4$_{pro-R}$) 3.86 (H-15)
			3.86	d, 12.4	3.70 (H-15)	3.70 (H-15)	46.9 (C-5) 56.4 (C-6) 75.9 (C-7)	1.03 (H-14) 3.70 (H-15)
16	13.0	CH$_3$	1.25	d, 6.5	2.83 (H-9)	2.83 (H-9) 3.48 (H-10) 4.77 (H-11)	44.1 (C-9) 52.5 (C-10) 213.6 (C-8)	2.83 (H-9) 3.48 (H-10)
1'	33.0	CH$_2$	3.43	dd, 14.8, 8.0	3.20 (H-1'$_{pro-S}$) 4.15 (H-2')	3.20 (H-1'$_{pro-S}$) 4.15 (H-2')	49.5 (C-13) 54.4 (C-2') 173.6 (C-3')	3.20 (H-1'$_{pro-S}$) 4.15 (H-2')
			3.20	dd, 14.8, 4.1	3.43 (H-1'$_{pro-R}$) 4.15 (H-2')	3.43 (H-1'$_{pro-R}$) 4.15 (H-2')	49.5 (C-13) 54.4 (C-2') 173.6 (C-3')	3.43 (H-1'$_{pro-R}$) 4.15 (H-2')
2'	54.4	CH	4.15	dd, 8.0, 4.1	3.20 (H-1'$_{pro-S}$) 3.43 (H-1'$_{pro-R}$)	3.20 (H-1'$_{pro-S}$) 3.43 (H-1'$_{pro-R}$)	33.6 (C-1') 173.6 (C-3')	3.43 (H-1'$_{pro-R}$) 3.20 (H-1'$_{pro-S}$)
3'	173.6	C						
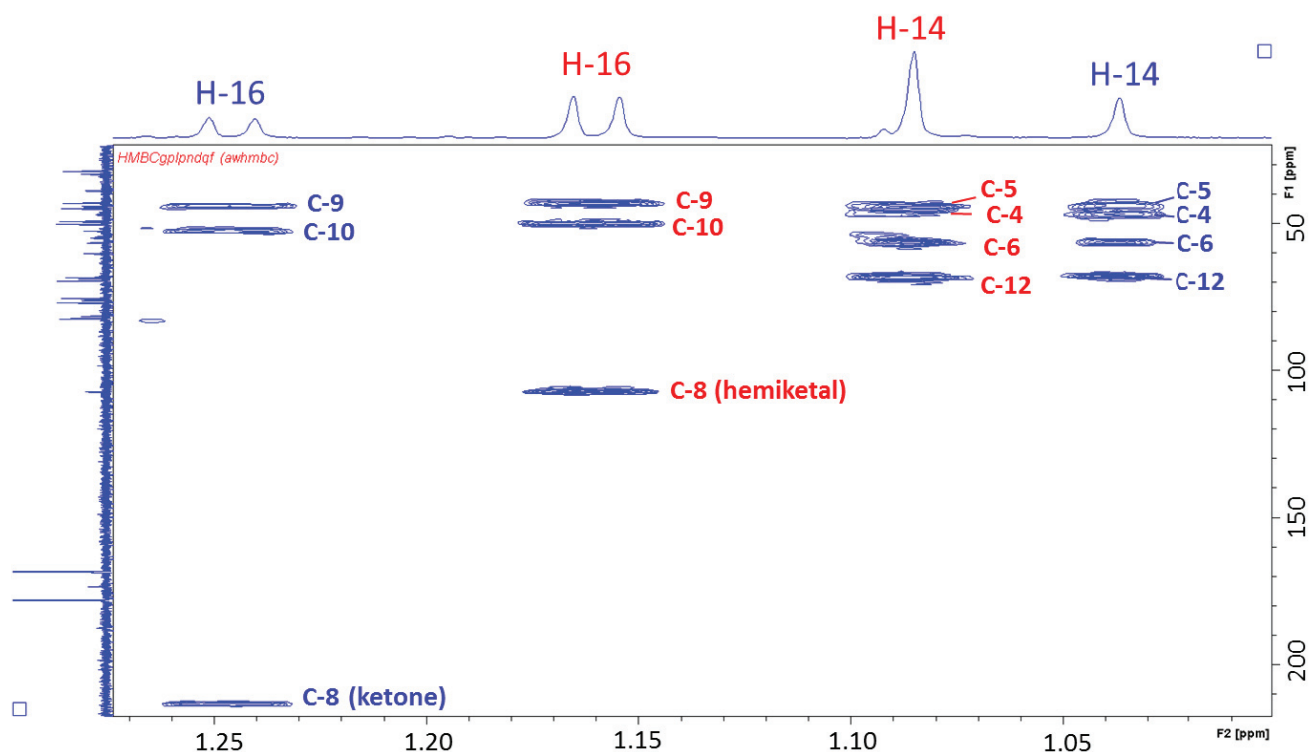
Figure 53. Selected area of HMBC spectrum of DON-10-Cys showing correlations from H-16 in the hemiketal and ketone isomers. Red and blue colors are used to help distinguish between major (hemiketal) and minor (ketone) isomer, respectively.

The rest of the ^{1}H-^{1}H connectivities were established using COSY, TOCSY and SELTOCSY experiments, and revealed six spin systems, very similar to the previously described DON-13-Cys epoxide adduct (Tables 2 and 3). Proton chemical shifts from the attached cysteine of both minor and major isomers were assigned from SELTOCSY experiments by irradiating 4.15/4.00 ppm (H-2′) and showing correlations to 3.46/3.43 ppm (H-1′$_{pro-R}$) and 3.15/3.20 ppm (H-1′$_{pro-S}$) (Figure 54).
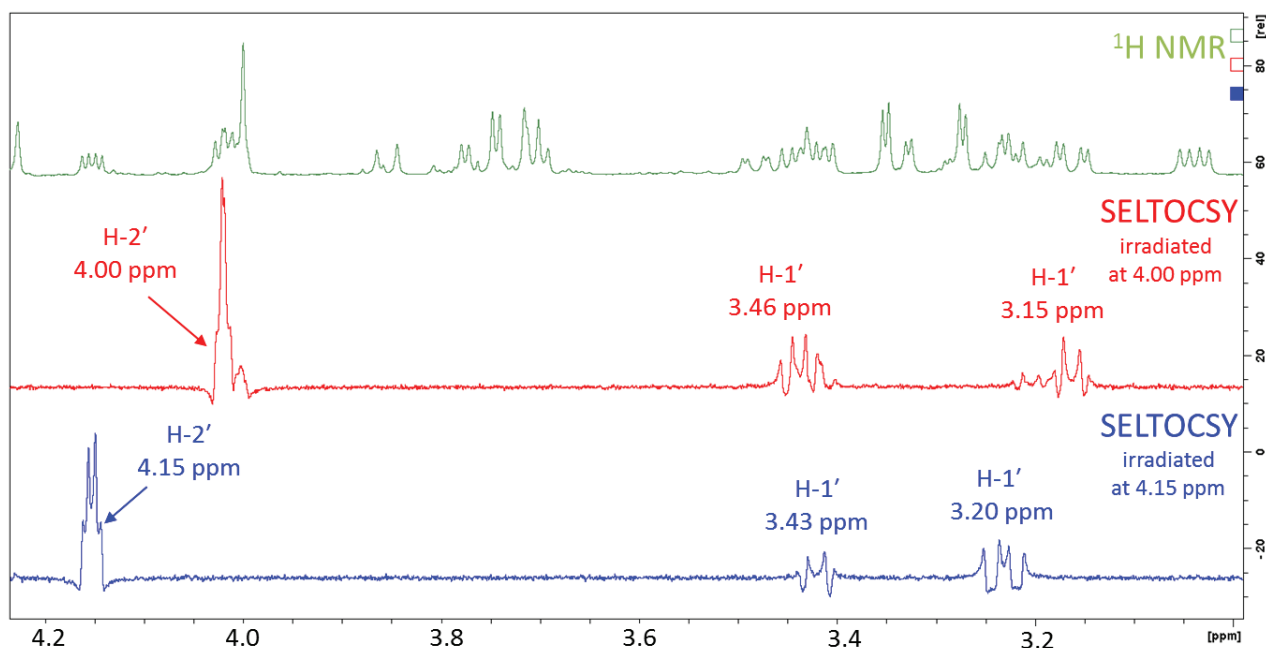
Figure 54. ^{1}H NMR spectrum and selective 1D TOCSY spectra of DON-10-Cys. Irradiation of H-2′ signals of major (hemiketal) and minor (ketone) isomers (4.00/4.15 ppm, red and blue, respectively) helped with resolving peaks and multiplets belonging to H-1′ protons of both, major and minor isomer.

The carbons these protons were attached to were identified from the HSQC spectrum of minor and major isomer (C-1′ (33.0/32.0 ppm) and C-2′ (54.4/54.9 ppm). The HMBC spectrum showed correlations from the cysteine side-chain methylene protons at 3.46/3.43 ppm (H-1′$_{pro-R}$) and 3.15/3.20 ppm (H-1′$_{pro-S}$) to C-10 (52.5/50.2 ppm) and C-2′ (54.5/54.9) and C-3′ (173.6/173.6 ppm) (Table 2, Figure 55), unambiguously confirming the attachment of cysteine via thiol group to C-10 of DON.
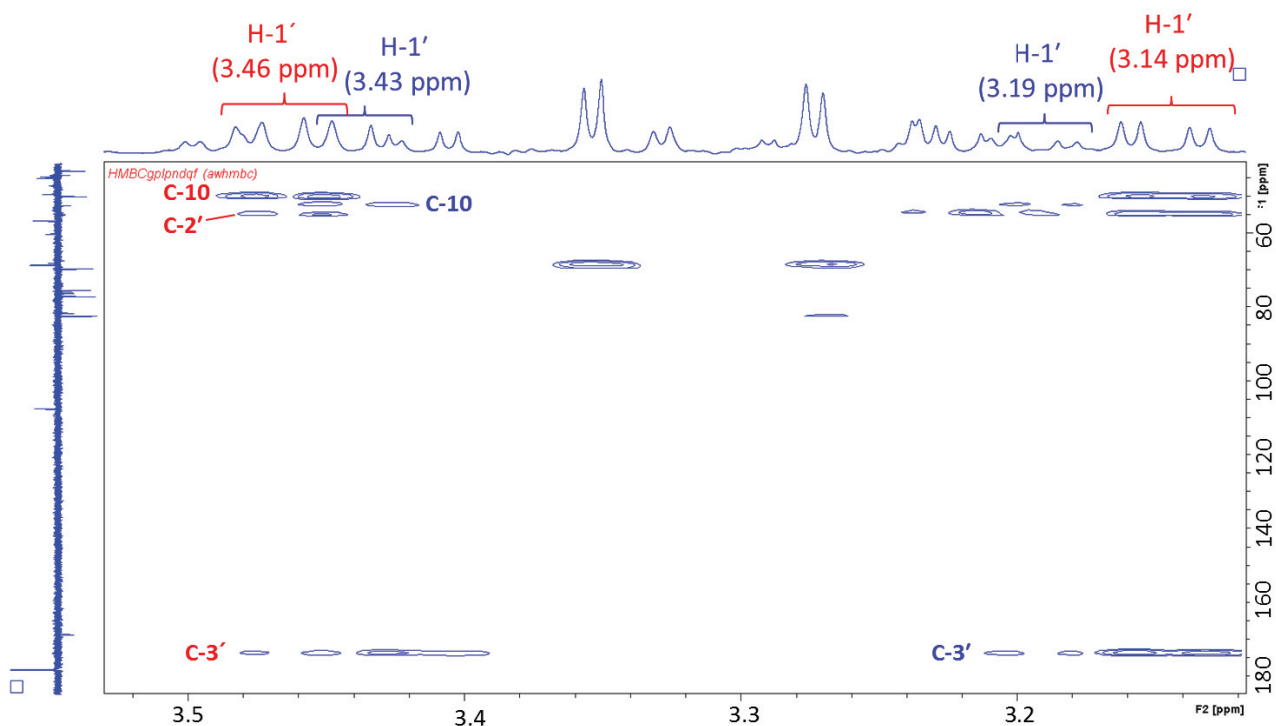
Figure 55. Selected HMBC area of DON-10-Cys showing correlations between attached cysteine C-1′ atom to C-10 atom of DON and to carboxylic atom C-3′, and C-2′. Red and blue colors are used to help distinguish between the signals of major and minor isomer, respectively.

HMBC correlations from H-10 (3.48/3.05 ppm) to C-1′ (33.0/32.0 ppm) and C-9 (44.1/43.0 ppm) confirmed the attachment position of cysteine to C-10.

Addition of thiol at C-10 can result in four diastereoisomeric products, where the thiol at C-10 and the methyl at C-9 are both on the same or opposite face as each other. All trichothecenes with 7-OH have a hydroxyl group α-oriented (below plane),[208] placing H-7 in β-orientation (above plane). In ROESY NMR experiments, the minor and major (ketone/hemiketal) DON-10-Cys isomers both showed NOE correlations between H-9 (2.83/1.86 ppm) and H-7 (4.80/3.99 ppm), indicating that the methyl at C-9 is below the plane. NOE correlations were also observed between H-10 (3.48/3.05 ppm) and H-11 (4.77/4.59 ppm) and H-16 (1.25/1.16 ppm), with the additional correlation from the major isomer H-10 (3.05 ppm) to H-15$_{pro-S}$ (3.70 ppm), placing the H-10 below plane and thus placing the attached cysteine in the β position (Tables 2 and 3, Figure 56).
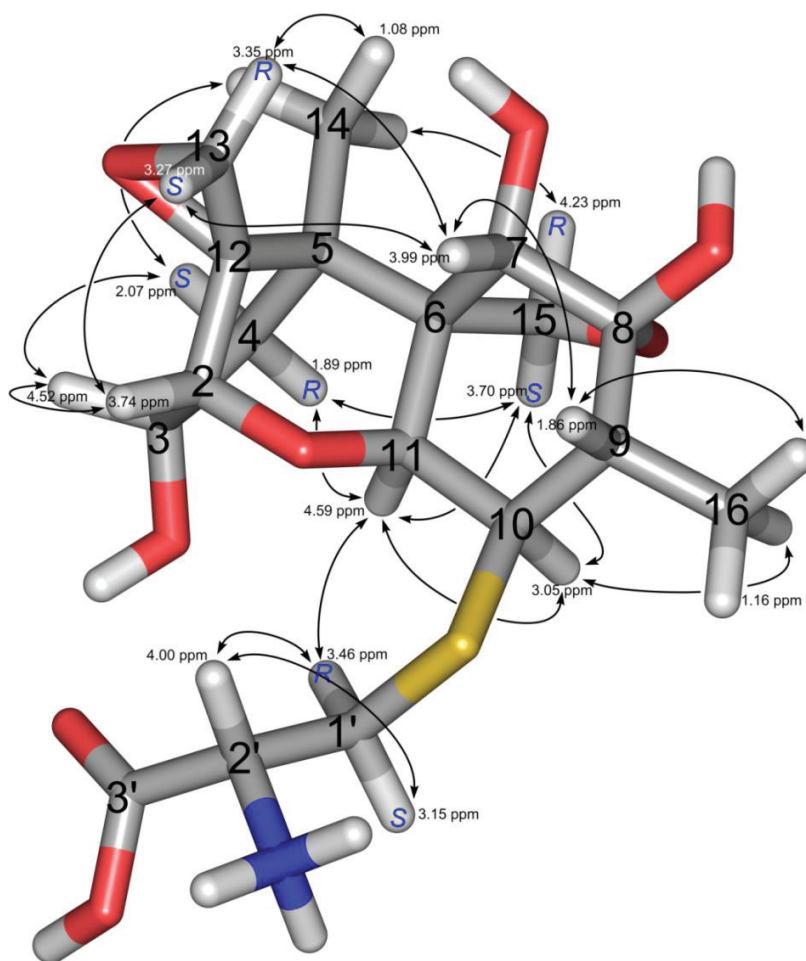
Figure 56. 3D model of the DON-10-Cys major hemiketal adduct, showing selected, structurally significant NOE correlations. Methylene protons marked S or R indicate pro-*R* or pro-*S* stereochemistry, respectively. This figure is adapted from Paper II, Figure 5.

5.3.2. Quantitation by NMR (qNMR)

As mentioned in the previous section, purified compounds were available in microgram amounts (Figure 57) and weighing would not be accurate enough for the preparation of quantitative analytical standards. A quantitative ¹H-NMR experiment, ERETIC2, was selected for quantitation (**Papers II** and **III**) due to several advantages over other NMR or LC–MS methods that would require an internal or external standard.
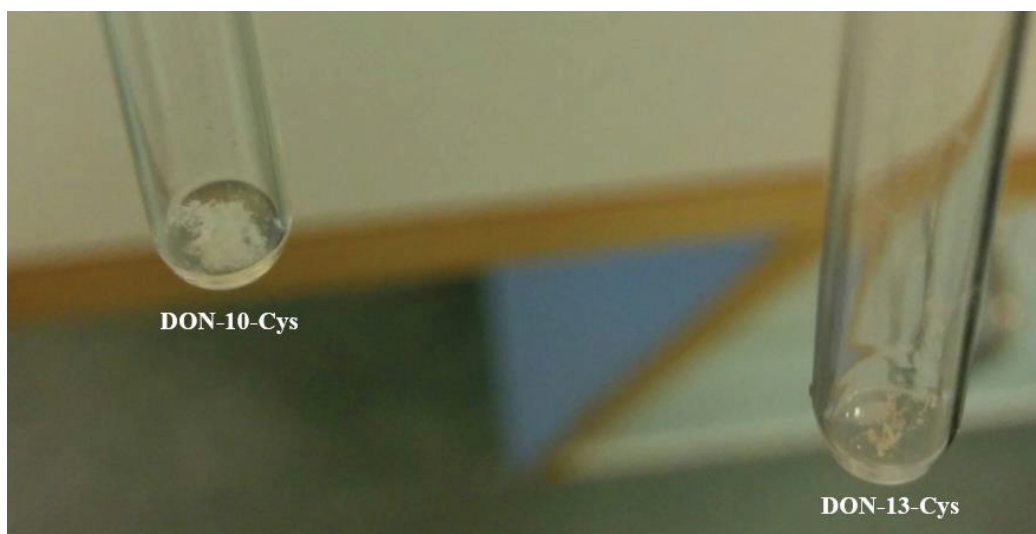
Figure 57. Purified DON–Cys adducts in the NMR tubes after the freeze-drying.

One of the advantages is that the reference compound does not need to be added to the sample, which was very important because the quantified samples were later used in cytotoxicity experiments. Furthermore, after the Fourier transformation of the acquired FID, the presence and the frequency position of the ERETIC signal can be freely chosen in the spectrum of the analyte so that the signal of the reference is not overlapping with the compound signals (Figure 58).

The intensity of ^{1}H signals is directly proportional to the number of nuclei and under certain conditions that are important to set up (a tuned and matched probe, a calibrated 90° pulse, a relaxation delay equal to at least 5T*1, sufficient signal-to-noise) prior to acquiring the spectra. It is also important to choose proton signals in the spectra that are not closely spaced or overlapping, and to integrate signal area as accurately as possible (by correct phasing and use of baseline correction). For each of the DON–thiol conjugates that were to be quantified, 10 consecutive qNMR experiments were carried out, and the H-14 and H-16 methyl signals and H-15 methylene protons were manually integrated, as these signals were sharp and well separated from other signals. The concentrations of the compounds were calculated (with reference to an ERETIC signal obtained from dioxane) by averaging the data. The accepted concentration was the one from the signal with the smallest standard deviation.
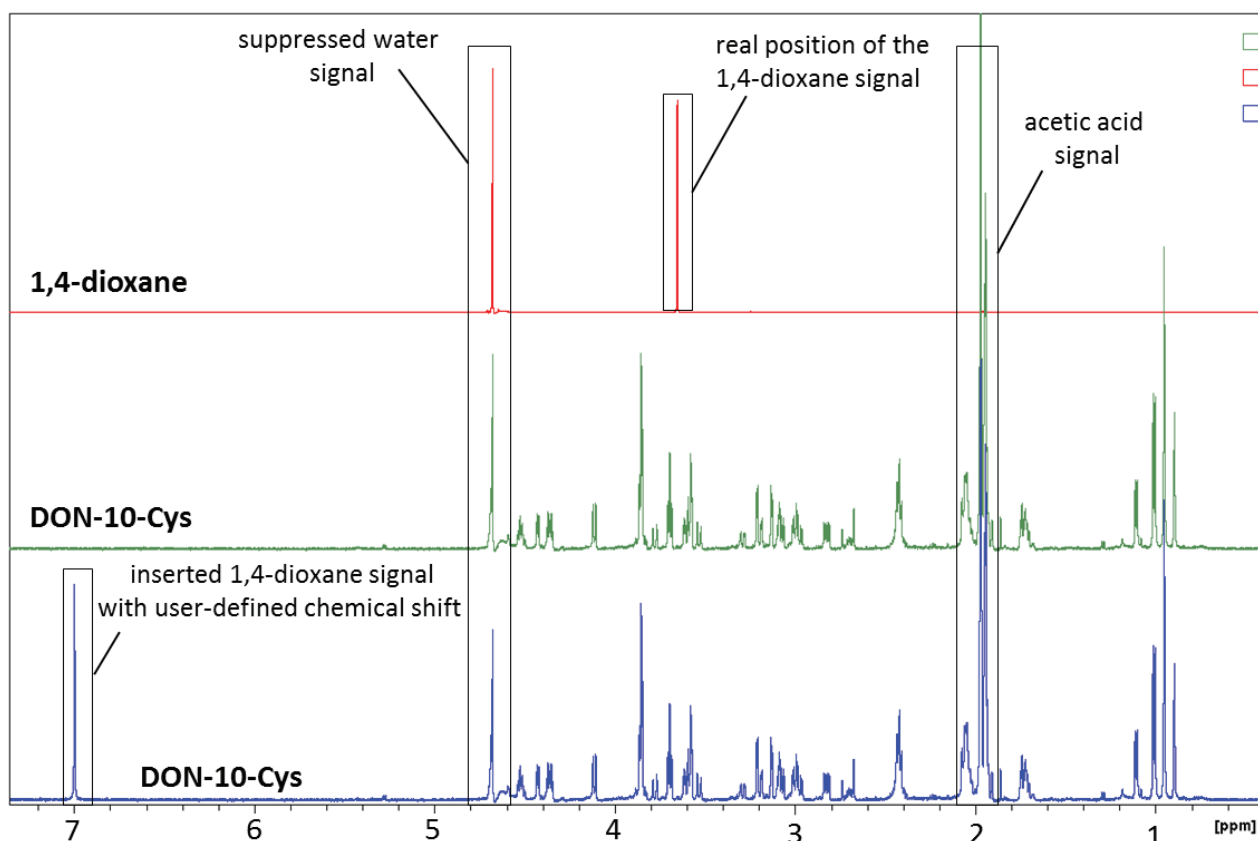
Figure 58. A solution of 1,4-dioxane in D$_2$O was taken as a calibration reference for the ERETIC signal. Its ^{1}H NMR spectrum shows a singlet at 3.75 ppm.[186] Once the ERETIC reference is defined, the user can define the chemical shift of the signal or choose if the ERETIC signal should be present in the spectrum or not.

5.3.3. Liquid chromatography-mass spectrometric analysis and characterization

LC–HRMS initially suggested the presence of both, mono- and diconjugates of DON-thiols is present in reaction mixtures, and C-10 or C-13 position of DON as the connection point of the thiol, which was later on confirmed by NMR spectroscopy. NMR spectra also revealed that intramolecular cyclization of the C-8 ketone form to an 8,15-hemiketal isomer is favorable for DON–thiol conjugates, and that the two forms are in the equilibrium. Thiol conjugation of DON at the C-10 position gives four possible diastereoisomers, where the methyl group at C-9 and the attached thiol on C-10 are both on the same side of the plane, or on opposite sides. All of this indicates the surprising complexity of the reaction. The NMR characterization of the major products was fundamental to the understanding of the reaction dynamics and for the interpretation of LC–MS chromatograms and the fragmentation patterns of the compounds.

In this study, LC–MS was used as a tool for different purposes, such as following the formation of the DON-thiol adducts with LC coupled to a low-resolution mass analyzer (linear ion trap) by real-time injections (**Papers I** and **II**) or by taking reaction mixture aliquots at different time points and diluting them (**Paper III**). Other experiments made use of LC coupled to a high resolution mass analyzer (Orbitrap), for example for determination of the elemental composition of reaction products or product ions from MS fragmentation. Orbitrap-based HRMS provides high resolution accurate mass ("HRAM") data that allows establishment of the elemental composition of ions with excellent accuracy. The fragmentation patterns gained from tandem MS/(HR)MS experiments are suitable for distinguishing the Michael adducts (C-10) and the epoxide adduct (C-13). DON–mercaptoethanol adducts (**Paper I**) afforded formate/acetate adducts (depending on the ingredients of the mobile phase used in LC), and their mass spectral fragmentation was therefore only studied in negative mode. To gain a better understanding of the product ions of DON–thiol conjugates, the fragmentation patterns were compared to those of the formate/acetate adducts of DON that were studied by multiple-stage ion trap MS^n. The most prominent product ions for DON were m/z 295, the deprotonated molecular ion of DON, m/z 265, due to loss of CH_2O, m/z 247 as a result of additional loss of water, and m/z 229, which was due to loss of an additional molecule of water, or m/z 217, which likely corresponded to an additional loss of CH_2O from m/z 247. The two losses of CH_2O could be assigned to the loss of the C-6 side chain or to loss of the epoxide group. Consistent with this assumption was the observation that the DON-13-mercaptoethanol monoadduct, as well as the 10,13-double adducts, afforded m/z 265, 247 and 229 product ions, and thus only a single loss of CH_2O, which is consistent with loss of the C-6 side chain. In contrast, C-10 Michael adducts afforded m/z 265, 247 and 217 fragments, which corresponded to loss of two CH_2O moieties. Another prominent product ion, present in the MS/MS spectra of Michael adducts, but not the C-13 epoxide adducts, was an m/z 138 ion. This ion was also observed in the MS/MS spectra from fragmentation of DON, suggesting that this ion could be connected with formation of a cyclohexene ring as shown in Figure 59. Proposed fragmentation pathways of DON-mercaptoethanol adducts are given in the Figures 59 and 60. MS fragmentation of the DON-mercaptoethanol Michael adduct afforded a major product ion with m/z 265. The same product ion was found in the epoxide adduct, however, it was not most prominent one and the fragmentation pathway to yield this ion is likely different for the two isomers (Figures 59 and 60). During the fragmentation of the DON-13-mercaptoethanol conjugate, a linkage between the 7-OH group and C-13 could be formed during the thiol elimination (Figure 59).
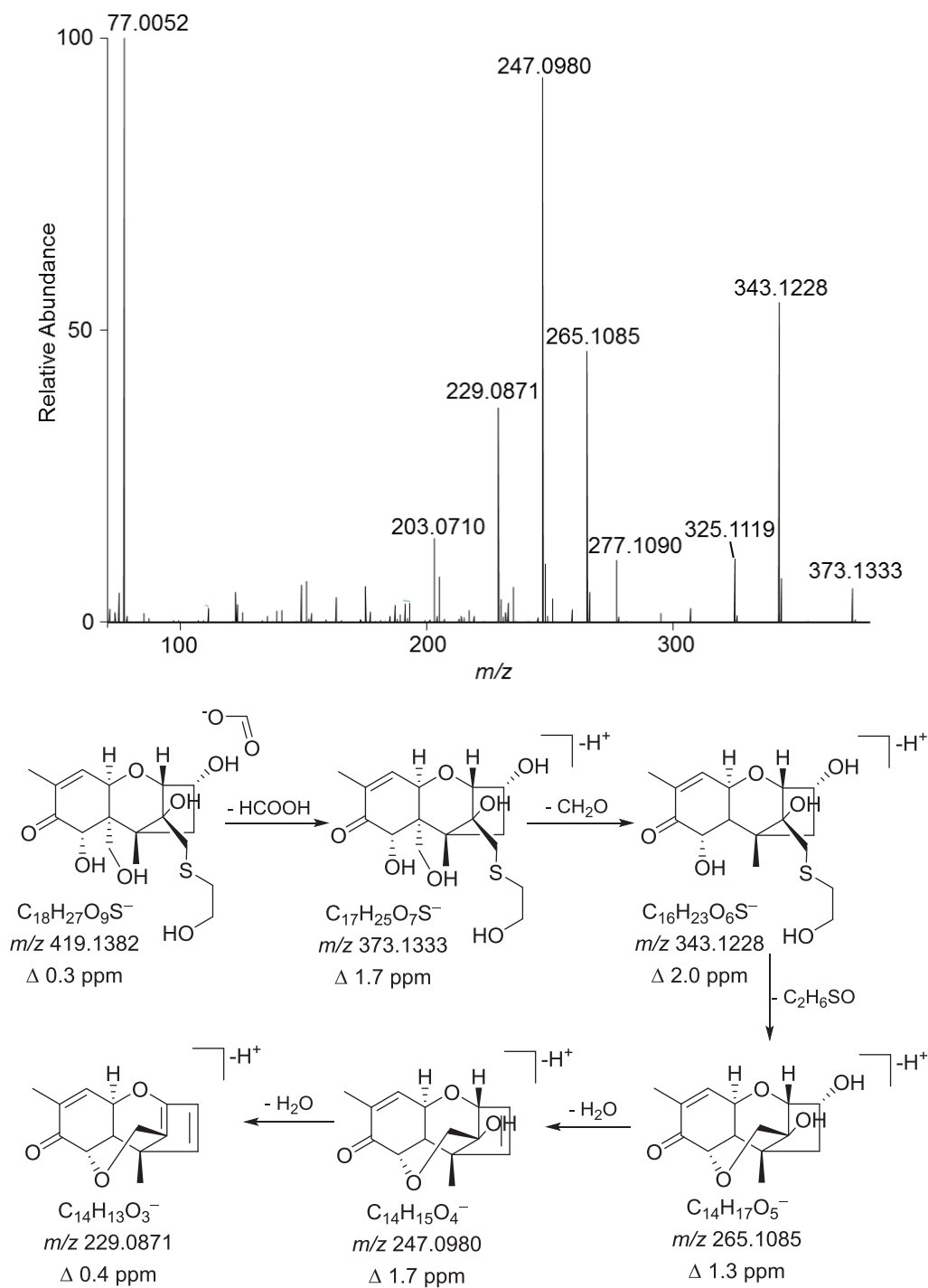
Figure 59. MS/HRMS spectrum of DON-13-mercaptoethanol adduct and its suggested negative ion mass spectral fragmentation pathway.
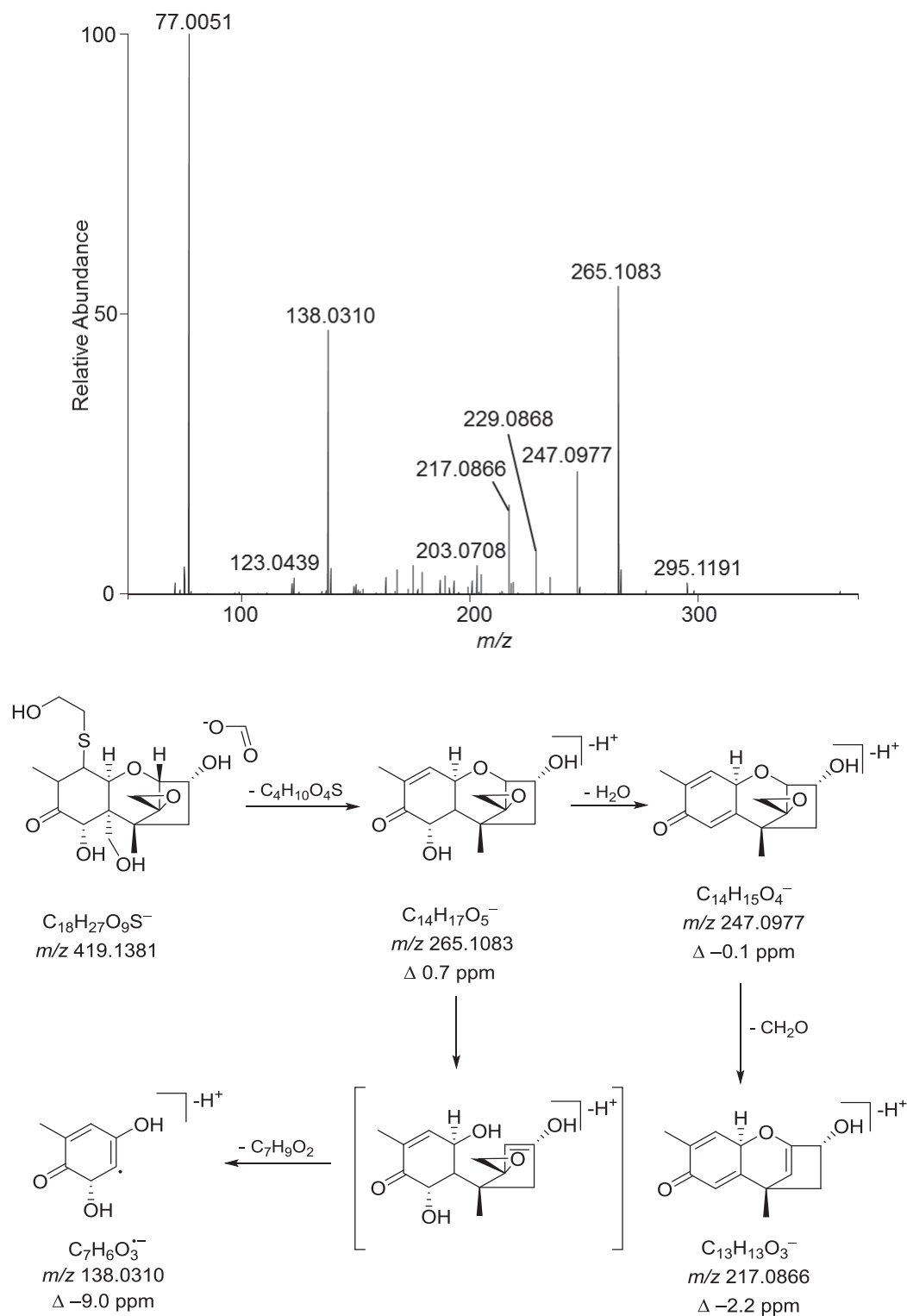
Figure 60. MS/HRMS spectrum of fastest forming DON-10-mercaptoethanol adduct and its suggested negative ion mass spectral fragmentation pathway, based on the fragmentation of DON suggested by Liu et al.[209]

As a result of the presence of the carboxylic and amino group(s) in the DON–Cys and DON–GSH adducts these ionized almost equally well in negative mode affording $[M{-}H]^-$, and in positive mode affording $[M{+}H]^+$ ions (Table 4). It was found that, at lower concentrations, the peak intensity was better in negative mode, while at higher concentrations it was better in positive mode. The product ion spectra in negative mode could discriminate between the epoxide and the Michael adducts. DON-13-Cys and DON-13-GSH (epoxide adducts) showed characteristic m/z 299.0958–299.0964 product ions corresponding to an elemental composition of $C_{14}H_{19}O_5S^-$ (Δ −0.3–1.7 ppm) showing that the sulfur was still attached to the trichothecene (**Paper II** and **III**). However, the most prominent product ion in the DON-13-GSH HRMS/MS spectrum was at m/z 272.0893 ($C_{10}H_{14}N_3O_6^-$, Δ 3.1 ppm), corresponding to deprotonated GSH that was lacking the sulfhydryl group. On the other hand, DON-10-Cys and DON-10-GSH (Michael adducts) afforded product ions that corresponding to $[Cys{-}H]^-$ and $[GSH{-}H]^-$, respectively, indicating that the thiol is more readily eliminated from the Michael adducts compared to their epoxide analogue. From the fragmentation patterns obtained in positive ion mode, it was possible to distinguish not only between the epoxide and the Michael adducts, but also among the different C-9,10-diastereoisomers. DON-13-Cys and DON-13-GSH both afforded three characteristic fragments with m/z 281.0836–281.0846 ($C_{14}H_{17}O_4S^+$, Δ −2.2–1.1), 263.0733–263.0739 ($C_{14}H_{15}O_3S^+$, Δ −1.3–0.9 ppm) and 231.1013–231.1021 ($C_{14}H_{15}O_3^+$, Δ −1.2–2.3 ppm). Again, the two major fragments (m/z 263.0733–263.0739 and 281.0836–281.0846) indicate sulfur attachment to DON after the fragmentation of the epoxide adduct. In general, the product ions from MS fragmentation of the C-10 conjugates are mostly related to the amino acids, while fragmentation of the C-13 conjugates yields predominantly product ions related to DON-part of the ionized molecules. The fragmentation patterns in positive mode of DON-10-Cys and DON-10-GSH are generally characterized by affording mostly identical product ions among the corresponding isomers, but with different relative intensities (**Papers II** and **III**, Table 4). Being aware that there are four possible Michael adducts that could be formed in thiol conjugation, and observing broad peaks in the chromatogram, efforts were made to separate the isomers. Initially, a fully porous octadecylsilane column was used, but subsequently by a column with a core-shell pentafluorophenylpropyl stationary phase, which has been shown to be suited for separating regio- and stereoisomers, was found to improve the chromatography of DON–thiol conjugates by reducing their LC–MS peak widths. However, not all of the DON-10-thiol diastereoisomers could be separated (Figure 61). When selected ions from the LC–HRMS/MS chromatogram in positive mode were extracted from an injection of the reaction mixture of DON with GSH, it became clear that there were at least two isomers present in the late eluting broad peak (Figure 61). The later-eluting broad peak observed in the LC–HRMS/MS chromatograms of the reaction mixture containing DON and GSH (Figure 62) was observed to move slightly to later retention time as the reaction progressed, indicating that the later-eluting isomer was the more prevalent in later stages of the reaction.
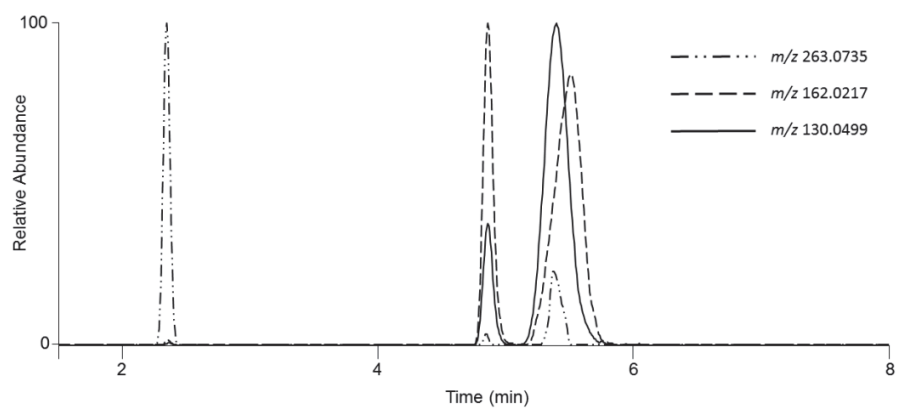
Figure 61. Extracted and stacked ion chromatograms of three product ions from LC-HRMS/MS of a mixture containing DON and GSH that had been allowed to react for 46.5 h at room temperature and pH 10.7. The different relative ratio of the product ions shows that the late-eluting broad peak is a mixture of at least two isomers. The separation was performed on an octadecylsilane stationary phase.
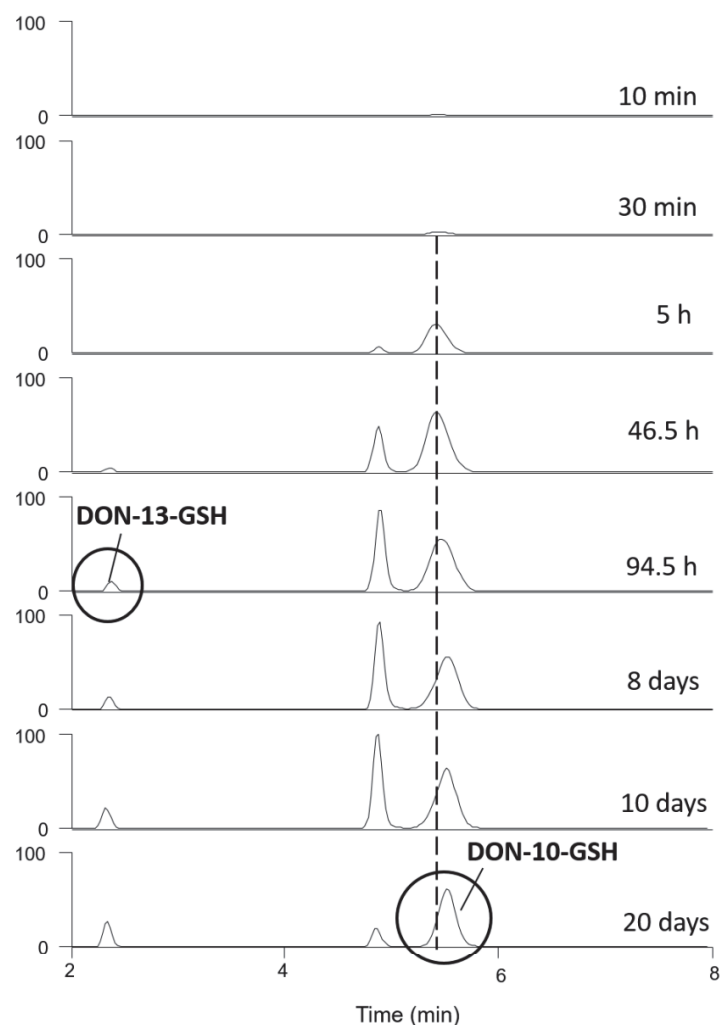
Figure 62. LC–MS extracted ion chromatograms (*m/z* 604.2) from the reaction of DON with GSH at pH 10.7 and room temperature. Highlighted peaks correspond to reaction products that have been purified and identified by NMR.

5.4. Natural occurrence of DON-thiol conjugates

Once the LC–MS method had been improved and the analytical standards were prepared, the next step was to analyze for the presence of DON–thiol conjugates in real samples. Because the C-8 ketone of DON is in equilibrium with the cyclic 8,15-hemiketal form and that four 9,10-diastereoisomers of C-10 thiol adduct could be formed, in theory there are ten possible mono- and eight di-conjugated toxin derivatives that could be formed per thiol. Furthermore, if such conjugates were present in the samples, the identification of the type of isomer could be

important, because the thiol binding could be reversible or irreversible depending on the attachment position, and the toxicity between the isomers could therefore vary.

Two different types of samples were analyzed for DON-thiol conjugates and compared using LC–HRMS/MS. The first type of sample analyzed was an extract from a wheat spikelet in the flowering stage, 96 h after being treated with DON. The second type was naturally-contaminated Norwegian wheat and oat samples, harvested at the end of the growing season. Both were compared to the obtained analytical standards (DON-10-Cys, DON-13-Cys, DON-10-GSH and DON-13-GSH, **Papers II** and **III**, respectively), as well as DON–GSH, –CysGly, –γ-GluCys,– Cys and – *N*-acetylcysteine (–NAC) reaction mixtures that were prepared by stopping the DON-thiol conjugation reaction at different time points by acidification to produce conjugates in different isomer ratios. The chromatogram of the wheat extract treated with DON revealed conjugates that were identical with the fast forming products in the reaction mixture. In contrast, the naturally-contaminated grains contained predominantly the epoxide DON–thiol adducts. Of all the analyzed samples, 63% contained at least one DON–thiol conjugate (all of which contained the DON-13-GSH), while 31% of all samples contained DON-13-Cys, 5% contained DON-13-CysGly, 11% contained DON-10-GSH and 5% contained DON-10-Cys. Selected sample extracts were upconcentrated to acquire LC–HRMS/MS data of good signal/noise in order to confirm the identities of the compounds.

The observation of DON-13-thiol adducts in natural samples is in the accordance with the observed reaction dynamics in *in vitro* experiments (**Papers I**, **II** and **III**). It was shown that DON reacts with thiols under different pH values, and initially gives fast- forming Michael adducts that were slowly replaced by other slower-forming Michael-addition isomers (i.e. C-9,10 diastereoisomers). At the same time, the epoxide adduct formed at a much slower rate, but became the most prominent product after approximately one month (under the highest pH conditions used). This pattern was observed for the reaction of DON with all of the thiols including 2-mercaptoethanol, cysteamine, sodium methanethiolate, sodium 2-mercaptoethanesulfonate (**Paper I**), cysteine (**Papers I** and **II**), glutathione (**Papers I** and **III**) and *N*-acetylcysteine, CysGly, and γ-GluCys (**Paper IV**). At neutral and mildly basic pH the reaction did not go to completion within an observation period of roughly 2 months, likely because of autooxidation of the thiols to disulfides. However, *in vivo*, GSH concentrations in cells can accumulate to millimolar concentrations,[210] and thus the reduced thiol is continuously available for reaction with DON over time to give the DON-13-GSH adduct as well as the corresponding breakdown products. As mentioned, in contrast to naturally-contaminated samples, the DON-treated wheat extract contained only the kinetically favored DON-GSH Michael conjugates and its breakdown products. This indicates that DON-thiol adducts are most likely products of a chemical and not an enzyme-catalyzed reaction, as one would also expect to find DON-13-thiol adducts in DON-treated wheat if it was an enzymatically catalyzed reaction.

In the reaction mixtures that were used as references for the analyses of the grain samples, the dipeptides CysGly and γ-GluCys were included to react with DON in order to identify the

possible presence of DON–GSH breakdown products. DON–CysGly was the only dipeptide conjugate detected, and no DON–γ-GluCys was found in any of the naturally contaminated grain samples or the DON-treated wheat. GSH-conjugates may be degraded by carboxypeptidase inside vacuoles,[211] however, the breakdown pathway starts with the membrane-bound (in animals) or vacuolar (in plants) enzyme γ-glutamyl transpeptidase that degrades the γ-linked glutamate and cysteine.[212] Due to the small amounts of putative DON-13-CysGly in grain samples, it was not possible to verify its identity by LC-HRMS/MS, but their retention times and calculated elemental composition (*m/z* 475.1744, $C_{20}H_{31}O_9N_2S^+$, Δ -0.04 ppm and *m/z* 473.1605, $C_{20}H_{29}O_9N_2S^-$, Δ 1.3 ppm) were in good agreement with the corresponding conjugates in the reaction mixture. Once CysGly-conjugates are in the vacuole of the plant cell, carboxypeptidase catalyzes the degradation of the glycine residue, leading to the formation of the cysteine-conjugate. An interesting observation was made, in which the peak areas of DON-13-GSH and DON-13-Cys conjugates, as well as the area of DON-3-Glc, correlated to those of DON. The quantitation of the DON-thiol conjugates was not done, but based on the response of these molecules in the LC–HRMS it could be concluded that the thiol concentrations were significantly lower than for DON and DON-3-Glc.

The precise fate of the cysteine conjugates as breakdown products in plants is still uncertain. As mentioned earlier (section 1.3.1.), there are two metabolic pathways described in plants for glutathione-conjugates, which are species-dependent. After being transferred to the vacuoles and after transformation to cysteine conjugates, they can either be cleaved to mercaptans or they can form an *N*-malonylcysteine conjugate. In contrast, in animal cells *N*-acetylcysteine conjugates are the most often formed, while mercaptans formed less often.[213] Even though DON–NAC conjugates have not been reported in plants, in this study we specifically searched for these conjugates in the samples. To do that, the reaction between DON and *N*-acetylcysteine (NAC) was carried out using optimized conditions as for all the other thiol reactions and followed using LC–HRMS (**Paper IV**). Compounds were tentatively assigned as C-13 epoxide adducts or Michael adducts, based on their retention times and fragmentation patterns from LC–HRMS/MS experiments. DON–NAC conjugates were best observed in negative ion mode, likely because the carboxylic acid group is the structural part that is most easily ionized. The product ions observed in the HRMS/MS spectra of DON-13-thiol conjugates in negative ion mode from previous experiments (Table 4) (**Papers I, II** and **III**) were essentially the same for DON–NAC. Thus, *m/z* 299.0957 and *m/z* 265.1078 (corresponding to $C_{14}H_{19}O_5S^-$ and $C_{14}H_{17}O_5^-$, respectively) were the most prominent product ions. In case of DON-10-NAC, thiol was eliminated from the molecule affording [NAC−H]$^-$ product ions with *m/z* 162.0219 ($C_5H_8O_3NS^-$, Δ -7.1). None of the DON–NAC conjugates were found in the DON-treated wheat spikelet sample, but 26% of the grain samples contained a putative DON-13-NAC, and 5% contained what was tentatively assigned as DON-10-NAC.

Although not directly related to the major aims of this work, the new LC method for the analysis of grain extracts separated 3ADON and 15ADON. Employing the method for the analysis of grain samples for the first time showed the presence of 15ADON in Norwegian grain.

The glutathione metabolic pathway of DON in wheat is now mainly identified. Kluger et al.[135] also reported the presence of a minor compound they assigned as DON−2H−*S*-glutathione. Therefore, to fully characterize the pathway, identification of that product is also desirable. We speculated that one of the possibilities is that 9,10-double bond of DON was oxidized to epoxide through phase I metabolism, and that GSH attached to the 12,13-epoxide ring.

Table 4. Summary of major product ions from DON–thiol adducts. Bold are *m/z* values of the product ions common for all DON-13-thiol conjugates, italic are m/z values of the product ion common for all DON-10-thiol conjugates and underlined are m/z product ions of ionized thiols.

	Positive mode			Negative mode		
	Product ion	Elemental composition	Error (ppm)	Product ion	Elemental composition	Error (ppm)
DON-13-GSH	529.1852	$C_{23}H_{33}O_{10}N_2S^+$	0.3	254.0783	$C_{10}H_{12}O_5N_3^-$	0.2
	499.1738	$C_{22}H_{31}O_9N_2S^+$	−1.4	210.0881	$C_9H_{12}O_3N_3^-$	−1.5
	445.1630	$C_{19}H_{29}O_8N_2S^+$	−2.0	143.0451	$C_5H_7O_3N_2^-$	−7.8
	281.0836	$C_{14}H_{17}O_4S^+$	−2.1	128.0340	$C_5H_7O_3N^-$	−10.3
	263.0733	$C_{14}H_{15}O_3S^+$	−1.3	272.0893	$C_{10}H_{14}O_6N_3^-$	1.8
	231.1013	$C_{14}H_{15}O_3^+$	−1.2	**299.0958**	$C_{14}H_{19}O_5S^-$	−0.2
DON-13-CysGly	439.1530	$C_{20}H_{27}O_7N_2S^+$	−0.8	**299.0955**	$C_{14}H_{19}O_5S^-$	−1.2
	391.1326	$C_{19}H_{23}O_5N_2S^+$	1	**265.1077**	$C_{14}H_{17}O_5^-$	−1.7
	299.0615	$C_{16}H_{13}O3NS^+$	1.5	**247.0960**	$C_{14}H_{15}O_4^-$	−6.4
	281.0833	$C_{14}H_{17}O_4S^+$	−3.2	143.0448	$C_2H_9O_6N^-$	9.0
	263.0728	$C_{14}H_{15}O_3S^+$	−3.1			
	231.1013	$C_{14}H_{15}O_3^+$	−1.2			
	203.1069	$C_{13}H_{15}O_2^+$	1.2			
	179.0488	$C_5H_{11}O_3N_2S^+$	1.7			
	162.0219	$C_5H_8O_3NS^+$	−0.3			
	145.0605	$C_5H_9O_3N_2^+$	−1.8			
DON-13-Cys	388.1427	$C_{17}H_{26}O_7NS^+$	0.6	**299.0964**	$C_{14}H_{19}O_5S^-$	1.8
	281.0846	$C_{14}H_{17}O_4S^+$	1.4	**265.1088**	$C_{14}H_{17}O_5^-$	2.5
	263.0739	$C_{14}H_{15}O_3S^+$	1.0	**247.0976**	$C_{14}H_{15}O_4^-$	0.1
	231.1021	$C_{14}H_{15}O_3^+$	2.3			
DON-13-NAC	–	–	–	**299.0952–299.0955**	$C_{14}H_{19}O_5S^-$	−2.2– −1.2
				265.1077	$C_{14}H_{17}O_5^-$	−1.7
				247.0975	$C_{14}H_{15}O_4^-$	−0.3
				128.0340	$C_5H_6O_3N^-$	−10.2
DON-10-GSH	529.1837–529.1846	$C_{23}H_{33}O_{10}N_2S^+$	−2.5 – −0.8	306.0771–306.0773	$C_{10}H_{16}O_6N_3S^-$	1.9–2.5
	475.1733–475.1740	$C_{20}H_{31}O_9N_2S^+$	−2.5 – −1.0	272.0893–272.0895	$C_{10}H_{14}O_6N_3^-$	1.8–2.5
	458.1470	$C_{20}H_{28}O_9NS^+$	−2.0	254.0781–254.0784	$C_{10}H_{12}O_5N_3^-$	−0.6
	297.1327–297.1328	$C_{15}H_{21}O_6^+$	−1.9– −1.6			
	179.0482–179.0483	$C_5H_{11}O_3N_2S^+$	−1.6– −1.1			
	162.0217	$C_5H_8O_3NS^+$	−1.5			
	130.0498	$C_5H_8O_3N^+$	−0.5			
DON-10-CysGly	458.1473	$C_{20}H_{28}O_9NS^+$	−1.4	177.0327–177.0328	$C_5H_9O_3N_2S^-$	−7.0– −6.4
	329.1043	$C_{15}H_{21}O_6 S^+$	−3.1	143.0447	$C_2H_9O_6N^-$	−8.1
	297.1324–297.1329	$C_{15}H_{21}O_6^+$	−2.9– −1.2			
	179.0479–179.0480	$C_5H_{11}O_3N_2S^+$	−3.3– −2.7			
	162.0214–162.0215	$C_5H_8O_3NS^+$	−3.3– −2.7			
DON-10-Cys	*297.1333–297.1335*	$C_{15}H_{21}O_6^+$	0.1–0.8	329.1068–329.1070	$C_{15}H_{21}O_6S^-$	1.1–1.7
	279.1228	$C_{15}H_{19}O_5^+$	0.4	120.0113	$C_3H_6O_2NS^-$	−9.7
	249.1122	$C_{14}H_{17}O_4^+$	0.3			
	231.1017	$C_{14}H_{15}O_3^+$	0.6			
	122.0274	$C_3H_8O_2NS^+$	3.0			
DON-10-NAC	–	–	–	329.1061–329.1063	$C_{15}H_{21}O_6S^-$	−1.0– −0.4
				162.0217	$C_5H_8O_3NS^-$	−8.3

5.5. Cytotoxicity of DON-thiol conjugates

The DON-conjugates were expected to be less toxic than DON itself, as the C-9,10 double bond and 12,13-epoxide ring are considered as essential structural features for the toxicity.[74]

The effects of DON-conjugates on cellular proliferation and metabolic activity were measured using the Alamar Blue assay in THP-1 monocytes (**Papers I** and **II**). Alamar Blue is a non-fluorescent dye, resazurin, which is reduced to a highly fluorescent, pink compound, resorufin, in functional mitochondria.[214] While DON inhibited the proliferation, the synthetic DON–mercaptoethanol or DON–Cys epoxide derivatives (**Papers I** and **II**), as well as the DON–mercaptoethanol double adduct (**Paper I**) did not display any inhibitory effects at the measured concentration (4 µM). Slight inhibition was only detected for DON–Cys Michael adduct (**Paper II**), which was attributed to DON contamination (ca. 10 mol %). Proliferation was also measured at different time points up to 72 h by treating THP-1 monocytes with different concentrations of the DON–Cys conjugates (2, 4, and 6 µM), where no significant effect on the proliferation detected at any time point or concentration. This result was in the accordance with the result from Fruhman et al., who showed that a methanethiol Michael conjugate reduced *in vitro* translation to 50% at approximately 10 times higher concentration (22.5 µM) than DON (2.1 µM).[89] After the proliferation test, cell extracts were subjected to semi-quantitative LC–HRMS analysis. In the cell extracts treated with either DON, DON-13-Cys epoxide conjugate or DON-10-Cys adduct after 0, 24 and 48 h, there was no detectable metabolism (i.e. de-conjugation) or oxidation. Moreover, the ratio between DON and the DON-10-Cys containing 10 mol % DON was also constant throughout the cell culture test, indicating that there was no detectable de-conjugation of the Michael adduct to DON.

DON causes cellular effects by targeting ribosomes[151] and induces expression of several pro-inflammatory cytokines including tumor necrosis factor α (TNFα), interleukin-1 beta (IL-1β), IL-6 and IL-8.[82] Secreted cytokines (TNFα, IL-1β) were measured in an immortalized human monocytic cell line (THP-1), with and without pretreatment with lipopolysaccharide (LPS), after the exposure to DON, deepoxy-DON and DON-13-mercaptoethanol and DON-10,13-dimercaptoethanol conjugate (**Paper I**). LPS is known to potentiate the cytokine expression,[215] but regardless of its presence there was an increase in TNF-α and IL-1β in response to DON exposure, but not with any of the other derivatives. These experiments support the common understanding that epoxide ring is an important structural feature for the toxicity of DON (and other trichothecenes).[87] Based on these observations on the structure–activity relationship of DON–mercaptoethanol adducts, it was anticipated that DON-13-Cys, and also DON-10-Cys adduct will have similar effect, i.e. no effect. When TNF-α levels were measured in THP-1 macrophages following exposure to DON-13-Cys and DON-10-Cys (**Paper II**), in the absence of LPS, all the compounds gave a statistically significant increase in response in comparison to the

control. When macrophages were primed with LPS, only DON gave a noticeably increased response compared to control, whereas the DON-10-Cys adduct gave a slight increase (which was again attributed to DON contamination), while DON-13-Cys epoxide adduct did not show any effect. Cell culture medium and cell extracts were separated and analyzed using LC–HRMS. Tested compounds were all present in the media, and again, calculated concentrations provided no evidence of metabolism of the compounds.

CellTox Green dye was used to assess the general cell toxicity and to confirm that the concentration of DON and its cysteine conjugates were in a noncytotoxic concentration range for cytokine measurments (**Paper II**). CellTox Green measures the changes in membrane integrity that occur as a result of cell death by using a proprietary asymmetric cyanine dye. The dye is excluded from viable cells, but binds to DNA of dead cells, enhancing their fluorescence. The fluorescent signal produced is proportional to cytotoxicity.[216] None of the tested compounds, including DON, induced cytotoxicity at the used concentrations.

5.6. Oxidation to sulfoxides

While following the reaction between mercaptoethanol and DON (**Paper I**), minor compounds affording ions that were shifted to 16 Da higher *m/z* compared to the DON–mercaptoethanol conjugate were detected in the LC–MS chromatograms. These were tentatively assigned as the products of thiol oxidation to sulfoxides. In order to confirm this assumption, hydrogen peroxide (H_2O_2) was added to an aliquot of the reaction mixture, which was then followed by the LC–MS. This oxidant was chosen because of its availability, lack of environmentally unfavorable co-products and high effective-oxygen content.[217] The oxidation products were identical to those observed in the untreated conjugates, based on their *m/z* and retention times. In order to reduce the autoxidation, vials containing the reaction mixtures were flushed with argon. When purified DON–Cys conjugates were analyzed using LC–HRMS after being stored for two months at −20 °C, trace levels of the sulfoxides were also observed (**Paper II**). Again, aliquots of each purified Cys–conjugate were oxidized using H_2O_2 for the purpose of confirmation. The LC–HRMS analysis revealed two main oxidation products for both the DON-10-Cys and epoxide DON-13-Cys adduct with *m/z* corresponding to addition of one oxygen, and were detected in both positive and negative ion mode (**Paper II**). These were attributed to diastereoisomeric pairs of sulfoxide. Another slowly growing peak was detected due to a compound affording ions with *m/z* corresponding to addition of two oxygen atoms in H_2O_2 treated DON–Cys conjugates, and was attributed to sulfone. When DON-10-Cys and DON-13-Cys sulfoxides were subjected to targeted LC–HRMS/MS, they displayed different fragmentation features and could easily be distinguished. The major product ion that was observed in the positive and negative MS/HRMS spectra of DON-10-Cys sulfoxides (but not of DON-13-Cys) had *m/z* corresponding to oxidized cysteine (**Paper II**). This was consistent with our previous observation that Michael adducts eliminate thiol (sulfoxide) more easily than the epoxide adduct. Because of this, oxidation of sulfides to sulfoxides followed with LC–MS/MS could become an analytical tool for identifying

the presence of such conjugates in samples. This was tested and used in **Paper IV** by adding H_2O_2 to a Norwegian oats extract that contained DON-13-GSH and comparing it to a reaction mixture of synthesized DON–GSH adducts that were also treated with H_2O_2 . The LC–HRMS chromatogram revealed the formation of two compounds assigned as sulfoxides in both the samples based on their *m/z* and retention time.

It is also important to note that oxidation of sulfur-containing amino acids like methionine and cysteine is common in living organisms,[218] so it cannot be excluded that DON–Cys or DON–GSH conjugates could be metabolized to their corresponding sulfoxides or sulfones.

5.7. Enzymatic reaction with GST

As described in section 1.3., the glutathione pathway is one of the most important detoxification pathways for conjugation of xenobiotics utilizing a group of enzymes called glutathione transferases (GSTs). To examine if the reaction between DON and GSH could be enzyme catalyzed, they were incubated with and without GST and the reaction was followed using LC-MS for 18 h (**Paper III**). The peaks that were observed in both mixtures were the kinetically favored DON-10-GSH adducts. DON-13-GSH was not detected throughout the experiment, which was expected because of the rather short reaction time. The peak areas for DON and the sum of all DON-GSH conjugates were plotted against time and fitted to exponential curves (decay and rise, respectively) and in both incubations, regardless of the presence of GST, the DON depletion rates, as well as the product ratios, were fundamentally identical. These observations indicate that the conjugation reaction is not enzyme catalyzed. The observations of the product profiles from the naturally DON-contaminated grain samples and wheat treated with DON (**Paper IV**) also indicate that the reaction is not enzyme catalyzed, as does the fact that DON is a polar compound[80] and GSTs in general catalyze the *S*-conjugation of GSH to compounds that are hydrophobic in nature in order to increase their polarity.[219] Still, it cannot be excluded that another GST might catalyse the conjugation reaction. GSTs show a high level of specificity toward GSH, but the electrophilic substrate can significantly vary between and within classes of GST.[219] Human alpha and mu GSTs used in the experiment are only specific for mammals, while for example, theta and zeta GSTs have counterparts in animals and plants, and phi GST is plant specific.[119]

6. ADDITIONAL FINDINGS

To date, conjugates of DON with natural thiols have only been reported *in planta*. As the biotransformation reactions occurring in plants and animals are generally similar, it was important to test whether these conjugates occur in animal cells. Königs et al.[220] studied the effects of DON in human primary hepatocytes and compared them to the HepG2 cells, an immortalized human hepatocellular liver carcinoma cell line, and subsequently analyzed cell

extracts using LC–MS/MS. Calculated DON recoveries after 8, 24 and 48 h incubation time indicated that there was no detectable metabolism of DON in the cells. In more recent studies by Juan-Garcia et al.,[221,222] HepG2 cells were treated with 3ADON and 15ADON, and cell extracts were analyzed with LC–MS/MS. The studies claim to (tentatively) identify 3ADON- and 15ADON–GSH and –γGluCys conjugates. However, very little information and evidence was provided in these reports, e.g. there were no reference standards available, no LC-MS/MS chromatograms were provided, no retention times and only low resolution MS spectra of low signal/noise were presented. Once the analytical standards of DON–Cys and DON–GSH conjugates were obtained (**Paper II** and **Paper III**), and the reaction mixtures containing DON–GlyCys and –γ-GluCys (**Paper IV**) were prepared, it was a relatively simple task to check if the glutathione biotransformation pathway occurs in the animal cells. The HepG2 cell line was selected as the liver is the main organ for metabolic reactions.

HepG2 cells were incubated for 24 h with either DON, U-[^{13}C$_{15}$]-DON, deepoxy-DON, and T-2 tetraol. At the end of the exposure period, cells where frozen and later left to thaw, after which they were filtered and centrifuged. Acetic acid was added to filtrates to prevent de-conjugation of any Michael adducts. Samples were subjected to LC-HRMS/MS analysis using the method described in **Paper IV**. The chromatogram obtained from the HepG2 cells treated with deepoxy-DON and T-2 tetraol showed the same pattern of DON–GSH conjugates as was reported in **Paper I** for the chemical reaction in base—only a single conjugate for T-2 tetraol and several for deepoxy-DON, which is consistent with conjugation of T-2 tetraol at the epoxide ring, and attachment of thiol at C-10 in deepoxy-DON. In the case of DON, the same biotransformation products were identified in HepG2 cells as in wheat treated with DON (**Paper IV**, Figure 63), i.e. the relatively fast-forming kinetically-favored C-10 Michael addition products. Another major biotransformation product of DON was, as expected, DON-3-GlcA. However, the exact concentrations were not calculated, and the degree of conversion is thus unknown. Based on the previous observations on relative responses of the molecules in LC-HRMS, it is possible to conclude that DON-3-GlcA is more abundant than the DON–thiol conjugates. A low degree of conversion to a kinetically favored DON-thiol conjugate again suggests that their formation is not enzyme-dependent.
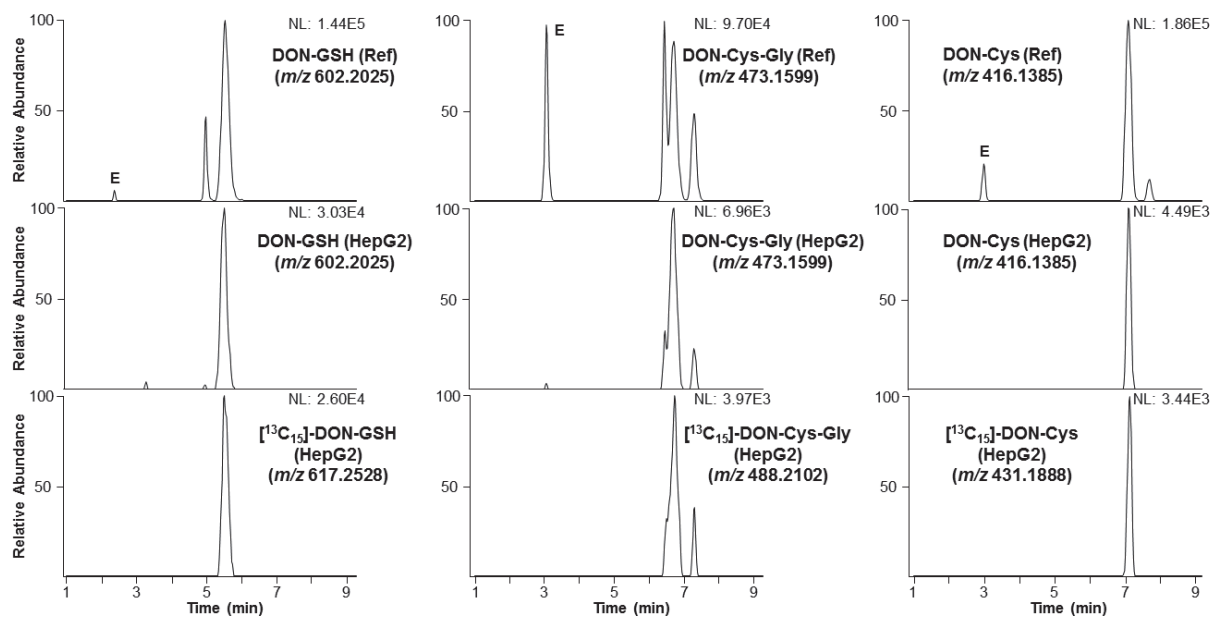
Figure 63. Extracted ion chromatograms ([M−H]⁻, Δ ± 5 ppm) from LC-HRMS showing different DON–GSH adducts and its breakdown products DON-CysGly and DON–Cys. Upper traces are from a reaction mixture containing DON (0.34 mM) and 30 mM each of glutathione, cysteinyl-glycine and L-cysteine (pH 10.7), while middle and lower traces are from extracts of HepG2 cells and medium after exposure to 40 µM DON or U-[^{13}C$_{15}$]-DON for 24 h. Epoxide adducts are labelled ("E").

7. CONCLUDING REMARKS AND FUTURE PROSPECTS

The research presented in this thesis showed that the reaction between DON and thiols proved to be very complex, as the LC–HRMS and NMR studies showed that thiols bind both reversibly to the C-9,10 conjugated double bond of DON creating 4 possible diastereoisomers, and slowly but irreversibly to C-13 of the 12,13-epoxide ring (Figure 64). DON and DON-thiol conjugates are present as a mixture of isomers in the ketone and hemiketal forms, with the thiol conjugates preferring the hemiketal form.
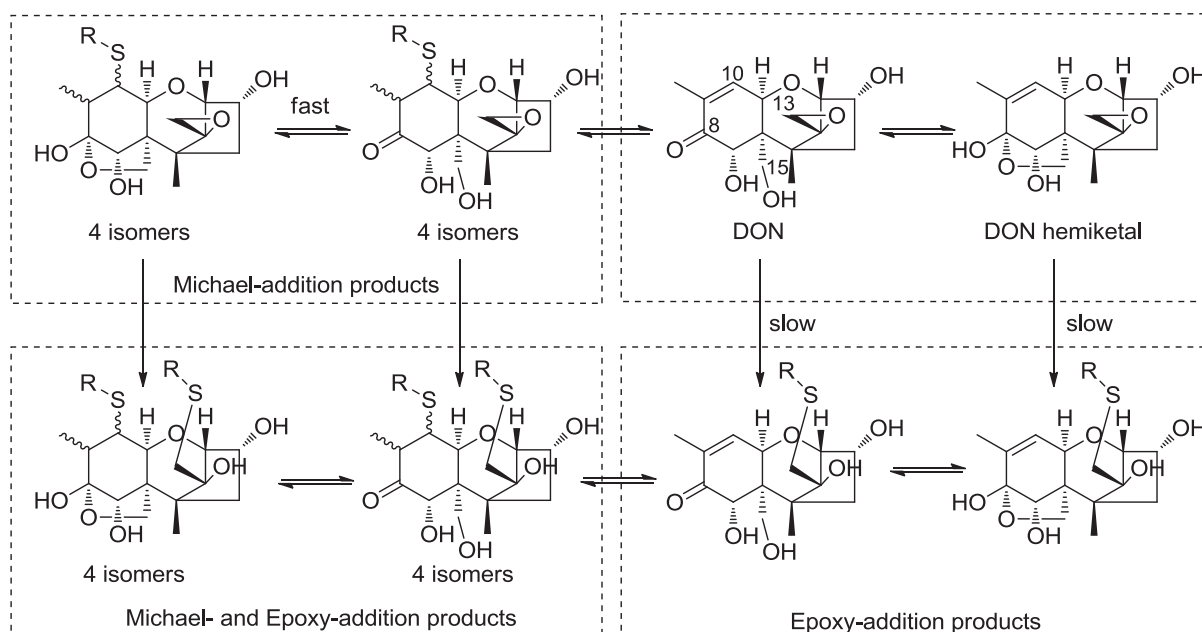
Figure 64. Generalized scheme showing reaction products of DON and thiol (RSH), as well as hemiketal–ketone equilibration at C-8.

The analytical standards of DON–Cys and DON–GSH Michael and epoxide adducts were prepared and quantified using NMR ERETIC2 method. The *in vitro* preliminary cytotoxicity assessment of DON-13-mercaptoethanol, DON-10,13-dimercaptoethanol, DON-10-Cys and DON-13-Cys relative to DON and deepoxy-DON was performed by measuring the expression of cytokines and proliferation of the cells, and showed that none of the compounds displayed any noticeable toxicity in comparison to DON and the control.

The present work also confirmed the presence of DON–GSH and its biodegradation products DON–CysGly, DON–Cys in DON-treated wheat and HepG2 cells, as well as in real, naturally contaminated samples. However, the main difference between these samples was the type of isomer of DON–thiol conjugate that was detected. Samples that had been stored for a longer period had the epoxide adduct as the main product, in contrast to DON-treated wheat and HepG2 cells, which contained only the kinetically-favored Michael adduct. This indicates that the reaction is most likely to be chemical, rather than enzymatic. The observed DON-thiol isomers found in extracts of the natural samples was consistent with the observation of the reaction dynamics between DON and thiols *in vitro*.

During this study, the reaction between DON and GSH was followed, with and without addition of the human alpha and mu GST enzymes. These GST showed no effect on the reaction rates or on the observed products. Despite the results, the possibility remains that a GST from another mammalian or plant source might catalyze the conjugation reaction. Thus, testing the catalytic

power of different types of GSTs on DON and GSH reaction could be something to investigate further. However, the presence of kinetically favored products in DON-treated wheat and HepG2 cells suggest that this is not the case.

Even though a lot of theory regarding the chemistry behind the formation of DON–thiol conjugates is now much clearer, to gain a full understanding it is still necessary to characterize and prepare the standards of the kinetically favored products, which have not yet been isolated.

DON and naturally-present thiol conjugates have not been reported so far in tissues of DON. One of the following goals should be to analyze samples from different animal sources, and to check for the presence of these conjugates.

As it is now known that DON reacts with thiols, there is a possibility that DON could also bind to bigger proteins containing cysteine, which could also have a significant role in DON excretion and its toxicology, and one of the major future goals should be to study and identify these DON-protein conjugates.

8. REFERENCES

(1)   Whittaker, R. H., On the broad classification of organisms. *Q. Rev. Biol.* **1959**, *34*, 210–226.

(2)   Wikipedia, Kingdom (biology). https://en.wikipedia.org/wiki/Kingdom_(biology) (Accessed: 26 July 2016)

(3)   Adl, S. M.; Simpson, A. G. B.; Farmer, M. A.; Andersen, R. A.; Anderson, O. R.; Barta, J. R.; Bowser, S. S.; Brugerolle, G. U. Y.; Fensome, R. A.; Fredericq, S.; James, T. Y.; Karpov, S.; Kugrens, P.; Krug, J.; Lane, C. E.; Lewis, L. A.; Lodge, J.; Lynn, D. H.; Mann, D. G.; McCourt, R. M.; Mendoza, L.; Moestrup, Ø.; Mozley-Standridge, S. E.; Nerad, T. A.; Shearer, C. A.; Smirnov, A. V.; Spiegel, F. W.; Taylor, M. F. J. R., The new higher level classification of eukaryotes with emphasis on the taxonomy of protists. *J. Eukaryotic Microbiol.* **2005**, *52*, 399–451.

(4)   Hibbett, D. S.; Binder, M.; Bischoff, J. F.; Blackwell, M.; Cannon, P. F.; Eriksson, O. E.; Huhndorf, S.; James, T.; Kirk, P. M.; Lücking, R.; Thorsten Lumbsch, H.; Lutzoni, F.; Matheny, P. B.; McLaughlin, D. J.; Powell, M. J.; Redhead, S.; Schoch, C. L.; Spatafora, J. W.; Stalpers, J. A.; Vilgalys, R.; Aime, M. C.; Aptroot, A.; Bauer, R.; Begerow, D.; Benny, G. L.; Castlebury, L. A.; Crous, P. W.; Dai, Y.-C.; Gams, W.; Geiser, D. M.; Griffith, G. W.; Gueidan, C.; Hawksworth, D. L.; Hestmark, G.; Hosaka, K.; Humber, R. A.; Hyde, K. D.; Ironside, J. E.; Kõljalg, U.; Kurtzman, C. P.; Larsson, K.-H.; Lichtwardt, R.; Longcore, J.; Miądlikowska, J.; Miller, A.; Moncalvo, J.-M.; Mozley-Standridge, S.; Oberwinkler, F.; Parmasto, E.; Reeb, V.; Rogers, J. D.; Roux, C.; Ryvarden, L.; Sampaio, J. P.; Schüßler, A.; Sugiyama, J.; Thorn, R. G.; Tibell, L.; Untereiner, W. A.; Walker, C.; Wang, Z.; Weir, A.; Weiss, M.; White, M. M.; Winka, K.; Yao, Y.-J.; Zhang, N., A higher-level phylogenetic classification of the fungi. *Mycol. Res.* **2007**, *111*, 509–547.

(5)   Keeling, P.; Leander, B. S.; Simpson, A., Tree of Life web project. http://tolweb.org/Eukaryotes/3 (Accessed: July 26 2016)

(6)   Bruns, T., Evolutionary biology: a kingdom revised. *Nature* **2006**, *443*, 758–761.

(7)   Finlay, R. D., Ecological aspects of mycorrhizal symbiosis: with special emphasis on the functional diversity of interactions involving the extraradical mycelium. *J. Exp. Bot.* **2008**, *59*, 1115–1126.

(8)   Klionsky, D. J.; Herman, P. K.; Emr, S. D., The fungal vacuole: composition, function, and biogenesis. *Microbiol. Rev.* **1990**, *54*, 266–292.

(9)   Lopez-Romero, E.; Ruiz-Herrera, J., The role of chitin in fungal growth and morphogenesis. In *Chitin in Nature and Technology*, Muzzarelli, R.; Jeuniaux, C.; Gooday, G. W., Eds. Springer US: Boston, MA, 1986; pp 55–62.

(10)   Sun, S.; Heitman, J., Is sex necessary? *BMC Biol.* **2011**, *9*, 1–4.

(11)   Guarro, J.; Gené, J.; Stchigel, A. M., Developments in Fungal Taxonomy. *Clin. Microbiol. Rev.* **1999**, *12*, 454–500.

(12)   Engelkirk, P. G.; Duben-Engelkirk, J. L.; Burton, G. R. W., *Burton's Microbiology for the Health Sciences*. Wolters Kluwer Health/Lippincott Williams & Wilkins: 2011; 433 pp. https://books.google.no/books?id=RaVKCQI75voC

(13)   Boundless, Fungi reproduction. https://www.boundless.com/biology/textbooks/boundless-biology-textbook/fungi-24/characteristics-of-fungi-149/fungi-reproduction-591-11810/ (Accessed: July 26 2016)

(14)   Piercey-Normore, M. D.; DePriest, P. T., Algal switching among lichen symbioses. *Am. J. Bot.* **2001**, *88*, 1490–1498.

(15)   Bennett, J. W.; Klich, M., Mycotoxins. *Clin. Microbiol. Rev.* **2003**, *16*, 497–516.

(16)   Richard, J. L., Some major mycotoxins and their mycotoxicoses—an overview. *Int. J. Food Microbiol.* **2007**, *119*, 3–10.

(17)   Pitt, J. I., Toxigenic fungi and mycotoxins. *Br. Biomed. Bull* **2000**, *56*, 184–192.

(18)   Di Menna, M. E.; Smith, B. L.; Miles, C. O., A history of facial eczema (pithomycotoxicosis) research. *N. Z. J. Agric. Res.* **2009**, *52*, 345–376.

(19)   Fridrichsons, J.; Mathieson, A. M., The structure of sporidesmin: causative agent of facial eczema in sheep. *Tetrahedron Lett.* **1962**, *3*, 1265–1268.

(20)   Zain, M. E., Impact of mycotoxins on humans and animals. *J. Saudi Chem. Soc.* **2011**, *15*, 129–144.

(21)   Keller, N. P.; Turner, G.; Bennett, J. W., Fungal secondary metabolism—from biochemistry to genomics. *Nat. Rev. Microbiol.* **2005**, *3*, 937–947.

(22)   Fox, E. M.; Howlett, B. J., Secondary metabolism: regulation and role in fungal biology. *Curr. Opin. Microbiol.* **2008**, *11*, 481–487.

(23)   Rohlfs, M.; Albert, M.; Keller, N. P.; Kempken, F., Secondary chemicals protect mould from fungivory. *Biol. Lett.* **2007**, *3*, 523–525.

(24)   Jansen, C.; von Wettstein, D.; Schäfer, W.; Kogel, K.-H.; Felk, A.; Maier, F. J., Infection patterns in barley and wheat spikes inoculated with wild-type and trichodiene synthase gene disrupted *Fusarium graminearum*. *Proc. Natl. Acad. Sci. U. S. A.* **2005**, *102*, 16892–16897.

(25)   Ponts, N.; Pinson-Gadais, L.; Verdal-Bonnin, M. N.; Barreau, C.; Richard-Forget, F., Accumulation of deoxynivalenol and its 15-acetylated form is significantly modulated by oxidative stress in liquid cultures of *Fusarium graminearum*. *FEMS Microbiol. Lett.* **2006**, *258*, 102–107.

(26)   Yin, W.-B.; Reinke, A. W.; Szilágyi, M.; Emri, T.; Chiang, Y.-M.; Keating, A. E.; Pócsi, I.; Wang, C. C. C.; Keller, N. P., bZIP transcription factors affecting secondary metabolism, sexual development and stress responses in *Aspergillus nidulans*. *Microbiology* **2013**, *159*, 77–88.

(27)   McCormick, S. P.; Stanley, A. M.; Stover, N. A.; Alexander, N. J., Trichothecenes: from simple to complex mycotoxins. *Toxins* **2011**, *3*, 802–814.

(28)   Huffman, J.; Gerber, R.; Du, L., Recent advancements in the biosynthetic mechanisms for polyketide-derived mycotoxins. *Biopolymers* **2010**, *93*, 764–776.

(29)   Kennedy, J.; Auclair, K.; Kendrew, S. G.; Park, C.; Vederas, J. C.; Hutchinson, C. R., Modulation of polyketide synthase activity by accessory proteins during lovastatin biosynthesis. *Science* **1999**, *284*, 1368–1372.

(30)   Clough, J. M., The strobilurin fungicides—from mushroom to molecule to market. In *Biodiversity: New Leads for the Pharmaceutical and Agrochemical Industries*, Wrigley, S. K.; Hayes, M. A.; Thomas, R.; Chrystal, E. J. T.; Nicholson, N., Eds. The Royal Society of Chemistry: 2000; pp 277–282.

(31)   McLean, A. E. M.; Marshall, A., Reduced carcinogenic effects of aflatoxin in rats given phenobarbitone. *Br. J. Exp. Pathol.* **1971**, *52*, 322–329.

(32)   Bbosa, G. S.; Kitya, D.; Lubega, A.; Ogwal-Okeng, J.; Anokbonggo, W. W.; Kyegombe, D. B., Review of the biological and health effects of aflatoxins on body organs and body systems. In *Aflatoxins - Recent Advances and Future Prospects*, 2013.

(33)   Thrasher, J. D., Aflatoxins. http://www.drthrasher.org/aflatoxins (Accessed: 26 July 2016)

(34)   Food and Agriculture Organization (FAO), Aflatoxin analytical methods for groundnuts. http://www.fao.org/docrep/X5036E/x5036E0m.htm (Accessed: July 26 2016)

(35)   Clifford, J. I.; Rees, K. R., The interaction of aflatoxins with purines and purine nucleosides. *Biochem. J.* **1967**, *103*, 467–471.

(36)   Waśkiewicz, A.; Beszterda, M.; Goliński, P., Occurrence of fumonisins in food – an interdisciplinary approach to the problem. *Food Control* **2012**, *26*, 491–499.

(37)   Qi, T. F.; Renaud, J. B.; McDowell, T.; Seifert, K. A.; Yeung, K. K.; Sumarah, M. W., Diversity of mycotoxin-producing black aspergilli in Canadian vineyards. *J. Agric. Food Chem.* **2016**, *64*, 1583–1589.

(38)   Renaud, J. B.; Kelman, M. J.; Qi, T. F.; Seifert, K. A.; Sumarah, M. W., Product ion filtering with rapid polarity switching for the detection of all fumonisins and AAL-toxins. *Rapid Commun. Mass Spectrom.* **2015**, *29*, 2131–2139.

(39)   Kőszegi, T.; Poór, M., Ochratoxin A: molecular interactions, mechanisms of toxicity and prevention at the molecular level. *Toxins* **2016**, *8*, 1–25, doi: 10.3390/toxins8040111.

(40)   Bayman, P.; Baker, J. L., Ochratoxins: a global perspective. *Mycopathologia* **2006**, *162*, 215–223.

(41)   Vogel, J., Watch out for moldy corn. http://farmprogress.com/story-watch-moldy-corn-9-34082 (Accessed: 26 July 2016)

(42)   Zinedine, A.; Soriano, J. M.; Moltó, J. C.; Mañes, J., Review on the toxicity, occurrence, metabolism, detoxification, regulations and intake of zearalenone: an oestrogenic mycotoxin. *Food Chem. Toxicol.* **2007**, *45*, 1–18.

(43)   EFSA Panel on Contaminants in the Food Chain, Appropriateness to set a group health-based guidance value for zearalenone and its modified forms. *EFSA Journal* **2016**, *14*.

(44)   Chen, X. X.; Yang, C. W.; Huang, L. B.; Niu, Q. S.; Jiang, S. Z.; Chi, F., Zearalenone altered the serum hormones, morphologic and apoptotic measurements of genital organs in post-weaning gilts. *Asian-Australasian Journal of Animal Sciences* **2015**, *28*, 171–179.

(45)   Hidy, P. H.; Baldwin, R. S.; Greasham, R. L.; Keith, C. L.; McMullen, J. R., Zearalenone and some derivatives: production and biological activities. *Adv. Appl. Microbiol.* **1977**, *22*, 59–82.

(46)   Finking, R.; Marahiel, M. A., Biosynthesis of nonribosomal peptides. *Annu. Rev. Microbiol.* **2004**, *58*, 453–488.

(47)   Bushley, K. E.; Turgeon, B. G., Phylogenomics reveals subfamilies of fungal nonribosomal peptide synthetases and their evolutionary relationships. *BMC Evol. Biol.* **2010**, *10*, 1–23.

(48)   Hoffmeister, D.; Keller, N. P., Natural products of filamentous fungi: enzymes, genes, and their regulation. *Nat. Prod. Rep.* **2007**, *24*, 393–416.

(49)   Felnagle, E. A.; Jackson, E. E.; Chan, Y. A.; Podevels, A. M.; Berti, A. D.; McMahon, M. D.; Thomas, M. G., Nonribosomal peptide synthetases involved in the production of medically relevant natural products. *Mol. Pharmaceutics* **2008**, *5*, 191–211.

(50)   Wikipedia, β-lactam antibiotic. https://en.wikipedia.org/wiki/%CE%92-lactam_antibiotic (Accessed: 26 July 2016)

(51)   Sauvage, E.; Kerff, F.; Terrak, M.; Ayala, J. A.; Charlier, P., The penicillin-binding proteins: structure and role in peptidoglycan biosynthesis. *FEMS Microbiol. Rev.* **2008**, *32*, 234–258.

(52)   Pöggeler, S.; Wöstemeyer, J., *Evolution of Fungi and Fungal-Like Organisms*. Springer Science & Business Media: 2011; Vol. 14 of the Mycota, 345 pp.

(53)   Guerre, P., Ergot alkaloids produced by endophytic fungi of the genus *Epichloë*. *Toxins* **2015**, *7*, 773–790.

(54)   Roberts, J. D.; Caserio, M. C., *Basic Principles of Organic Chemistry, second edition*. W. A. Benjamin, Inc.: Menlo Park, CA, 1977;

(55)   University of Calgary, Terpenes. http://www.chem.ucalgary.ca/courses/351/Carey5th/Ch26/ch26-4-1.html (Accessed: 26 July 2016)

(56)   Nelson, J. H., Production of blue cheese flavor via submerged fermentation by *Penicillium roqueforti*. *J. Agric. Food Chem.* **1970**, *18*, 567–569.

(57)   Hohn, T. M.; Plattner, R. D., Purification and characterization of the sesquiterpene cyclase aristolochene synthase from *Penicillium roqueforti*. *Arch. Biochem. Biophys.* **1989**, *272*, 137–143.

(58)   Saikia, S.; Nicholson, M. J.; Young, C.; Parker, E. J.; Scott, B., The genetic basis for indole–diterpene chemical diversity in filamentous fungi. *Mycol. Res.* **2008**, *112*, 184–199.

(59)   Shank, R. A.; Foroud, N. A.; Hazendonk, P.; Eudes, F.; Blackwell, B. A., Current and future experimental strategies for structural analysis of trichothecene mycotoxins—a prospectus. *Toxins* **2011**, *3*, 1518–1553.

(60)   Karlovsky, P., Biological detoxification of the mycotoxin deoxynivalenol and its use in genetically engineered crops and feed additives. *Appl. Microbiol. Biotechnol.* **2011**, *91*, 491–504.

(61)   Clark, C. A.; Hyun, J. W.; Hoy, M. W., Relationships among wilt-inducing isolates of *Fusarium oxysporum* from sweetpotato and tobacco. *Plant Dis.* **1998**, *82*, 530–536.

(62)   Sánchez-Peña, P.; Cauich-Pech, S. O.; Núñez-Farfán, J.; Núñez-Cebreros, R. D.; Hernández-Verdugo, S.; Parra-Terraza, S.; Villarreal-Romero, M., Incidence of *Fusarium oxysporum* f. sp. *lycopersici* races in tomato in Sinaloa, Mexico. *Plant Dis.* **2010**, *94*, 1376–1376.

(63)   Jarvis, B. B.; Mazzocchi, D. B.; Ammon, H. L.; Mazzola, E. P.; Flippen-Anderson, J. L.; Gilardi, R. D.; George, C. F., Conformational effects in trichothecenes: structures of 15-hydroxy C4 and C8 ketones. *J. Org. Chem.* **1990**, *55*, 3660−3662.

(64)   Ueno, Y., The toxicology of mycotoxins. *Crit. Rev. Toxicol.* **1985**, *14*, 99–132.

(65)   Deshpande, S. S., *Handbook of Food Toxicology*. Taylor & Francis: New York, USA, 2002; 920 pp.

(66)   Tamm, C.; Jeker, N., Synthesis of macrocyclic trichothecene mycotoxins. *Tetrahedron* **1989**, *45*, 2385–2415.

(67)   Rotter, B. A.; Prelusky, D. B.; Pestka, J., Toxicology of deoxynivalenol (vomitoxin). *J. Toxicol. Environ. Health* **1996**, *48*, 1–34.

(68)   Babich, H.; Borenfreund, E., Cytotoxicity of T-2 toxin and its metabolites determined with the neutral red cell viability assay. *Appl. Environ. Microbiol.* **1991**, *57*, 2101–2103.

(69)   Garreau de Loubresse, N.; Prokhorova, I.; Holtkamp, W.; Rodnina, M. V.; Yusupova, G.; Yusupov, M., Structural basis for the inhibition of the eukaryotic ribosome. *Nature* **2014**, *513*, 517–522.

(70)   Pace, J. G.; Watts, M. R.; Canterbury, W. J., T-2 mycotoxin inhibits mitochondrial protein synthesis. *Toxicon* **1988**, *26*, 77–85.

(71)   Ueno, Y.; Matsumoto, H., Inactivation of some thiol-enzymes by trichothecene mycotoxins from *Fusarium* species. *Chem. Pharm. Bull.* **1975**, *23*, 2439–2442.

(72)   Suneja, S. K.; Wagle, D. S.; Ram, G. C., Effect of oral administration of T-2 toxin on glutathione shuttle enzymes, microsomal reductases and lipid peroxidation in rat liver. *Toxicon* **1989**, *27*, 995–1001.

(73)   Rocha, O.; Ansari, K.; Doohan, F. M., Effects of trichothecene mycotoxins on eukaryotic cells: a review. *Food Addit. Contam.* **2005**, *22*, 369–378.

(74)   Wu, Q.; Dohnal, V.; Kuca, K.; Yuan, Z., Trichothecenes: structure–toxic activity relationships. *Curr. Drug Metab.* **2013**, *14*, 641–660.

(75)   Streit, E.; Schatzmayr, G.; Tassis, P.; Tzika, E.; Marin, D.; Taranu, I.; Tabuc, C.; Nicolau, A.; Aprodu, I.; Puel, O.; Oswald, I. P., Current situation of mycotoxin contamination and co-occurrence in animal feed—focus on Europe. *Toxins* **2012**, *4*, 788–809.

(76)   Mesterházy, Á., Role of deoxynivalenol in aggressiveness of *Fusarium graminearum* and *F. culmorum* and in resistance to *Fusarium* head blight. *Eur. J. Plant Pathol.* **2002**, *108*, 675–684.

(77)   Wegulo, S. N., Factors influencing deoxynivalenol accumulation in small grain cereals. *Toxins* **2012**, *4*, 1157–1180.

(78)   Audenaert, K.; Vanheule, A.; Hofte, M.; Haesaert, G., Deoxynivalenol: a major player in the multifaceted response of *Fusarium* to its environment. *Toxins* **2014**, *6*, 1–19.

(79)   Bhat, R.; Rai, R. V.; Karim, A. A., Mycotoxins in food and feed: present status and future concerns. *Compr. Rev. Food Sci. Food Saf.* **2010**, *9*, 57–81.

(80)   Sobrova, P.; Adam, V.; Vasatkova, A.; Beklova, M.; Zeman, L.; Kizek, R., Deoxynivalenol and its toxicity. *Interdiscip. Toxicol.* **2010**, *3*, 94–99.

(81)   Pestka, J. J., Deoxynivalenol−induced proinflammatory gene expression: mechanisms and pathological sequelae. *Toxins* **2010**, *2*, 1300−1317.

(82)   Arunachalam, C.; Doohan, F. M., Trichothecene toxicity in eukaryotes: cellular and molecular mechanisms in plants and animals. *Toxicol. Lett.* **2013**, *217*, 149−158.

(83)   Desmond, O. J.; Manners, J. M.; Stephens, A. E.; Maclean, D. J.; Schenk, P. M.; Gardiner, D. M.; Munn, A. L.; Kazan, K., The *Fusarium* mycotoxin deoxynivalenol elicits hydrogen peroxide production, programmed cell death and defence responses in wheat. *Mol. Plant Pathol.* **2008**, *9*, 435–445.

(84)   Ponts, N.; Couedelo, L.; Pinson-Gadais, L.; Verdal-Bonnin, M. N.; Barreau, C.; Richard-Forget, F., *Fusarium* response to oxidative stress by H_2O_2 is trichothecene chemotype-dependent. *FEMS Microbiol. Lett.* **2009**, *293*, 255−262.

(85)   Gardiner, D. M.; Kazan, K.; Praud, S.; Torney, F. J.; Rusu, A.; Manners, J. M., Early activation of wheat polyamine biosynthesis during *Fusarium* head blight implicates putrescine as an inducer of trichothecene mycotoxin production. *BMC Plant Biol.* **2010**, *10*, 1–13.

(86)   Cundliffe, E.; Cannon, M.; Davies, J., Mechanism of inhibition of eukaryotic protein synthesis by trichothecene fungal toxins. *Proc. Natl. Acad. Sci. USA* **1974**, *71*, 30−34.

(87)   Ueno, Y.; Nakajima, M.; Sakai, K.; Ishii, K.; Sato, N., Comparative toxicology of trichothec mycotoxins: inhibition of protein synthesis in animal cells. *J. Biochem.* **1973**, *74*, 285–296.

(88)   Swanson, S. P.; Nicoletti, J.; Rood, H. D., Jr.; Buck, W. B.; Cote, L. M.; Yoshizawa, T., Metabolism of three trichothecene mycotoxins, T-2 toxin, diacetoxyscirpenol and deoxynivalenol, by bovine rumen microorganisms. *J. Chromatogr.* **1987**, *414*, 335–342.

(89)   Fruhmann, P.; Weigl-Pollack, T.; Mikula, H.; Wiesenberger, G.; Adam, G.; Varga, E.; Berthiller, F.; Krska, R.; Hametner, C.; Frohlich, J., Methylthiodeoxynivalenol (MTD): insight

into the chemistry, structure and toxicity of thia-Michael adducts of trichothecenes. *Org. Biomol. Chem.* **2014**, *12*, 5144−5150.

(90)   Suzuki, T.; Iwahashi, Y., Comprehensive gene expression analysis of type B trichothecenes. *J. Agric. Food Chem.* **2012**, *60*, 9519−9527.

(91)   Alassane-Kpembi, I.; Kolf-Clauw, M.; Gauthier, T.; Abrami, R.; Abiola, F. A.; Oswald, I. P.; Puel, O., New insights into mycotoxin mixtures: the toxicity of low doses of Type B trichothecenes on intestinal epithelial cells is synergistic. *Toxicol. Appl. Pharmacol.* **2013**, *272*, 191−198.

(92)   Williams, R. T., *Detoxification Mechanisms: the Metabolism of Drugs and Allied Organic Compounds*. J. Wiley: 1947; https://books.google.no/books?id=49_0oQEACAAJ

(93)   Iyer, R. S.; Voehler, M. W.; Harris, T. M., Adenine adduct of aflatoxin B1 epoxide. *J. Am. Chem. Soc.* **1994**, *116*, 8863−8869.

(94)   Testa, B.; Pedretti, A.; Vistoli, G., Reactions and enzymes in the metabolism of drugs and other xenobiotics. *Drug Discovery Today* **2012**, *17*, 549−560.

(95)   Berthiller, F.; Lemmens, M.; Werner, U.; Krska, R.; Hauser, M. T.; Adam, G.; Schuhmacher, R., Short review: metabolism of the *Fusarium* mycotoxins deoxynivalenol and zearalenone in plants. *Mycotoxin Res.* **2007**, *23*, 68−72.

(96)   Coleman, J.; Blake-Kalff, M.; Davies, E., Detoxification of xenobiotics by plants: chemical modification and vacuolar compartmentation. *Trends Plant Sci. 2*, 144−151.

(97)   Xu, C.; Li, C. Y.-T.; Kong, A.-N. T., Induction of phase I, II and III drug metabolism/transport by xenobiotics. *Arch. Pharmacal Res.* **2005**, *28*, 249−268.

(98)   Liska, D.; Lyon, M.; Jones, D. S., Detoxification and biotransformational imbalances. *Explore (New York, N.Y.)* **2006**, *2*, 122−140.

(99)   Jancova, P.; Anzenbacher, P.; Anzenbacherova, E., Phase II drug metabolizing enzymes. *Biomed. Pap.* **2010**, *154*, 103−116.

(100)   Bártíková, H.; Skálová, L.; Stuchlíková, L.; Vokřál, I.; Vaněk, T.; Podlipná, R., Xenobiotic-metabolizing enzymes in plants and their role in uptake and biotransformation of veterinary drugs in the environment. *Drug Metab. Rev.* **2015**, *47*, 374−387.

(101)   Cvilink, V.; Lamka, J.; Skálová, L., Xenobiotic metabolizing enzymes and metabolism of anthelminthics in helminths. *Drug Metab. Rev.* **2009**, *41*, 8−26.

(102)   Murray, R.; Bender, D.; Botham, K.; Kennelly, P.; Rodwell, V.; Weil, P., Metabolism of xenobiotics. In *Harper's Illustrated Biochemistry, 29e*, McGraw-Hill: 2012

(103)   Matsumura, F.; Krishna Murti, C. R., *Biodegradation of Pesticides*. Plenum Press: New York, US, 1982; 307 pp. https://books.google.no/books?id=ek4yBwAAQBAJ

(104)   Gamage, N.; Barnett, A.; Hempel, N.; Duggleby, R. G.; Windmill, K. F.; Martin, J. L.; McManus, M. E., Human sulfotransferases and their role in chemical metabolism. *Toxicol. Sci.* **2006**, *90*, 5−22.

(105)   Knights, K. M.; Sykes, M. J.; Miners, J. O., Amino acid conjugation: contribution to the metabolism and toxicity of xenobiotic carboxylic acids. *Expert Opin. Drug Metab. Toxicol.* **2007**, *3*, 159−168.

(106)   Döring, B.; Petzinger, E., Phase 0 and phase III transport in various organs: combined concept of phases in xenobiotic transport and metabolism. *Drug Metab. Rev.* **2014**, *46*, 261−282.

(107)   Berthiller, F.; Crews, C.; Dall'Asta, C.; Saeger, S. D.; Haesaert, G.; Karlovsky, P.; Oswald, I. P.; Seefelder, W.; Speijers, G.; Stroka, J., Masked mycotoxins: a review. *Mol. Nutr. Food Res.* **2013**, *57*, 165−186.

(108)   Yang, Y. M.; Noh, K.; Han, C. Y.; Kim, S. G., Transactivation of genes encoding for Phase II enzymes and Phase III transporters by phytochemical antioxidants. *Molecules* **2010**, *15*, 6332–6348.

(109)   Munoz, M.; Henderson, M.; Haber, M.; Norris, M., Role of the MRP1/ABCC1 multidrug transporter protein in cancer. *IUBMB life* **2007**, *59*, 752–757.

(110)   Lin, J. H.; Yamazaki, M., Role of P-glycoprotein in pharmacokinetics. *Clin. Pharmacokinet.* **2003**, *42*, 59–98.

(111)   Wang, W.; Ballatori, N., Endogenous glutathione conjugates: occurrence and biological functions. *Pharmacol. Rev.* **1998**, *50*, 335–356.

(112)   Noctor, G.; Mhamdi, A.; Chaouch, S.; Han, Y.; Neukermans, J.; Marquez-Garcia, B.; Queval, G.; Foyer, C. H., Glutathione in plants: an integrated overview. *Plant, Cell Environ.* **2012**, *35*, 454–484.

(113)   LoPachin, R. M.; Gavin, T.; DeCaprio, A.; Barber, D. S., Application of the hard and soft, acids and bases (HSAB) theory to toxicant–target interactions. *Chem. Res. Toxicol.* **2012**, *25*, 239–251.

(114)   Pickett, C. B.; Lu, A. Y., Glutathione *S*-transferases: gene structure, regulation, and biological function. *Annu. Rev. Biochem.* **1989**, *58*, 743–764.

(115)   Leustek, T.; Martin, M. N.; Bick, J. A.; Davies, J. P., Pathways and regulation of sulfur metabolism revealed through molecular and genetic studies. *Annu. Rev. Plant Physiol. Plant Mol. Biol.* **2000**, *51*, 141–165.

(116)   Brazier-Hicks, M.; Evans, K. M.; Cunningham, O. D.; Hodgson, D. R.; Steel, P. G.; Edwards, R., Catabolism of glutathione conjugates in *Arabidopsis thaliana*. Role in metabolic reactivation of the herbicide safener fenclorim. *J. Biol. Chem.* **2008**, *283*, 21102–21112.

(117)   Dixon, D. P.; Lapthorn, A.; Edwards, R., Plant glutathione transferases. *Genome Biol.* **2002**, *3*, 1–10.

(118)   Edwards, R.; Dixon, D. P.; Walbot, V., Plant glutathione *S*-transferases: enzymes with multiple functions in sickness and in health. *Trends Plant Sci.* **2000**, *5*, 193–198.

(119)   Dixon, D. P.; Edwards, R., Glutathione transferases. *The Arabidopsis Book* **2010**, *8*, e0131.

(120)   Berthiller, F.; Maragos, C.; Dall'Asta, C., Introduction to masked mycotoxins. In *Masked Mycotoxins in Food : Formation, Occurrence and Toxicological Relevance*, Royal Society of Chemistry: Cambridge, UK, 2015; pp 1–13.

(121)   Prange, A.; Modrow, H.; Hormes, J.; Krämer, J.; Köhler, P., Influence of mycotoxin producing fungi (*Fusarium*, *Aspergillus*, *Penicillium*) on gluten proteins during suboptimal storage of wheat after harvest and competitive interactions between field and storage fungi. *J. Agric. Food Chem.* **2005**, *53*, 6930–6938.

(122)   Berthiller, F.; Schuhmacher, R.; Adam, G.; Krska, R., Formation, determination and significance of masked and other conjugated mycotoxins. *Anal. Bioanal. Chem.* **2009**, *395*, 1243–1252.

(123)   Rychlik, M.; Humpf, H.-U.; Marko, D.; Dänicke, S.; Mally, A.; Berthiller, F.; Klaffke, H.; Lorenz, N., Proposal of a comprehensive definition of modified and other forms of mycotoxins including "masked" mycotoxins. *Mycotoxin Res.* **2014**, *30*, 197–205.

(124)   Miller, J. D.; Young, J. C.; Trenholm, H. L., *Fusarium* toxins in field corn. I. Time-course of fungal growth and production of deoxynivalenol and other mycotoxins. *Can. J. Bot.* **1983**, *61*, 3080–3087.

(125)   Sewald, N.; von Gleissenthall, J. L.; Schuster, M.; Müller, G.; Aplin, R. T., Structure elucidation of a plant metabolite of 4-desoxynivalenol. *Tetrahedron: Asymmetry* **1992**, *3*, 953−960.

(126)   Berthiller, F.; Dall'Asta, C.; Schuhmacher, R.; Lemmens, M.; Adam, G.; Krska, R., Masked mycotoxins: determination of a deoxynivalenol glucoside in artificially and naturally contaminated wheat by liquid chromatography-tandem mass spectrometry. *J. Agric. Food Chem.* **2005**, *53*, 3421−3425.

(127)   Lemmens, M.; Scholz, U.; Berthiller, F.; Dall'Asta, C.; Koutnik, A.; Schuhmacher, R.; Adam, G.; Buerstmayr, H.; Mesterhazy, A.; Krska, R.; Ruckenbauer, P., The ability to detoxify the mycotoxin deoxynivalenol colocalizes with a major quantitative trait locus for *Fusarium* head blight resistance in wheat. *Mol. Plant-Microbe Interact.* **2005**, *18*, 1318−1324.

(128)   Tran, S. T.; Smith, T. K.; Girgis, G. N., A survey of free and conjugated deoxynivalenol in the 2008 corn crop in Ontario, Canada. *J. Sci. Food Agric.* **2012**, *92*, 37−41.

(129)   Malachova, A.; Dzuman, Z.; Veprikova, Z.; Vaclavikova, M.; Zachariasova, M.; Hajslova, J., Deoxynivalenol, deoxynivalenol-3-glucoside, and enniatins: the major mycotoxins found in cereal-based products on the Czech market. *J. Agric. Food Chem.* **2011**, *59*, 12990−12997.

(130)   Lancova, K.; Hajslova, J.; Poustka, J.; Krplova, A.; Zachariasova, M.; Dostalek, P.; Sachambula, L., Transfer of *Fusarium* mycotoxins and 'masked' deoxynivalenol (deoxynivalenol-3-glucoside) from field barley through malt to beer. *Food Addit. Contam., Part A* **2008**, *25*, 732−744.

(131)   Dall'Erta, A.; Cirlini, M.; Dall'Asta, M.; Del Rio, D.; Galaverna, G.; Dall'Asta, C., Masked mycotoxins are efficiently hydrolyzed by human colonic microbiota releasing their aglycones. *Chem. Res. Toxicol.* **2013**, *26*, 305−312.

(132)   Gratz, S. W.; Duncan, G.; Richardson, A. J., The human fecal microbiota metabolizes deoxynivalenol and deoxynivalenol-3-glucoside and may be responsible for urinary deepoxy-deoxynivalenol. *Appl. Environ. Microbiol.* **2013**, *79*, 1821−1825.

(133)   Gardiner, S. A.; Boddu, J.; Berthiller, F.; Hametner, C.; Stupar, R. M.; Adam, G.; Muehlbauer, G. J., Transcriptome analysis of the barley−deoxynivalenol interaction: evidence for a role of glutathione in deoxynivalenol detoxification. *Mol. Plant Microbe Interact.* **2010**, *23*, 962−976.

(134)   Kluger, B.; Bueschl, C.; Lemmens, M.; Berthiller, F.; Haubl, G.; Jaunecker, G.; Adam, G.; Krska, R.; Schuhmacher, R., Stable isotopic labelling-assisted untargeted metabolic profiling reveals novel conjugates of the mycotoxin deoxynivalenol in wheat. *Anal. Bioanal. Chem.* **2013**, *405*, 5031−5036.

(135)   Kluger, B.; Bueschl, C.; Lemmens, M.; Michlmayr, H.; Malachova, A.; Koutnik, A.; Maloku, I.; Berthiller, F.; Adam, G.; Krska, R.; Schuhmacher, R., Biotransformation of the mycotoxin deoxynivalenol in *Fusarium* resistant and susceptible near isogenic wheat lines. *PloS one* **2015**, *10*, e0119656.

(136)   Warth, B.; Fruhmann, P.; Wiesenberger, G.; Kluger, B.; Sarkanj, B.; Lemmens, M.; Hametner, C.; Frohlich, J.; Adam, G.; Krska, R.; Schuhmacher, R., Deoxynivalenol-sulfates: identification and quantification of novel conjugated (masked) mycotoxins in wheat. *Anal. Bioanal. Chem.* **2014**, *407*, 1033−1039.

(137)   Alexander, N. J.; McCormick, S. P.; Waalwijk, C.; van der Lee, T.; Proctor, R. H., The genetic basis for 3-ADON and 15-ADON trichothecene chemotypes in *Fusarium*. *Fungal Genet. Biol.* **2011**, *48*, 485−495.

(138) Côté, L.-M.; Dahlem, A.; Yoshizawa, T.; Swanson, S.; Buck, W., Excretion of deoxynivalenol and its metabolite in milk, urine, and feces of lactating dairy cows. *J. Dairy Sci.* **1986**, *69*, 2416–2423.

(139) Prelusky, D. B.; Veira, D. M.; Trenholm, H. L.; Hartin, K. E., Excretion profiles of the mycotoxin deoxynivalenol, following oral and intravenous administration to sheep. *Fundam. Appl. Toxicol.* **1986**, *6*, 356–363.

(140) Eriksen, G. S.; Pettersson, H.; Lindberg, J. E., Absorption, metabolism and excretion of 3-acetyl DON in pigs. *Arch. Anim. Nutr.* **2003**, *57*, 335–345.

(141) Nagl, V.; Schwartz, H.; Krska, R.; Moll, W. D.; Knasmuller, S.; Ritzmann, M.; Adam, G.; Berthiller, F., Metabolism of the masked mycotoxin deoxynivalenol-3-glucoside in rats. *Toxicol. Lett.* **2012**, *213*, 367–373.

(142) Lattanzio, V. M.; Solfrizzo, M.; De Girolamo, A.; Chulze, S. N.; Torres, A. M.; Visconti, A., LC-MS/MS characterization of the urinary excretion profile of the mycotoxin deoxynivalenol in human and rat. *J. Chromatogr. B: Anal. Technol. Biomed. Life Sci.* **2011**, *879*, 707–715.

(143) Meky, F. A.; Turner, P. C.; Ashcroft, A. E.; Miller, J. D.; Qiao, Y. L.; Roth, M. J.; Wild, C. P., Development of a urinary biomarker of human exposure to deoxynivalenol. *Food Chem. Toxicol.* **2003**, *41*, 265–273.

(144) Turner, P. C.; Hopton, R. P.; White, K. L. M.; Fisher, J.; Cade, J. E.; Wild, C. P., Assessment of deoxynivalenol metabolite profiles in UK adults. *Food Chem. Toxicol.* **2011**, *49*, 132–135.

(145) Uhlig, S.; Ivanova, L.; Faeste, C. K., Enzyme-assisted synthesis and structural characterization of the 3-, 8-, and 15-glucuronides of deoxynivalenol. *J. Agric. Food Chem.* **2013**, *61*, 2006–2012.

(146) Turner, P. C.; White, K. L. M.; Burley, V. J.; Hopton, R. P.; Rajendram, A.; Fisher, J.; Cade, J. E.; Wild, C. P., A comparison of deoxynivalenol intake and urinary deoxynivalenol in UK adults. *Biomarkers* **2010**, *15*, 553–562.

(147) Schwartz-Zimmermann, H. E.; Hametner, C.; Nagl, V.; Slavik, V.; Moll, W.-D.; Berthiller, F., Deoxynivalenol (DON) sulfonates as major DON metabolites in rats: from identification to biomarker method development, validation and application. *Anal. Bioanal. Chem.* **2014**, *406*, 7911–7924.

(148) Schwartz-Zimmermann, H. E.; Fruhmann, P.; Danicke, S.; Wiesenberger, G.; Caha, S.; Weber, J.; Berthiller, F., Metabolism of deoxynivalenol and deepoxy-deoxynivalenol in broiler chickens, pullets, roosters and turkeys. *Toxins* **2015**, *7*, 4706–4729.

(149) Warth, B.; Del Favero, G.; Wiesenberger, G.; Puntscher, H.; Woelflingseder, L.; Fruhmann, P.; Sarkanj, B.; Krska, R.; Schuhmacher, R.; Adam, G.; Marko, D., Identification of a novel human deoxynivalenol metabolite enhancing proliferation of intestinal and urinary bladder cells. *Scientific Reports* **2016**, *6*, 33854.

(150) Ran, R.; Wang, C.; Han, Z.; Wu, A.; Zhang, D.; Shi, J., Determination of deoxynivalenol (DON) and its derivatives: current status of analytical methods. *Food Control* **2013**, *34*, 138–148.

(151) Maresca, M., From the gut to the brain: journey and pathophysiological effects of the food-associated trichothecene mycotoxin deoxynivalenol. *Toxins* **2013**, *5*, 784–820.

(152) Bretz, M.; Beyer, M.; Cramer, B.; Knecht, A.; Humpf, H. U., Thermal degradation of the *Fusarium* mycotoxin deoxynivalenol. *J. Agric. Food. Chem.* **2006**, *54*, 6445–6451.

(153) Zachariasova, M.; Vaclavikova, M.; Lacina, O.; Vaclavik, L.; Hajslova, J., Deoxynivalenol oligoglycosides: new "masked" *Fusarium* toxins occurring in malt, beer, and breadstuff. *J. Agric. Food Chem.* **2012**, *60*, 9280–9291.

(154)   Wood, W. F., New components in defensive secretion of the striped skunk, *Mephitis mephitis*. *J. Chem. Ecol.* **1990**, *16*, 2057–2065.

(155)   Troccaz, M.; Borchard, G.; Vuilleumier, C.; Raviot-Derrien, S.; Niclass, Y.; Beccucci, S.; Starkenmann, C., Gender-specific differences between the concentrations of nonvolatile (*R*)/(*S*)-3-methyl-3-sulfanylhexan-1-ol and (*R*)/(*S*)-3-hydroxy-3-methyl-hexanoic acid odor precursors in axillary secretions. *Chem. Senses* **2009**, *34*, 203–210.

(156)   Lo Conte, M.; Carroll, K. S., The chemistry of thiol oxidation and detection. In *Oxidative Stress and Redox Regulation*, Springer Netherlands: 2013; pp 1–42.

(157)   Ziegler, D. M., Role of reversible oxidation-reduction of enzyme thiols-disulfides in metabolic regulation. *Annu. Rev. Biochem.* **1985**, *54*, 305–329.

(158)   Wall, S. B.; Oh, J.-Y.; Diers, A. R.; Landar, A., Oxidative modification of proteins: an emerging mechanism of cell signaling. *Front. Physiol.* **2012**, *3*, 1–9.

(159)   Turell, L.; Radi, R.; Alvarez, B., The thiol pool in human plasma: The central contribution of albumin to redox processes. *Free Radical Biol. Med.* **2013**, *65*, 244–253.

(160)   Loudon, M., *Organic Chemistry*. 5th Edition ed.; Roberts and Company Publishers: Colorado, USA, 2009; 1353 pp.

(161)   Clayden, J.; Greeves, N.; Warren, S.; Wothers, P., *Organic Chemistry*. 1st ed.; Oxford University Press: New York, USA, 2001; 1491 pp.

(162)   Noda, L. H.; Kuby, S. A.; Lardy, H. A., Properties of thiolesters: kinetics of hydrolysis in dilute aqueous media. *J. Am. Chem. Soc.* **1953**, *75*, 913–917.

(163)   Danehy, J. P.; Parameswaran, K. N., Acidic dissociation constants of thiols. *J. Chem. Eng. Data* **1968**, *13*, 386–389.

(164)   University of California, Davis, ChemWiki: Michael additions, β-eliminations and reactions with electron sink cofactors. http://chemwiki.ucdavis.edu/Textbook_Maps/Organic_Chemistry_Textbook_Maps/Map%3A_Organic_Chemistry_With_a_Biological_Emphasis_(Soderberg)/Chapter_14%3A_Reactions_with_stabilized_carbanion_intermediates,_part_II/Section_14.1%3A_Michael_additions,_%CE%B2_eliminations_and_reactions_with_electron_sink_cofactors (Accessed: 26 July 2016)

(165)   Mather, B. D.; Viswanathan, K.; Miller, K. M.; Long, T. E., Michael addition reactions in macromolecular design for emerging technologies. *Prog. Polym. Sci.* **2006**, *31*, 487–531.

(166)   Parker, R. E.; Isaacs, N. S., Mechanisms of epoxide reactions. *Chem. Rev.* **1959**, *59*, 737–799.

(167)   Wikipedia, Acetal. https://en.wikipedia.org/wiki/Acetal (Accessed: July 26 2016)

(168)   Khan, N. Novel methods for the synthesis of septanose sugars/extended ring systems from hexose sugars. Doctoral thesis, Seton Hall University, South Orange, New Jersey, USA, 2012.

(169)   Brown, W. H.; Iverson, B. L.; Anslyn, E. V.; Foote, C. S., *Organic Chemistry*. 7th Edition ed.; Wadsworth Cengage Learning: Belmont, CA, United States, 2014; 1312 pp.

(170)   Smith, R. M., Before the injection—modern methods of sample preparation for separation techniques. *J. Chromatogr. A* **2003**, *1000*, 3–27.

(171)   Danaceau, J., Successful sample preparation strategies for LC/MS/MS analysis of drugs in complex biological matrices for forensic toxicology applications. http://www.waters.com/webassets/cms/events/docs/FINALSamplePrepStrategiesClinical_Forensic11_5_13.pdf (Accessed: 11 July 2016)

(172)   Bueno, D.; Istamboulie, G.; Muñoz, R.; Marty, J. L., Determination of mycotoxins in food: a review of bioanalytical to analytical methods. *Appl. Spectrosc. Rev.* **2015**, *50*, 728–774.

(173)   Manisha, C.; Manisha, S.; Swati, D., Significance of various chromatographic techniques in drug discovery and development. *Int. J. Res. Pharm. Chem.* **2013**, *3*, 282–289.

(174)   Zöllner, P.; Leitner, A.; Jodlbauer, J.; X. Mayerc, B.; Linder, W., Improving LC–MS/MS analyses in complex food matrices, Part II — mass spectrometry. *LC·GC Europe* **2003**, 354–362.

(175)   Mansoor, M. A., Liquid chromatography. In *eLS*, John Wiley & Sons, Ltd: Chichester, United Kingdom [http://dx.doi.org/10.1038/npg.els.0003917], 2015.

(176)   Zwir-Ferenc, A.; Biziuk, M., Solid phase extraction technique—trends, opportunities and applications. *Pol. J. Environ. Stud.* **2006**, *15*, 677–690.

(177)   Andrade-Eiroa, A.; Canle, M.; Leroy-Cancellieri, V.; Cerdà, V., Solid-phase extraction of organic compounds: a critical review (Part I). *TrAC, Trends Anal. Chem.* **2016**, *80*, 641–654.

(178)   Greaves, J.; Roboz, J., *Mass Spectrometry for The Novice*. Taylor and Francis Group: Boca Raton, FL, United States, 2014; 275 pp.

(179)   Flamini, R.; Traldi, P., *Mass Spectrometry in Grape and Wine Chemistry*. John Wiley & Sons, Inc.: Hoboken, NJ, United States, 2010; 366 pp.

(180)   Schwartz, J. C.; Senko, M. W.; Syka, J. E. P., A two-dimensional quadrupole ion trap mass spectrometer. *J. Am. Soc. Mass Spectrom.* **2002**, *13*, 659–669.

(181)   Soininen, P. Quantitative ^{1}H NMR Spectroscopy. Doctoral thesis,, University of Kuopio, Finland, 2008.

(182)   Claridge, T. D. W., *High-resolution NMR Techniques in Organic Chemistry*. Second ed.; Elsevier: Oxford, UK, 2009; Vol. 27, 383 pp.

(183)   Lipid Library AOCS, Pulsed Nuclear Magnetic Resonance Spectrometry. http://lipidlibrary.aocs.org/Biochemistry/content.cfm?ItemNumber=40797 (Accessed: 2 August 2016)

(184)   University of California, San Diego, Processing: the Fourier Transform. http://sopnmr.blogspot.no/2015/11/processing-fourier-transform.html (Accessed: 2 August 2016)

(185)   Coxon, B., Developments in the Karplus equation as they relate to the NMR coupling constants of carbohydrates. *Adv. Carbohydr. Chem. Biochem.* **2009**, *62*, 17–82.

(186)   Gottlieb, H. E.; Kotlyar, V.; Nudelman, A., NMR chemical shifts of common laboratory solvents as trace impurities. *J. Org. Chem.* **1997**, *62*, 7512–7515.

(187)   Richards, S. A.; Hollerton, J. C., *Essential Practical NMR for Organic Chemistry*. John Wiley and Sons, Ltd.: Sussex, UK, 2011; 228 pp.

(188)   Hwang, T. L.; Shaka, A. J., Water suppression that works. Excitation sculpting using arbitrary wave-forms and pulsed-field gradients. *J. Magn. Reson., Ser. A* **1995**, *112*, 275–279.

(189)   Schirra, H. J., One Dimensional NMR Spectroscopy. http://www.cryst.bbk.ac.uk/PPS2/projects/schirra/html/1dnmr.htm (Accessed: 2 August 2016)

(190)   Hassan, J.; Nabulsi, A. A., A new graphical user interface for teaching NMR. *Am. Educ. Res. J.* **2014**, *2*, 240–244.

(191)   Wilkins, A. L.; Miles, C. O., Structure determination of new algal toxins using NMR methods. *Chem. N. Z* **2006**, *70*, 70–74.

(192)   Singh, K.; Blümich, B., NMR spectroscopy with compact instruments. *TrAC, Trends Anal. Chem.* **2016**, *83, Part A*, 12–26.

(193)   Freeman, R., Selective excitation in high-resolution NMR. *Chem. Rev.* **1991**, *91*, 1397–1412.

(194)   Claridge, T. D. W.; Perez-Victoria, I., Enhanced ^{13}C resolution in semi-selective HMBC: a band-selective, constant-time HMBC for complex organic structure elucidation by NMR. *Org. Biomol. Chem.r* **2003**, *1*, 3632–3634.

(195)   Monakhova, Y. B.; Kohl-Himmelseher, M.; Kuballa, T.; Lachenmeier, D. W., Determination of the purity of pharmaceutical reference materials by ^{1}H NMR using the standardless PULCON methodology. *J. Pharm. Biomed. Anal.* **2014**, *100*, 381−386.

(196)   Bharti, S. K.; Roy, R., Quantitative ^{1}H NMR spectroscopy. *TrAC, Trends Anal. Chem.* **2012**, *35*, 5−26.

(197)   Burton, I. W.; Quilliam, M. A.; Walter, J. A., Quantitative ^{1}H NMR with external standards: use in preparation of calibration solutions for algal toxins and other natural products. *Anal. Chem.* **2005**, *77*, 3123−3131.

(198)   Cullen, C. H.; Ray, G. J.; Szabo, C. M., A comparison of quantitative nuclear magnetic resonance methods: internal, external, and electronic referencing. *Magn. Reson. Chem.* **2013**, *51*, 705−713.

(199)   Akoka, S.; Barantin, L.; Trierweiler, M., Concentration measurement by proton NMR using the ERETIC method. *Anal. Chem.* **1999**, *71*, 2554−2557.

(200)   Mehr, K.; John, B.; Russell, D.; Avizonis, D., Electronic referencing techniques for quantitative NMR: pitfalls and how to avoid them using amplitude-corrected referencing through signal injection. *Anal. Chem.* **2008**, *80*, 8320−8323.

(201)   Wider, G.; Dreier, L., Measuring protein concentrations by NMR spectroscopy. *J. Am. Chem. Soc.* **2006**, *128*, 2571−2576.

(202)   Hong, R. S.; Hwang, K. H.; Kim, S.; Cho, H. E.; Lee, H. J.; Hong, J. T.; Moon, D. C., Survey of ERETIC2 NMR for quantification. *J. Korean Magn. Reson. Soc.* **2013**, *17*, 98−104.

(203)   Finley, D.; Stephenson, L.; Benedick, J., *Cell-based assays*. Sigma-Aldrich: 2010; Vol. 5, 31 pp. http://www.sigmaaldrich.com/content/dam/sigma-aldrich/docs/Sigma-Aldrich/General_Information/1/biofiles_v5_n8.pdf

(204)   Buckle, A. E.; Sanders, M. F., An appraisal of bioassay methods for the detection of mycotoxins—a review. *Lett. Appl. Microbiol.* **1990**, *10*, 155−160.

(205)   Gutleb, A. C.; Morrison, E.; Murk, A. J., Cytotoxicity assays for mycotoxins produced by *Fusarium* strains: a review. *Environ. Toxicol. Pharmacol.* **2002**, *11*, 309−320.

(206)   Beloeil, J. C.; Morellet, N.; Pasquier, C.; Dauphin, G.; Jeminet, G., Study of a δ-hydroxy ketone-hemiketal equilibrium by 2D-NMR exchange spectroscopy for the antibiotic grisorixin: involvement in cationic transport through membranes. *Biochimie* **1989**, *71*, 125−135.

(207)   Breitmaier, E., *Structure Elucidation by NMR in Organic Chemistry*. Third revised ed.; John Wiley & Sons, Ltd: 2003; 258 pp. http://dx.doi.org/10.1002/0470853069.ch3

(208)   Savard, M. E.; Blackwell, B. A.; Greenhalgh, R., An ^{1}H nuclear magnetic resonance study of derivatives of 3-hydroxy-12,13-epoxytrichothec-9-enes. *Can. J. Chem.* **1987**, *65*, 2254−2262.

(209)   Liu, Z.-Y.; Yu, C.-H.; Wan, L.; Sun, Z.-L., Fragmentation study of five trichothecenes using electrospray hybrid ion trap/time-of-flight mass spectrometry with accurate mass measurements. *Int. J. Mass spectrom.* **2012**, *309*, 133−140.

(210)   Noctor, G.; Foyer, C. H., Ascorbate and glutathione: keeping active oxygen under control. *Annu. Rev. Plant Physiol. Plant Mol. Biol.* **1998**, *49*, 249−279.

(211)   Wolf, A. E.; Dietz, K.-J.; Schröder, P., Degradation of glutathione *S*-conjugates by a carboxypeptidase in the plant vacuole. *FEBS Lett.* **1996**, *384*, 31−34.

(212)   Ohkama-Ohtsu, N.; Zhao, P.; Xiang, C.; Oliver, D. J., Glutathione conjugates in the vacuole are degraded by gamma-glutamyl transpeptidase GGT3 in *Arabidopsis*. *Plant J.* **2007**, *49*, 878−888.

(213)   Cooper, A. J. L.; Krasnikov, B. F.; Niatsetskaya, Z. V.; Pinto, J. T.; Callery, P. S.; Villar, M. T.; Artigues, A.; Bruschi, S. A., Cysteine *S*-conjugate β-lyases: important roles in the

metabolism of naturally occurring sulfur and selenium-containing compounds, xenobiotics and anticancer agents. *Amino Acids* **2011**, *41*, 7–27.

(214)   Springer, J. E.; Azbill, R. D.; Carlson, S. L., A rapid and sensitive assay for measuring mitochondrial metabolic activity in isolated neural tissue. *Brain Res. Protoc.* **1998**, *2*, 259−263.

(215)   Islam, Z.; Pestka, J. J., LPS priming potentiates and prolongs proinflammatory cytokine response to the trichothecene deoxynivalenol in the mouse. *Toxicol. Appl. Pharmacol.* **2006**, *211*, 53−63.

(216)   Promega Corporation, *CellTox™ Green Cytotoxicity Assay, TM375 Revised 5/15*. 2015; 21 pp. https://no.promega.com/~/media/files/resources/protocols/technical%20manuals/101/celltox%20green%20cytotoxicity%20assay%20protocol.pdf

(217)   Sato, K.; Hyodo, M.; Aoki, M.; Zheng, X.-Q.; Noyori, R., Oxidation of sulfides to sulfoxides and sulfones with 30% hydrogen peroxide under organic solvent- and halogen-free conditions. *Tetrahedron* **2001**, *57*, 2469–2476.

(218)   Jacob, C., A scent of therapy: pharmacological implications of natural products containing redox-active sulfur atoms. *Nat. Prod. Rep.* **2006**, *23*, 851−863.

(219)   Salinas, A. E.; Wong, M. G., Glutathione *S*-transferases−a review. *Curr. Med. Chem.* **1999**, *6*, 279–309.

(220)   Königs, M.; Schwerdt, G.; Gekle, M.; Humpf, H.-U., Effects of the mycotoxin deoxynivalenol on human primary hepatocytes. *Mol. Nutr. Food Res.* **2008**, *52*, 830–839.

(221)   Juan-Garcia, A.; Juan, C.; Konig, S.; Ruiz, M. J., Cytotoxic effects and degradation products of three mycotoxins: alternariol, 3-acetyl deoxynivalenol and 15-acetyl deoxynivalenol in liver hepatocellular carcinoma cells. *Toxicol. Lett.* **2015**, *235*, 8-16.

(222)   Juan-Garcia, A.; Juan, C.; Manyes, L.; Ruiz, M. J., Binary and tertiary combination of alternariol, 3-acetyl deoxynivalenol and 15-acetyl deoxynivalenol on HepG2 cells: toxic effects and evaluation of degradation products. *Toxicol. In Vitro* **2016**, *34*, 264–273.